GEOLOGICA ULTRAIECTINA

Mededelingen van de
Faculteit Aardwetenschappen
Universiteit Utrecht

No. 118

# Solid state NMR study of minerals and glasses

## Application of off-resonance nutation spectroscopy

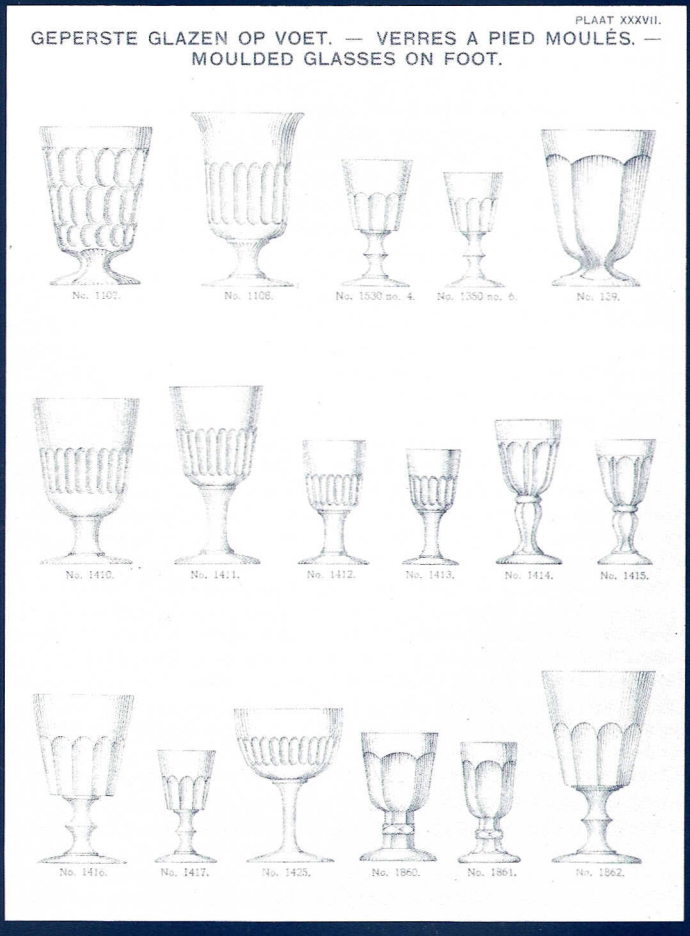


Peter Dirken

# Solid state NMR study of minerals and glasses

**Application of off-resonance nutation spectroscopy**

## Vaste stof NMR studie van mineralen en glazen

**Toepassing van off-resonance nutatie spectroscopie**

(met een samenvatting in het Nederlands)

Proefschrift

ter verkrijging van de graad van doctor
aan de Universiteit Utrecht
op gezag van de Rector Magnificus, Prof. Dr. J.A. van Ginkel,
ingevolge het besluit van het college van dekanen
in het openbaar te verdedigen
op maandag 7 maart 1994 des namiddags te 4.15 uur

door

Petrus Johannes Dirken

geboren op 1 augustus 1967 te Geleen

Promotores: Prof. Dr. R.D. Schuiling.
Verbonden aan de faculteit Aardwetenschappen
van de Universiteit Utrecht.
Prof .G. Blasse.
Verbonden aan de faculteit Scheikunde
van de Universiteit Utrecht.

Co-promotores: Dr. A.P.M. Kentgens.
Verbonden aan het NSR Center for Molecular Structure, Design and Synthesis, SON/NWO HF-NMR Faciliteit te Nijmegen.
Dr. J.B.H. Jansen.
Voorheen verbonden aan de faculteit Aardwetenschappen van de Universiteit Utrecht; nu werkzaam bij Bowagemi B.V. te Driebergen.

CIP-GEGEVENS KONINKLIJKE BIBLIOTHEEK, DEN HAAG

Dirken, Petrus Johannes

Solid state NMR study of minerals and glasses :
application of off-resonance nutation spectroscopy /
Petrus Johannes Dirken. - Utrecht : Faculteit
Aardwetenschappen, Universiteit Utrecht. - (Geologica
Ultraiectina, ISSN 0072-1026 ; no. 118)
Proefschrift Universiteit Utrecht. - Met lit. opg. - Met
samenvatting in het Nederlands.
ISBN 90-71577-72-4
Trefw.: NMR / vaste-stoffysica.

Front cover: Glass can be of great practical use..
From the Leerdam glass collection 1878-1930.
Printed with permission of publishing
company Antiek Lochem in Lochem.

## DAS VEILCHEN

*Ein Veilchen auf der Wiese stand,*
*Gebückt in sich und unbekannt;*
*Es war ein herzig's Veilchen.*
*Da kam eine junge Schäferin,*
*Mit leichtem Schritt und munterm Sinn,*
*Daher, daher,*
*Die Wiese her, und Sang.*

*Ach,! denkt das Veilchen; war ich nur*
*Die schönste Blume der Natur,*
*Ach nur ein kleines Weilchen,*
*Bis mich das Liebchen abgepflückt,*
*Und an dem Busen matt gedrückt!*
*Ach nur, ach nur,*
*Ein Viertelstündchen lang!*

*Ach! aber ach! das Mädchen kam,*
*Und nicht in Acht das Veilchen nahm,*
*Ertrat das arme Veilchen.*
*Es sang und starb und freut sich noch:*
*Und sterb' ich denn, so sterb 'ich doch*
*Durch sie, durch sie,*
*Zu ihren Füßen doch.*
*1775.*

*Tekst: J. W. von Goethe*
*Op muziek gezet door W.A. Mozart*
*(KV476)*

## Table of contents.

Chapter 2 has been published in *the American Mineralogist, 77, 718-724 (1992)*
Co-authors J. Ben H. Jansen and Roelof D. Schuiling

Chapter 3 has been submitted to *the American Mineralogist*
Co-authors Arno P. M. Kentgens, Gerda.H. Nachtegaal, Ad M. J. van der Eerden and J. Ben H. Jansen

Chapter 4 has been submitted to *the Journal of Physical Chemistry*
Co-authors Arno P. M. Kengtens, Gerda.H. Nachtegaal and J. Ben H. Jansen

Chapter 5 is intended for publication in *Solid State Nuclear Magnetic Resonance Spectroscopy.*

## Dankwoord

Dit proefschrift is grotendeels de optelsom van de hulp en steun van een aantal mensen. Hier wil ik hun daarvoor bedanken.

Allereerst en bovenal wil ik mijn "Geochemie" co-promotor Ben Jansen bedanken. Ten eerste natuurlijk, omdat hij degene was die mij eind 1989 vroeg in het HPT lab te komen werken. Maar nog veel meer, om zijn vermogen mij telkens weer uit de bekende "dooie" momenten te slepen. Zijn geweldige enthousiasme en kundige suggesties zijn altijd een enorme stimulans geweest.

Mijn dank gaat zeker ook uit naar Arno Kentgens, mijn "NMR" co-promotor, van wie ik veel geleerd heb over deze veelomvattende en fascinerende techniek. Dankzij hem kon ik kennis maken met nutatie NMR technieken en in het bijzonder "state of the art" off-resonance nutatie NMR. De kwaliteit van de afzonderlijke hoofdstukken heeft veel voordeel gehad van zijn grote kennis van zaken en zeer kritische houding.

Prof. Dr. R. Schuiling en Prof. G. Blasse bedank ik in de eerste plaats voor het feit, dat ze bereid waren op te treden als promotor voor dit project en in de tweede plaats voor hun suggesties, ieder op zijn eigen vakgebied, met betrekking tot de manuscripten. Vooral dankzij het intensieve contact met Prof Blasse kon dit project binnen de daarvoor gestelde tijdspanne afgerond worden.

Ad van der Eerden ben ik dankbaar niet alleen voor zijn schier onuitputtelijke voorraad praktische ideën in het lab, maar ook voor het gewillige oor dat ik vond als er weer eens wat tegenslag was of als ik "zomaar wat" wilde kletsen. Na het vertrek van Ben nam hij voor een groot gedeelte diens stimulerende invloed over.

Gerda Nachtegaal dank ik voor haar hulp tijdens de NMR sessies. Altijd maar weer stond ze klaar om problemen tijdens de metingen op te lossen, metingen voor mij te doen (!), of te helpen bij het uitwerken van die metingen. Mede dankzij haar was het altijd een plezier om in Nijmegen te werken.

Voor het goed tot een eind brengen van een promotie zijn een goede sfeer van groot belang. Daarvoor wil ik dan ook mijn kamergenoten en collega's bedanken (in willekeurige volgorde): Jan, Nellie, Marc, Thijs, Ineke, Gerko, Ronald, Theo, Paul, Roland, en Jeroen in Utrecht en Ernst, Ferry, en nog vele anderen in Nijmegen.

Vianney Govers en Thea Broer dank ik voor de XRD analysen, Tilly Bouten voor de hulp bij de microprobe analysen, Pim van Maurik en Joop Pieters voor het electronenmicroscopie werk, Paul Anten voor de ICP analysen, en Theo van Zessen voor de XRF analysen.

Nellie Slaats bedank ik voor haar hulp bij het voorbereiden van SEM preparaten en tal van kleine dingen. Kees Woensdregt bedank ik voor zijn steun vooral in het laatste jaar na de overheveling naar de vakgroep Geologie. Jan van Os, Jos Joordens en Hans Janssen wil ik bedanken voor hun technische ondersteuning en humor tijdens de NMR metingen.

Verder wil ik graag al het personeel van de werkplaats, bibliotheek, de slijpkamer, de Audiovisuele dienst, bedanken voor hun vakkunde.

Margret (Jezus, Peter, maak die mok nou eens schoon) en Berna (hé, Tjippie) bedank ik voor hun enthousiaste culinaire inzet in de kantine en tijdens borrels.

Mijn ouders, broer, zussen en vrienden en vriendinnen bedank ik voor hun vertrouwen en belangstelling voor alles wat voor mij belangrijk was en nog is.

Jan Viguurs bedank ik voor het zeer kritisch doorlezen van hoofdstuk 1 en hoofdstuk 5. Ingo Horn, Sieger van der Laan and their colleagues at the Mineralogisches-Petrologisches Institut der Universität Göttingen are thanked for trying to perform HP experiments and of course for the great time I've had there.

I'd like to thank Prof. Ray Dupree, Andy Howes and Simon Kohn of the University of Warwick in the U.K. for their hospitality and help during my 5 weeks visit to Coventry.

Prof. A. Koster van Groos, University of Illinois, Chicago zou ik willen bedanken voor het doen van een run op de Internally Heated apparatuur aldaar en zijn zeer gastvrije ontvangst in Chicago. Prof. J. Kirkpatrick, University of Illinois, Urbana and Prof. J. Stebbins of Stanford University, U.S.A. are thanked for giving me the opportunity to visit their lab and for giving a talk at their institute.

## Samenvatting

Dit proefschrift beschrijft NMR experimenten aan een aantal natuurlijke en synthetische verbindingen en glazen. Het doel van die experimenten is na te gaan, hoe samenstelling en structuur van die verbindingen aan elkaar gerelateerd zijn. Dit is van belang, omdat tal van eigenschappen, of dat nu (geo)chemische, fysische of andere eigenschappen zijn, afhankelijk zijn van de samenstelling.

Na een algemene inleiding (hoofdstuk 1), worden in hoofdstuk 2 vaste stof NMR experimenten aan een vijftal synthetische en natuurlijke alkalifluoroaluminaten beschreven. Deze verbindingen bestaan uit $AlF_6$ octaeders die, net als $SiO_4$ tetraeders, aan elkaar geschakeld kunnen worden. Daarbij ontstaan plaatstructuren, netwerkstructuren of structuren met geïsoleerde octaeders. Zowel de $^{23}Na$ als de $^{27}Al$ chemical shift zijn afhankelijk van het type structuur. De $^{27}Al$ chemical shift wordt - analoog aan Si chemical shifts in silicaten - steeds negatiever gaande van geïsoleerde $AlF_6$ octaeders naar octaeders in plaatstructuren en netwerkstructuren. Voor het eerst wordt rechtstreeks aangetoond, dat ook de $^{23}Na$ chemical shift afhankelijk is van het aantal liganden: $NaF_6$-groepen hebben een minder negatieve chemical shift dan $NaF_8$-groepen. Tevens laat hoofdstuk 2 zien, dat de $^{27}Al$ chemical shifts in oxiden meer dan 20 ppm hoger zijn dan die van equivalente fluoriden.

In hoofdstuk 3 worden NMR experimenten beschreven aan een tweetal zeldzame mineralen, zunyiet en harkeriet, die een bijzondere kristallografische groep bevatten. Deze groep is opgebouwd uit een centrale $TO_4$ tetraeder (T=Si voor zunyiet en Al voor harkeriet) met 4 $SiO_4$ tetraeders eromheen. De T-O-Si hoeken zijn 176° (harkeriet) of 180° (zunyiet). Het mineraal zunyiet heeft een overschot aan Al. Met $^{27}Al$ NMR wordt aannemelijk gemaakt dat dit, net als bij harkeriet in de centrale tetraeder wordt ingebouwd. Een bekende correlatie tussen de $^{27}Al$ chemical shift en de Al-O-Si intertetraedrische hoek voor netwerk aluminosilicaat structuren kan daardoor uitgebreid worden naar hoeken van 176° (was 153.7°).

In hoofdstuk 4 wordt off-resonance nutatie NMR spectroscopie toegepast op een vijftal synthetische glazen. Deze glazen hebben een samenstelling nauw verwant aan een graniet, waarbij de alkali ionen vervangen zijn door respectievelijk Li, Na, K, Rb of Cs. De off-resonance nutatie NMR spectroscopie techniek, ontwikkeld bij de HF NMR faciliteit in Nijmegen, blijkt zeer goed bruikbaar om de kwadrupole interactie van Al in amorfe systemen te bepalen. Hierdoor kan ook de isotrope $^{27}Al$ chemical shift nauwkeuriger bepaald worden. De kwadrupool interactie van Al en zijn isotrope chemical shift nemen af als de iongrootte van het alkali ion toeneemt. Hierbij wordt de in hoofdstuk 3 beschreven correlatie tussen de $^{27}Al$ chemical shift en de Al-O-Si intertetraedrische hoek gebruikt om aan te tonen, dat de toename van de ionstraal van het alkali ion gepaard gaat met een vergroting van de ringen waaruit deze glazen zijn opgebouwd. Het feit, dat de kwadrupool interactie van de Al kernen in het glas en de polariteit van het alkali ion een lineair verband vertonen. toont aan, dat er een sterke interactie tussen beide typen ionen bestaat en waarschijnlijk dicht bij elkaar zitten. Ditzelfde verband wordt voorspeld door een theoretisch model.

Hoofdstuk 5 gaat in op de vraag of korund ($\alpha$-$Al_2O_3$) gebruikt kan worden als een standaard in kwantitatieve Al NMR. Het kwadrupoolkarakter van Al zorgt ervoor, dat kwantitatieve metingen aan een aantal voorwaarden moeten voldoen om vergelijkingen

tussen intensiteiten van verschillende verbindingen te kunnen maken. Hoofdstuk 5 vergelijkt de intensiteiten van een aantal synthetische en natuurlijke korund monsters en toont aan, dat zelfs als aan alle voorwaarden voldaan is de intensiteiten ver uiteenlopen. Korund gemaakt door het verhitten van $Al(OH)_3$ levert goede resultaten op, maar de natuurlijke korunden en een synthetisch éénkristal van korund laten een groot verlies aan intensiteit zien. Waarschijnlijk worden de verschillen in intensiteit veroorzaakt door een verschil in relaxatie gedrag. Korund als standaard voor kwantitatieve Al NMR metingen lijkt alleen dan zinvol, als het een zuiver, goedgekarakteriseerd monster betreft.

## Summary

In this thesis solid state NMR experiments on a variety of minerals and glasses are described with the aim of studying the dependence of their structure on the chemical composition. Chapter 1 introduces the reader to the subject.

Chapter 2 describes $^{23}Na$ and $^{27}Al$ NMR experiments on a number of alkali fluoroaluminates. These substances consist of $AlF_6$ octahedra which can be linked together to form a variety of structures, similar to the way in which $SiO_4$ and $AlO_4$ tetrahedra are linked together in aluminosilicates. The $^{23}Na$ and $^{27}Al$ chemical shifts correlate well with the type of structure. $AlF_3$ is a network structure and has the most negative $^{27}Al$ chemical shift (-16 ppm). The chemical shift increases from -3 and -1 ppm in the sheet structure chiolite ($Na_5Al_3F_{14}$) to 0 ppm in cryolite ($Na_3AlF_6$). The $^{23}Na$ chemical shift is dependent of the number of fluorines coordinating Na: Na in an $NaF_6$ group has a more positive chemical shift than Na in $NaF_8$. Additionally, $^{27}Al$ chemical shifts for oxides are shown to be at least 20 ppm less shielded than those in similar fluorides.

Chapter 3 studies pentameric $(Si,Al)_5O_{16}$ groups with (almost) straight intertetrahedral Al-O-Si angles in a zunyite with excess Al and in harkerite. The excess Al in the zunyite lattice is shown to occupy the central tetrahedral Si(1) site. The $^{27}Al$ chemical shift correlation with the Al-O-Si angle is extended to 176°

Chapter 4 reports the first application of off-resonance nutation spectroscopy to five alkali aluminosilicate glasses. These glasses have a chemical composition similar to that of a granite, with the alkali's replaced by Li, Na, K, Rb, and Cs. Off-resonance nutation spectroscopy, newly developed at the HF-NMR facility in Nijmegen, proves to be very powerful in determining the quadrupole interaction and subsequently the isotropic chemical shifts for Al in these glasses. The quadrupole interaction and the chemical shift decrease when the size of the charge-balancing counterion increases. The correlation of the $^{27}Al$ chemical shift with the Al-O-Si angle for framework aluminosilicate structures (see also chapter 3) is used to show, that the size of the alkali ion determines the size of the rings building up the glasses. Since the quadrupole interaction for Al is linearly correlated with the polarising power of the alkali ion, the aluminium and the alkali ions are believed to be closely bound. This is supported by a theoretical ionic model predicting this correlation.

Chapter 5 investigates the use of corundum ($\alpha$-$Al_2O_3$ ) as a standard in quantatative NMR measurements. As Al is a quadrupolar nucleus, a number of requirements have to be fullfilled in order to obtain reliable results. Most importantly, only the central transition is excited by using a very short rf pulse in order to be in the region of linear response. The intensities of five natural and synthetic corundum samples are compared. Despite the fact that all experimental conditions are identical and in the linear region, the intensities differ considerably. A synthetic corundum obtained by heating $Al(OH)_3$ has the highest intensity, close to the expected value, but the other samples have much too low intensities. Relaxation effects are shown to be responsible for this. It is proposed, that only in case of a well-characterized corundum sample without impurities $\alpha$-$Al_2O_3$ can be used as a standard for quantitative NMR measurements.

Chapter 1

# Introduction

## 1.1 General

Approximately 95% of the minerals and rocks in the earth's crust were originally formed by crystallization from silicate melts (Burnham, 1981). It is thus obvious, that these melts are of overwhelming importance in geochemistry.

An understanding of the melt structure is vital to understand its physical, chemical and thermal properties (Tossell and Vaughan, 1992). Directly or indirectly, most geological processes are influenced by these properties. For instance, partitioning behaviour between melts and fluids and/or crystals is a function of the chemical composition (Webster, 1990). A direct consequence of this functionality is the development of economically important ore-deposits. Eruption behaviour of volcanoes also depends on the type of magma involved, more specifically the viscosity($\eta$) and the gas content of the magma. The viscosity is probably the most important property of a silicate melt (Perchuk and Kushiro, 1991). Viscosities of $SiO_2$-rich magma (granitic/rhyolitic; $SiO_2$>68 wt%) are much higher ($\eta \approx 10^{12}$ Poise at 1100°C) than $SiO_2$-poor magma (alkali basalt, $\eta=10^2$-$10^3$ Poise at 1100 °C) (Cas and Wright, 1987). Clearly, viscosity is a function of the chemical composition, in this case the $SiO_2$ content. Other factors controlling viscosity are the volatile content ($H_2O$, F, Cl, $CO_2$), temperature, pressure, crystal content and bubble content. Additionally, $SiO_2$-rich melts can dissolve more $H_2O$ than $SiO_2$-poor melts (Cas and Wright, 1987). So not only is there a wide range of factors that influence the viscosity, and in fact all properties of natural magmas, they are also interconnected.

This complexity has urged experimental geochemists to study these factors separately in synthetic systems with all experimental techniques available. A vast majority of these studies involves glasses that were quenched rapidly to room temperature and atmospheric pressure in order to freeze the conditions of the melt.

Despite the fact that some authors question the validity of this assumption and the fact, that in situ measurements on melts are becoming more and more feasible (McMillan et al., 1992; Coté et al., 1992; Stebbins, 1991), much of our understanding of the behaviour and structure of silicate melts stems from glass studies.

## 1.2 The continuous random network model

Many, if not all spectroscopic methods available to modern-day geochemists have been applied to silicate glasses and minerals. Much of the initial understanding of glass structure comes from radial distribution functions (RDF's) from X-ray and neutron diffraction studies (Mozzi and Warren, 1969; Taylor and Brown, 1979a,b).

This technique has taught us, that (alumino)silicate melts are built up of $SiO_4$ (and $AlO_4$) tetrahedra. These tetrahedra are connected by bridging oxygens (figure 1) into Q-species with a range of compositions. Additionally, these tetrahedra can also be connected to network modifying cations by non-bridging oxygens. This description is also valid

for crystalline aluminosilicates. The key difference between the crystalline and the amorphous state is the lack of periodicity in the latter. This is caused by variations in the bond angle and distances to second-nearest neighbors. This description is the most widespread model for silicate glass structure and is usually called the continuous random network model (Zachariasen, 1932; Mysen, 1988).

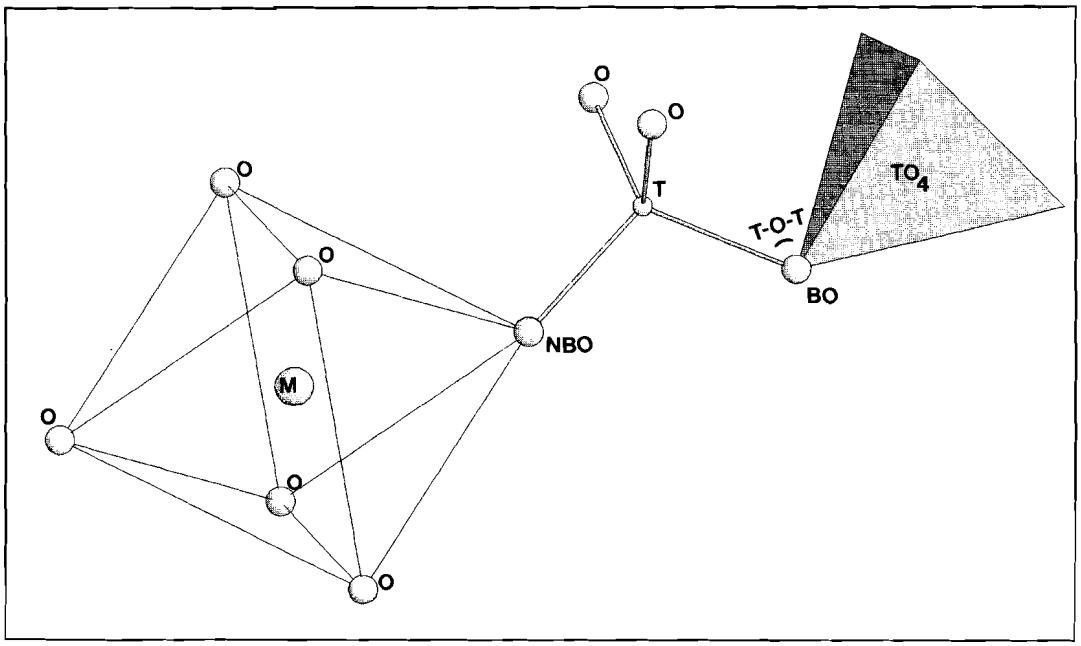


**Figure 1.** *The continuous random network model.*
*Two* $TO_4$ *tetrahedra (T=Si or Al) are connected through a bridging oxygen (BO). One of the tetrahedra is bonded to a network modifying cation (M) (for instance an alkali ion) through a non-bridging oxygen (NBO). T-O-T angles and bond lengths (M-O, T-O)are subject to large variations.*

The above mentioned radial distribution functions, from which much of the early data originated, become increasingly difficult to interpret as the number of constituents increases. Other techniques have emerged, which are used to determine the above mentioned Q-species and their distributions in the melt, the most important being vibrational spectroscopy (Mysen, 1988). This technique has been successful in the identification of the Q-species, but quantification is quite difficult because of calibration problems and overlap of broad bands encountered in vibrational spectra of amorphous systems. In case of the interaction of $H_2O$ with aluminosilicate melts, for instance, there is a lot of debate about the assignment of some absorption bands (Sykes and Kubicki, 1993; Kohn et al., 1992). From these bands, many conclusions are drawn; it is therefore of vital importance that these are checked with as many structural tools and as thoroughly as possible.

## 1.3 Solid state NMR spectroscopy

Solid state NMR is a relatively new technique, which has experienced an explosive growth since the advent of FT pulse technology in combination with high field superconducting magnets and Magic Angle sample Spinning (MAS).

Solid state NMR has a few unique features making it ideally suited for studying amorphous systems. First of all, NMR is element specific, and as a result it is, in principle, independent of the complexity of the system. Secondly, the NMR signal is proportional to the number of contributing nuclei, making it useful for quantitative applications. The third advantage of NMR is, that it is interaction specific. This implies, that by changing the experiment setup (pulse sequence, excitation of more than one kind of nucleus), we can tune into a specific interaction of interest. An example is the study of the homonuclear or heteronuclear dipolar interactions. This interaction can give information on internuclear distances between atoms of the same or of different types, respectively. Other interactions, which are of considerable structural significance are the chemical shift interaction (in fact the most widely used) and the quadrupole interaction.

Finally, NMR can give information on dynamic phenomena such as atomic or molecular motion and exchange via studies of NMR lineshapes and nuclear spin relaxation (Abragam, 1961; Slichter, 1992; Liu et al., 1987; Stebbins, 1988). The region in which NMR is sensitive to these processes spreads from Hz to 100's of MHz.

A disadvantage of NMR is, that the above mentioned interactions can be calculated ab-initio only with great difficulty. As a result, extraction of information from NMR spectra relies heavily on the availability of reference systems. Much of the effort in solid state NMR is put into the development of these systems.

In this thesis, $^{29}$Si, $^{23}$Na, and $^{27}$Al have been studied, with emphasis on $^{27}$Al. $^{29}$Si has spin I=½, 4.7 % natural abundance and often suffers from long $T_1$ relaxation times, making $^{29}$Si measurements rather time consuming. $^{29}$Si chemical shifts can be correlated with coordination state, tetrahedral polymerisation, number of Al next-nearest neighbors, mean Si-O-T bond angle per tetrahedron (T=Si, Al) and group electronegativity (Lippmaa et al., 1980; Lippmaa et al., 1981; Smith and Blackwell, 1983; Kirkpatrick, 1988).

$^{27}$Al has a 100% natural abundance, spin I=5/2 and is therefore a quadrupolar nucleus. Smith (1993) and Kirkpatrick and Phillips (1993) have recently given a thorough review of solid state $^{27}$Al NMR spectroscopy. Theoretical and experimental aspects of NMR of quadrupolar nuclei have been reviewed by Freude and Haase (1993).

### Quadrupole interaction

Nuclei with spin I>1/2 have a quadrupole moment (eQ), which is a result of a non-spherical charge distribution. This quadrupole moment interacts with the electric field gradient at the nucleus, causing an electrostatic interaction, the quadrupole interaction. This interaction is described by the quadrupole coupling constant (QCC) and asymmetry parameter ($\eta$ ) (Cohen and Reif, 1957). In case of spin I=1/2 nuclei there are only two nuclear energy levels, -1/2 and 1/2, so there is only one transition possible. In case of aluminium with spin I = 5/2, there are (2I+1) = 6 nuclear energy levels (figure 2). In the

absence of an external magnetic field $B_0$, these levels have an equal energy, but in case of $B_0 \neq 0$, these levels (m) get their own specific energy (Zeeman interaction). The transition energies are equal ($\Delta E$). The quadrupole interaction has an additional effect on the position of the nuclear energy levels. The six equally spaced levels are perturbed in first and second order, except for the central (-1/2, 1/2) transition, which is only affected in second order. The non-central (satellite) transitions are usually spread over a frequency range in the order of $\nu_Q$ (=3QCC/(2I(2I-1))), which can be in the MHz range. This is the reason why these satellite transitions are usually not observed in solid state NMR spectra. The central transition is affected only in second order. The lineshape is distorted and in the absence of other strong line broadening interactions it has a form characteristic for the quadrupole parameters QCC and $\eta$. This form is called a powder pattern (Samoson and Lippmaa, 1983b). Magic Angle Spinning (MAS) averages first order effects, but not the second order effects. As a result, line narrowing is incomplete and a powder pattern is preserved. Additionally, the line is shifted from its isotropic chemical shift value. As quadrupole effects are inversely proportional to the square of the magnetic field strength, resolution of solid state spectra benefits greatly from the use of very high (>11.7 T) magnetic fields.

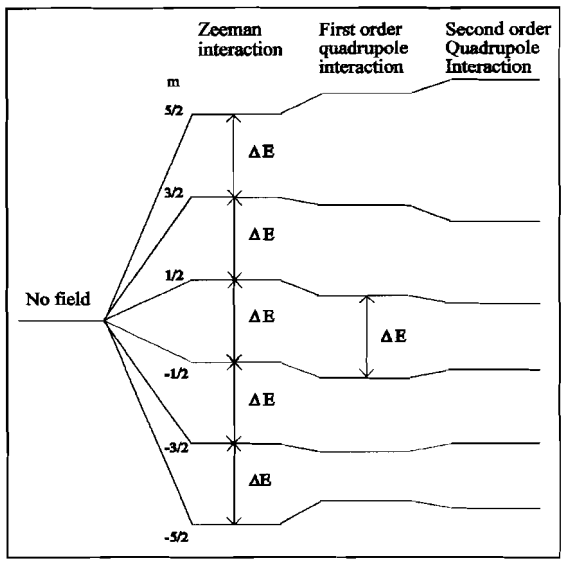


**Figure 2.** *Graphical representation of the Zeeman interaction and first and second order quadrupole interaction.*

$^{27}$Al NMR is sensitive to coordination state (Müller et al., 1981; de Jong et al., 1983), mean Al-O-Si angle (for $^{[4]}$Al in framework aluminosilicate structures; Lippmaa et al., 1986). For $^{[4]}$Al, $\delta_{iso}$ is also sensitive to the degree of polymerisation of the $AlO_4$ tetrahedra (Müller et al., 1986). The quadrupolar nature of Al can complicate the interpretation of the NMR spectra, but is also an extra source of structural information. It can be used to investigate the local symmetry of the first coordination sphere of Al. Ghose and Tsang (1973) studied a wide range of Al-containing phases and concluded, that the $^{27}$Al $e^2qQ/h$ (quadrupole coupling constant) is correlated with the distortion of the nearest neighbor oxygen polyhedron.

Getting information on the various interactions in amorphous phases is complicated by severe line-broadening effects due to a distribution of interactions. The amorphous character is due to variations in the bond angle and distances to second-nearest neighbors.

Important new developments in solid state NMR are Dynamic Angle Spinning (DAS) NMR (Llor and Virlet, 1988; Chmelka et al., 1989), Double Orientation Rotation (DOR) NMR (Samoson et al., 1988). DAS is a two-dimensional technique, in which there is a rapid flipping of the sample between two axes. In DOR NMR there is a simultaneous spinning of the sample around two axes. These techniques average the first and second order quadrupole broadening and as a result NMR signals are narrowed as compared to MAS NMR.

Additionally, satellite transitions can be studied. These transitions have an intrinsically narrower linewidth (Samoson, 1985). However, this technique, denoted as SATRAS by Jäger et al. (1992), seems to be limited to nuclei with spin I=5/2 (Freude and Haase, 1993).

A promising technique, which allows for an accurate determination of the quadrupole interaction in amorphous solids is an extension of nutation NMR spectroscopy, called off-resonance nutation NMR (Kentgens, 1993; Chapter 4 of this thesis).

## 1.4 Scope and organisation of this thesis

The aim of this thesis is to obtain a better insight into the structural dependence of $^{27}Al$ (and partly $^{23}Na$) NMR in mineral and glass structures. The mineral structure information can be used as a reference for future studies on mineral and glass structures.

**Chapter 2** deals with $^{23}Na$ and $^{27}Al$ MAS NMR on alkali fluoroaluminates. This type of substances is commonly encountered in synthetic and natural F-rich melts. This chapter can be used as a reference system for NMR studies of these melts.

**Chapter 3** extends the well-known correlation in $^{27}Al$ MAS NMR between the $^{27}Al$ isotropic chemical shift and the Al-O-Si angle for framework aluminosilicates to Al-O-Si angles of 176°. This is done by studying two rare minerals: zunyite and harkerite. These minerals contain similar $(Si,Al)_5O_{16}$ groups (pentamers) with (almost) straight intertetrahedral angles.

**Chapter 4** reports the first application of off-resonance nutation spectroscopy. It is used to study the role and position of the charge-balancing cation in a series of synthetic framework alkali aluminosilicate glasses (alkali = Li, Na, K, Rb, or Cs).

**Chapter 5** tries to evaluate the use of corundum ($\alpha$-$Al_2O_3$) as a standard in quantitative $^{27}Al$ NMR studies.

# Chapter 2

## Influence of Octahedral Polymerisation on Sodium-23 and Aluminum-27 MAS-NMR in Alkali Fluoroaluminates

### 2.1 Abstract

Solid state $^{23}Na$ and $^{27}Al$ MAS NMR spectra of NaF, $\alpha$- and $\beta$-$AlF_3$, cryolite ($Na_3AlF_6$), chiolite ($Na_5Al_3F_{14}$) and elpasolite ($K_2NaAlF_6$) have been studied. Structures and chemical compositions have been checked by X-ray diffraction, DTA/TGA and wet chemical analyses (ICP-AES, AAS, ISE). $^{27}Al$ NMR isotropic chemical shifts range from -13.2 to + 1.4 ppm, indicating octahedral coordination by fluorine, which is in agreement with crystallographic data. Compared to $AlO_6$ octahedra in aluminates, the $AlF_6$ octahedra in fluoroaluminates are at least 20 ppm more shielded. The $^{27}Al$ results show, that Al chemical shifts become more shielded as the degree of polymerisation of the $AlF_6$ octahedra increases. $S^0$ structures with isolated $AlF_6$ octahedra fall into a region around 0 ppm with a spread of only 2 ppm. Sheet-structures with $S^2$ and $S^4$ octahedra, have Al resonances at -1 to -3 ppm and Al in network structures resonates at -12.5 to -13.2 ppm. This trend is explained by a decrease in the number of non-bridging fluorines per octahedron (NBF/O). Consequently, $^{23}Na$ NMR depends on the type of $AlF_6$ polymerisation. Octahedrally coordinated Na stepwise becomes more shielded from 7.2 ppm for NaF, via 2.4 ppm for cryolite to -6 ppm for chiolite. Eight-coordinated Na resonates at more negative chemical shifts than six-coordinated Na, -9.3 ppm in cryolite and -21 ppm in chiolite. The observation of the $^{27}Al$ and $^{23}Na$ signals of two closely related structures, cryolite and elpasolite, indicates, that both $^{27}Al$ and $^{23}Na$ NMR are insensitive to cationic substitution within the lattice, probably because of the ionic character of the Al-F and Na-F bonds.

### 2.2 Introduction

Magic Angle Spinning Nuclear Magnetic Resonance (MAS-NMR) spectroscopy is an important technique to determine the coordination state and local symmetry of structural units such as $(Si,Al)O_4$, $AlO_5$ or $AlO_6$ polyhedra within crystalline and amorphous solids. In general, increased shielding of a nucleus by its ligands and an increase in coordination number results in a more negative chemical shift. In the case of Al, chemical shifts for 4-, 5- and 6-coordination fall into the range 50-80, 35-40 and -10-+15 respectively (Müller et al, 1981; Kirkpatrick, 1988; Akitt, 1989).

The degree of polymerisation of $SiO_4$ tetrahedra in crystalline as well as amorphous solids can be determined with one dimensional $^{29}Si$ NMR experiments (Smith et al. 1983; Magi et al. 1984; Stebbins, 1987; Kirkpatrick, 1988). Increased polymerisation causes an increased shielding of the silicon nuclei. The chemical shifts of Al in $AlO_4$ are considered to be insensitive to polymerisation effects and shift to higher fields if the tetrahedra are connected to $SiO_4$ tetrahedra (Müller et al, 1986). Müller and Bentrup (1989)

studied various hydrous alkali fluoroaluminates and concluded that $^{27}Al$ NMR is hardly affected by differences in condensation of $AlF_6$ octahedra. Na- (and Li-) fluoroaluminates were not considered, though the Na-Al-F-system is particularly suited for the study of $AlF_6$ condensation, as a variety of structures exists in this system with a similar cationic second sphere of Na atoms. Furthermore, $^{23}Na$ NMR chemical shifts can be compared to give additional information on polymerisation phenomena.

In this paper one dimensional solid state $^{23}Na$ and $^{27}Al$ magic angle spinning NMR spectroscopic results on compounds in the system Na-Al-F are presented.

The first aim is to find out whether chemical shift data of $^{23}Na$ and $^{27}Al$ correlate with structural features within these phases. In this way it may be possible to discriminate between various types of Al-F structure types. For this purpose, a crystallogra-phic review of all compounds considered is presented prior to any NMR data.

Recently, Kohn et al (1991) reported the existence of $^{[5]}Al$ and $^{[6]}Al$ complexes in melts of jadeite + NaF and jadeite + cryolite ($Na_3AlF_6$) compositions with $^{27}Al$ and $^{27}Al$-$^{19}F$ CP NMR at 22 and -5 ppm respectively. They, among others (Manning, 1981; Mysen and Virgo, 1985), suggest that Al and F are present in F-rich aluminosilicate melts as Na-Al-F complexes. In this study we use Magic Angle Spinning NMR spectroscopy to distinguish Al-O complexes from Al-F complexes directly by $^{27}Al$ chemical shifts.

$^{23}Na$ NMR can give information whether or not Al and F form clusters with Na which resemble crystalline sodium fluoroaluminates. Cationic effects on $^{27}Al$ chemical shifts are investigated by comparing $^{27}Al$ NMR data of two almost isostructural compounds. (cryolite, $Na_3AlF_6$ versus elpasolite, $K_2NaAlF_6$) and combining these with previous work on alkalifluoroaluminates (Müller and Bentrup, 1989).

## 2.3 Crystallography

In the system NaF-$AlF_3$, NaF, $AlF_3$ and $Na_5Al_3F_{14}$ exist as stable phases besides the well-known mineral cryolite ($Na_3AlF_6$). NaF and $Na_5Al_3F_{14}$ occur in nature as the minerals villiaumite and chiolite respectively. The crystal structures of these compounds have been determined and refined.

**Villiaumite (NaF)** has the halite structure (Barth and Lunde, 1927), a simple cubic closest packing of F with Na in the octahedral interstices.

$AlF_3$ has a stable $\alpha$-form; a beta-phase has been obtained by dehydration of $\alpha$-$AlF_3 \cdot 3H_2O$ (Christoph et al, 1965), a gamma-phase by thermal decomposition of $NH_4AlF_4$ (Shinn et al, 1966). Le Bail et al (1988) reexamined the $\beta$-phase prepared from dehydrating $\alpha$-$AlF_3 \cdot 3H_2O$, assuming that it was identical to the **$\gamma$-phase**. No structure-determination has been carried out for $\gamma$-$AlF_3$. The stable $\alpha$-$AlF_3$ crystallizes as a rhombohedral structure (Hoppe and Kissel, 1984). It can be regarded as a $VF_3$-type structure (Hepworth et al, 1957) which is built up by a distorted closest packing of fluorine atoms, with aluminum in octahedral sites. The highly regular $AlF^{3-}_6$ octahedra share corners, in a three dimensional network. The metastable **$\beta$-$AlF_3$** phase consists of a 3-dimensional network of very regular $AlF^{3-}_6$ octahedra with 2 distinct Al-sites. The structure can be regarded as a slightly deviated hexagonal tungsten bronze (HTB) structure (Magnelli, 1953), in which sheets of intercon-

nected $AlF^{3-}_6$ octahedra parallel to the a-b plane are stacked along the c-axis. At 500 °C $\beta$-$AlF_3$ irreversibly transforms to $\alpha$-$AlF_3$ (Le Bail et al, 1988).

The crystal structure of **cryolite ($Na_3AlF_6$)** is made up of isolated $AlF^{3-}_6$ octahedra linked by 6-coordinated Na, forming a regular octahedron and 8-coordinated Na, creating a highly distorted cubic antiprism (Hawthorne and Ferguson, 1975). The $AlF^{3-}_6$ octahedra are very regular. The structure has a pseudocubic, monoclinic symmetry, attaining a true cubic symmetry in the beta-cryolite phase, above the reversible transformation temperature of 561 °C (Majumdar and Roy, 1965).

**Elpasolite ($K_2NaAlF_6$)** has the cryolite structure with the two 8-coordinated Na atoms replaced by K. It has a cubic symmetry, with undistorted $AlF_6$ octahedra (Sabelli, 1987).

**Chiolite ($Na_5Al_3F_{14}$)** is a tetragonal phase, which structure was refined by Jacoboni (1981). Two types of octahedra form independent $[Al_3F_{14}]^{5n-}_n$ layers perpendicular to the c-axis. Within each layer octahedra having $2/_m$ or $4/_m$ symmetry alternate with each fourth octahedron replaced by a sodium atom. Two Na atoms are coordinated by eight F, the other eight by six F. One $AlF_6$ octahedron shares corners with 4 octahedra; the other octahedron with two octahedra.

In general, the structures involved can be divided into three types, depending on the polymerisation of the octahedra. The $\alpha$- and $\beta$-$AlF_3$ phases are three dimensional networks of $AlF_6$ units. $Na_5Al_3F_{14}$ is a sheet structure and $Na_3AlF_6$ can be considered as a 'nesostructure' since its AlF6 octahedra are entirely isolated.

## 2.4 Experimental

### Samples

**$Na_3AlF_6$** and **$Na_5Al_3F_{14}$** are available as the minerals cryolite and chiolite respectively, both from the Ivigtut deposit, Greenland (Bøggild, 1953). The synthetic equivalents and elpasolite (**$K_2NaAlF_6$**) are prepared using the methods described by Cowley and Scott (1948). **$\beta$-$AlF_3$** is prepared by decomposing $NH_4AlF_4$ at 315 °C under a nitrogen flow, a method described by Shinn et al (1966) and by dehydrating $\alpha$-$AlF_3 \cdot 3H_2O$ (Christoph et al., 1965). **NaF** is available as analytical grade reagent from MERCK (Art.6449). **$\alpha$-$AlF_3$** is put to our disposal by Billiton ore company. All compounds are checked for impurities by X-ray diffraction with a Philips PW 1050/25 diffractometer using CuK$\alpha$ radiation.

Chemical analyses of all the fluorides have been carried out by dissolving them in a 40 mol% $Li_2CO_3$-60 mol% $K_2CO_3$ flux at 550 °C. The flux is then dissolved in water and analysed for K and Al by ICP-AES (ARL 34000), for Na by atomic absorption spectroscopy (Perkin Elmer 460) and for F by means of a fluorine selective electrode (Orion, Fluoride Electrode, Model 9409 and Reference Electrode, Model 9001). Analytical errors are 5 % for fluorine and sodium, and 10 % for potassium and aluminum.

DTA/TGA measurements were conducted under a $N_2$-atmosphere with a Du Pont Instruments 1090 Thermal Analyzer at a heating rate of 10 °C/min. The temperatures are correct within 5 °C.

### NMR spectroscopy

The one dimensional solid state NMR spectra were collected on Bruker CXP-300, AM-500 and AM-600 solid state high resolution spectrometers, operating at 7.1 T, 11.7 T and 14.1 T respectively. To assure relative saturation of the $^{27}Al$ and $^{23}Na$ resonances, the spectra were measured with short pulse excitations, using typical pulse lengths of 1-2 μs, relaxation delays of 0.25-0.5 seconds and 40-100 kHz spectral widths. Per measurement 100-12000 FID's were collected. The $^{27}Al$ and $^{23}Na$ chemical shifts are measured relative to an external standard of aqueous $AlCl_3$ and NaCl solution respectively. Spinning rates are typically 12 kHz, unless stated otherwise.

$^{23}Na$ and $^{27}Al$ isotropic chemical shifts ($\delta_{iso}$) and quadrupole coupling constants (QCC) are determined by calculating the quadrupolar induced shift at different magnetic fields (7.1, 11.7 and 14.1 T), assuming $\eta = 0$ and that the lines are symmetric. Contributions of the quadrupole broadening to the line-width can be calculated (Engelhardt and Michel, 1987). In some cases does the calculated broadening exceed the experimental linewidth, which is an indication that the asymmetry parameter must be closer to 1. The asymmetry parameter has no influence on the $\delta_{iso}$ in the calculations, as a change in $\eta$ from 0 to 1 is compensated by a change in QCC of approximately 15 %. Peak positions are correct within 1 ppm just as $\delta_{iso}$. Taking the error in peak position into account, the error in the QCC increases to 1 MHz. In the case of chiolite, $\delta_{iso}$ and the QCC are extracted from the spectra by using the frequencies for the singularities (Müller, 1982; Engelhardt and Michel, 1987) at two ($^{23}Na$) and three magnetic fields ($^{27}Al$). An ASPECT 3000 based computer program called POWDER (Müller and Bentrup, 1989) is used to check the calculations on the $^{23}Na$ and $^{27}Al$ spectra of chiolite.

## 2.5 Results

### X-ray diffraction

The spectra of **NaF**, **α-$AlF_3$**, **natural cryolite** and **synthetic and natural chiolite** and **synthetic elpasolite** do not contain reflections of impurities. The synthetic cryolite sample contains approximately 5 wt% chiolite. This impurity is not detected in the $^{23}Na$ and $^{27}Al$ NMR spectra. The β-$AlF_3$ phases were identical, so the NMR study is limited to the β-$AlF_3$ phase obtained by dehydration of α-$AlF_3 \cdot 3H_2O$.

### DTA/TGA

All phases were examined by thermal analyses to obtain additional chemical and structural information. **NaF** displays no thermochemical effect in the temperature range 25-750 °C. The **α-$AlF_3$** DTA-spectrum has a small endothermic peak at 450 °C and a larger one at 750 °C. TGA results on α-$AlF_3$ show a 10 % weight loss over the temperature region 450-780 °C. The onset of this volatilization corresponds to the first endothermic peak in the

DTA. At this temperature the $\alpha$-phase transforms to a high temperature phase (Robie et al., 1978). The peak at 750 °C has not been reported in literature. The **$\beta$-$AlF_3$** phase displays an exothermic reaction at 720 °C. The reaction represents the structural transformation to $\alpha$-$AlF_3$. This result is in good agreement with the result of 720 °C claimed by Shinn et al (1966). However, Le Bail et al (1988) reported a transformation temperature of 500 °C for their $\beta$-$AlF_3$. DTA on the $\beta$-$AlF_3$ obtained by dehydration of $\alpha$-$AlF_3 \cdot 3H_2O$ does not display a transformation at 500 °C. It further justifies rejecting $\gamma$-$AlF_3$ as a separate phase.

Both **natural and synthetic cryolite** display an endothermic peak at 562 °C. The peak represents the reversible transformation of the monoclinic $\alpha$-cryolite to the cubic $\beta$-cryolite. The temperature is in excellent agreement with the temperature of 561 °C reported by Majumdar and Roy (1965). Additionally, the synthetic cryolite loses a few percent water at 125 °C. **Elpasolite** only displays one small DTA-peak at 113 °C, most probably caused by a water-loss of about 1 wt% from the sample.

The DTA-curve of **natural chiolite** shows a melting temperature of 700 °C, 75 °C lower than reported by Mesrobian et al. (1972). Their experiments were conducted under non-atmospheric pressures up to 400 bars, however, so an absolute comparison is not entirely justified. The **synthetic chiolite** displays one small peak at 175 °C resulting from loss of a few percent water.

### Chemistry

The F-content of $\alpha$-$AlF_3$ is low, probably because of an impurity of corundum, which is lower than the X-ray detection limit of about 5 wt%. Additional F is lost during analysis, due to the high vapour pressure of $AlF_3$. It is not to be expected, that the impurity influences in anyway the $^{27}Al$ NMR results.

All samples acquired by precipitation from an aqueous solution, i.e. synthetic cryolite, chiolite and elpasolite, have a sum smaller than 100 %. This is due to uptake of some water as evidenced by DTA/TGA. The stoichiometric compositions corrected for possible water losses are within analytical accuracy.

### $^{27}Al$ and $^{23}Na$ NMR

The $^{27}Al$ and $^{23}Na$ NMR data for $\alpha$- and $\beta$-$AlF_3$, NaF, $Na_3AlF_6$, $K_2NaAlF_6$ and $Na_5Al_3F_{14}$ are listed in table 1 and 2, respectively. The symbol $S^n$ is used on the analogy of Müller et al (1986) with Q (of Quaternary) replaced by S (of Senary). The superscript n indicates the number of bridging fluorines per octahedron. If n equals zero, the structure consists of isolated $AlF_6$ octahedra. If n equals 6, the octahedra have condensed into a three dimensional network. The intermediate types of octahedra, with n=2 and n=4, alternate in chiolite and form a sheet-structure.

The $^{27}Al$ isotropic chemical shifts in these fluoroaluminates range from -13.2 to +1.4 indicating an octahedral coordination of Al by F in all Al-bearing phases (Müller et al, 1981; Kirkpatrick, 1988; Akitt, 1989). This is in agreement with crystallographic data and with earlier studies on alkalifluoroaluminates (alkali = $NH_4$, K, Rb, Cs) by Grimmer et al (1982) and Müller and Bentrup (1989). Results from synthetic and natural samples are identical. In

**Table 1.** *$^{27}Al$ NMR results.*

| compound | $S^n$(Al) | $\delta_{iso}$ (ppm) | QCC (MHz) | $\eta$ | Width (Hz) | Q.B.* (Hz) |
|---|---|---|---|---|---|---|
| $Na_3AlF_6$ | 0 | 1.4 | 2.0 | 0 | 1050 | 220/60 |
| $K_2NaAlF_6$ | 0 | 0.8 | 1.4 | 0 | 1000 | 110/30 |
| $Na_5Al_3F_{14}$ | 2 | -1 | 8.2 | 0 | - | - |
| | 4 | -3 | 6.5 | 1 | - | - |
| $\alpha$-$AlF_3$ | 6 | -13.2 | 2.8 | 0 | 1450 | 430/100 |
| $\beta$-$AlF_3$ | 6 | -12.5 | 3.4 | 0 | 1200 | 640/160 |

* Q.B.: calculated second order quadrupole broadening for $\eta$ = 0 and 0.75, resp.

**Table 2.** *$^{23}Na$ NMR results.*

| compound | C.N.* | $\delta_{iso}$ (ppm) | | QCC (MHz) | | $\eta$ | | Width (Hz) | Q.B.** (Hz) |
|---|---|---|---|---|---|---|---|---|---|
| | | *1* | *2* | *1* | *2* | *1* | *2* | *1* | *1* |
| NaF | 6 | 7.2 | | 0 | | 0 | | 600 | 0 |
| $Na_3AlF_6$ | 6 | 2.4 | 4 | 0 | 0.9 | 0 | 1.0 | 400 | 0 |
| | 8 | -9.3 | -8 | 2.3 | 1.45 | 0.75 | 0.25 | 700 | 1400/330 |
| $K_2NaAlF_6$ | 6 | 2.1 | | 0 | | 0 | | 500 | 0 |
| $Na_5Al_5F_{14}$ | 6 | | -6 | | 3.2 | | 0.15 | - | - |
| | 8 | | -21 | | 1.5 | | 0 | - | - |

* C.N.: Na coordination number

** Q.B.: calculated second order quadrupole broadening for $\eta$ = 0 and 0.75, resp.,

1: This study; 2: J.F. Stebbins and X. Xue, written communication

some cases more than one set of values is presented in tables 1 and 2, indicating more than one crystallographic position. In the $^{23}Na$ and $^{27}Al$ spectra of chiolite the central transitions have complex lineshapes. They are reconstructed by using the frequency-equations for the singularities at two or three magnetic fields (Engelhardt and Michel, 1987), the field dependent 2nd order quadrupole shift and the computer simulation program POWDER (Müller and Bentrup, 1989). The $^{23}Na$ spectrum of chiolite (figure 1) has a line-shape which is characteristic for a crystallographic site with an asymme

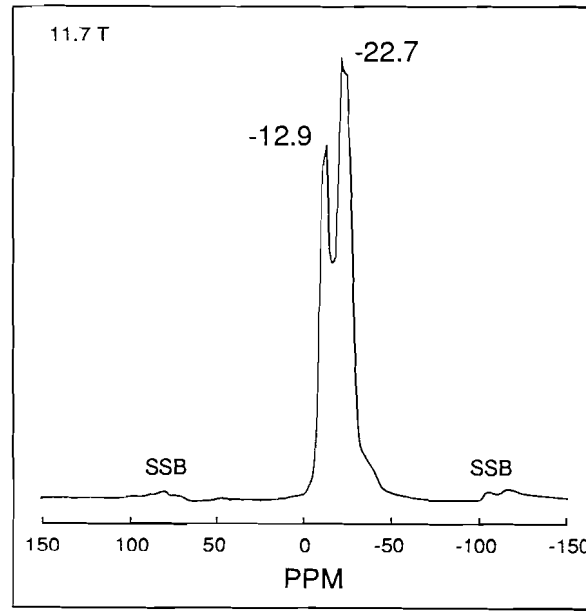


**Figure 1.** *$^{23}Na$ MAS NMR spectrum of chiolite. SSB=spinning sideband.*

try parameter of 0 (Kentgens et al., 1983). The high intensity of the right singularity points to an additional site with a small intensity overlapping the other site. The data in table 2 are from J.F. Stebbins and X. Xue (written communication), who collected spectra at 9.4 T. The lower magnetic field allows a more accurate estimation of the NMR data. We used these data to simulate our spectra and became very good results. In case of cryolite (figure 2), our variable field data are combined with the computer simulation data of Stebbins and Xue in order to compare the two approaches. Within the errors of estimates, the data correspond well. The lack of structure on the 4 ppm peak, even in the 9.4 T spectra, is responsible for the spread of $\eta$. Starting point for the analysis of the $^{27}$Al spectra of chiolite (figure 3) was the assumption that the outermost signals correspond to a site with $\eta = 0$, while the signal in the middle corresponds to a site with $\eta = 1$. Calculating QCC and $\delta_{iso}$ at the three magnetic fields resulted in three sets of data which are mutually consistent. This data set was then refined in a computer simulation. The shoulder at the low field side of the spectrum is the result of a background signal from the probe, for which we did not correct. Linewidths (Full Width at Half Height) are 1000-1500 Hz for $^{27}$Al and 400-700 Hz for $^{23}$Na. If the second order quadrupole broadening is substracted from these values and other contributions to the linewidth are ruled out, the broadening due to the coupling of Al and F and of Na and F becomes 600-1000 and 100-600, respectively.

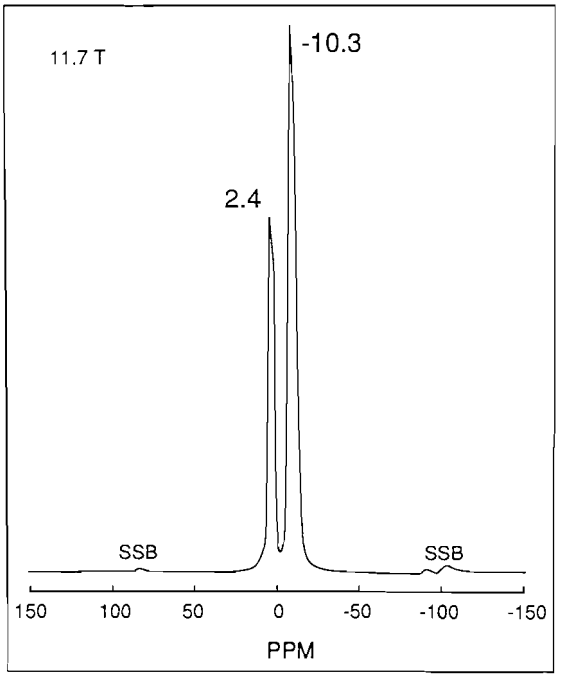


**Figure 2.** *$^{23}$Na MAS NMR spectrum of cryolite. SSB=spinning sideband.*

## 2.6 Discussion

### $^{27}$Al

The $^{27}$Al spectrum of **$\alpha$-$AlF_3$** displays one peak at -16 ppm at 11.7 T, which shifts to -15 ppm at 14.1 T, corresponding to a $\delta_{iso}$ of -13.2 ppm. The -16 ppm value has previously been reported by Kimura and Satoh (1989) and Satoh and Kimura (1990), who did not consider quadrupole induced shifts. Their -16 ppm value may indicate that the minor impurity in our $\alpha$-$AlF_3$ has no influence on the NMR results.

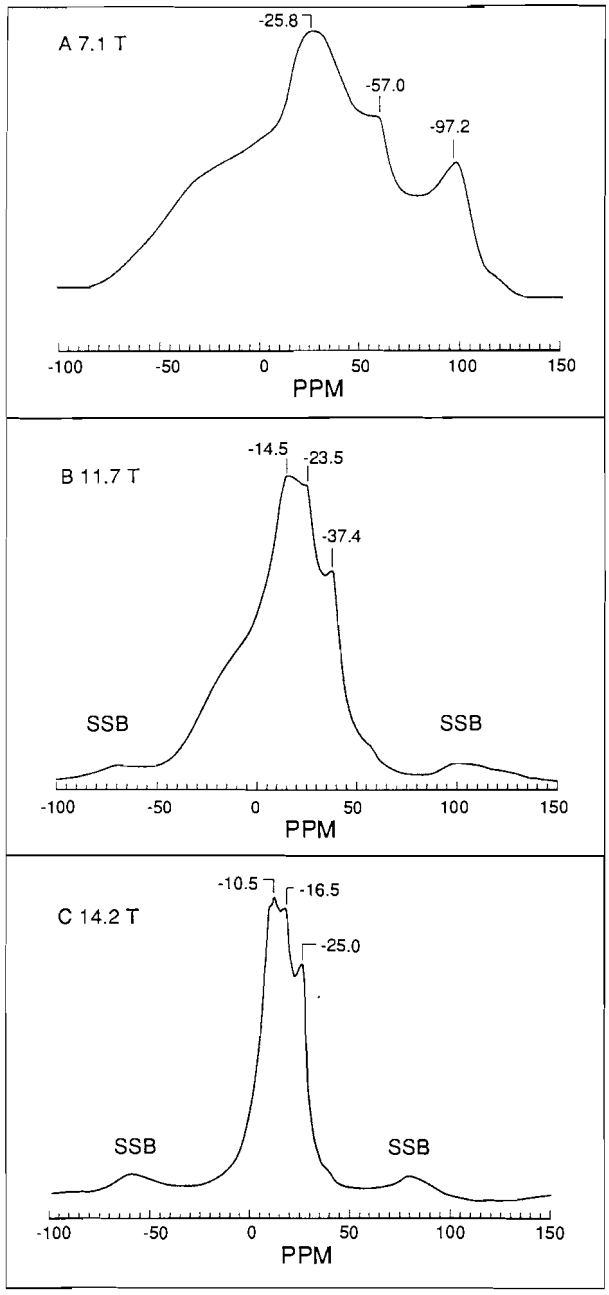


**Figure 3.** *$^{27}Al$ MAS NMR spectra of chiolite at different magnetic fields. Spinning speeds are (A) 13.9, (B) 9, and (C) 11 kHz, respectively. SSB = spinning sideband.*

**$\beta$-$AlF_3$** has an isotropic chemical shift of -12.5 ppm, with only one peak at both fields of 11.7 T and 14.1 T. According to the crystallography of $\beta$-$AlF_3$, the structure has two Alsites, which are almost identical. The differences between these two sites are too small to be detected as two separate NMR resonances.

$Na_5Al_3F_{14}$ has $^{27}Al$ chemical shifts of -1 ± 2 ppm and -3 ± 2 ppm. This is in agreement with the two different octahedral Al-sites in chiolite, known from structure determinations. Crystallographic data show, that the $S^4$-site occupies 33 % of all the Al and should have the lowest intensity in the $^{27}Al$ spectra. The Al-site with a chemical shift of -3 ppm, QCC = 6.5 ± 0.5 MHz and $\eta$ = 1 can be assigned to the $S^4$-site, the $S^2$-site must then be represented by the -1 ppm signal with QCC = 8.2 ± 0.5 MHz and $\eta$ = 0.

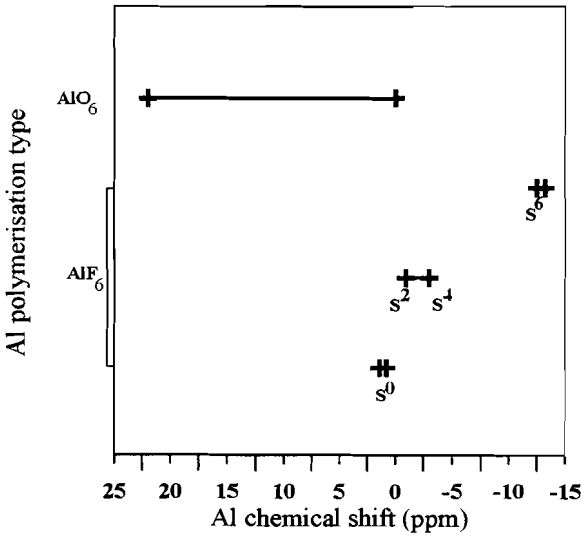


**Figure 4.** *Graphical representation of the $^{27}Al$ chemical shifts of $AlX_6$ octahedra in oxoaluminates and fluoroaluminates.*

The isolated $AlF_6$ octahedra in cryolite (**$Na_3AlF_6$**) have an $^{27}Al$ isotropic chemical shift of 1.4 ppm. Previously, Müller and Bentrup (1989) reported $^{27}Al$ chemical shifts of -0.6 and -0.1 ppm in similar compounds, $(NH_4)_3AlF_6$ and $K_3AlF_6$, respectively. The cubic elpasolite (**$K_2NaAlF_6$**) structure is strongly related to the (pseudocubic) monoclinic cryolite structure. Two of three Na atoms are replaced by K atoms. Like cryolite, the $^{27}Al$ NMR isotropic chemical shift is ± 1 ppm. The spread in peak positions of these four hexafluoroaluminates is only 2 ppm. This observation leads us to the conclusion, that second sphere influences of Na, K, or $NH_4$ on the shielding of Al by F are of very small importance in alkalifluoroaluminates. The cation effects are even smaller than the 6.4 ppm range for interconnected $AlO_4$ tetrahedra in K-, Li-, and Na- aluminates (Müller et al., 1986). The Al nucleus is more effectively shielded from its surroundings and less sensitive to second sphere substitutions, due to the more ionic character of the Al-F bond.

Figure 4 displays a graphical presentation of the isotropic chemical shifts of Al in alkalifluoroaluminates. The $^{27}Al$ chemical shifts decrease from 1 ppm in $S^0$- to -1 in $S^2$-, -3 in $S^4$- and -13 to -15 in $S^6$-structures. It follows, that $^{27}Al$ chemical shifts decrease as the degree of polymerisation increases, analogous to $^{29}Si$ results in aluminosilicates (Engelhardt and Michel, 1987). The number of non-bridging fluorines per octahedron (NBF/O, equal to 6-n) decreases from 6 in $S^0$ to 4 in $S^2$, 2 in $S^4$ and 0 in $S^6$-structures. Non-bridging fluorines control the residual charge on the Al-nucleus and thereby its shielding. The observed trend in the $^{27}Al$ chemical shift can be explained by a decrease in NBF/O with polymerisation.

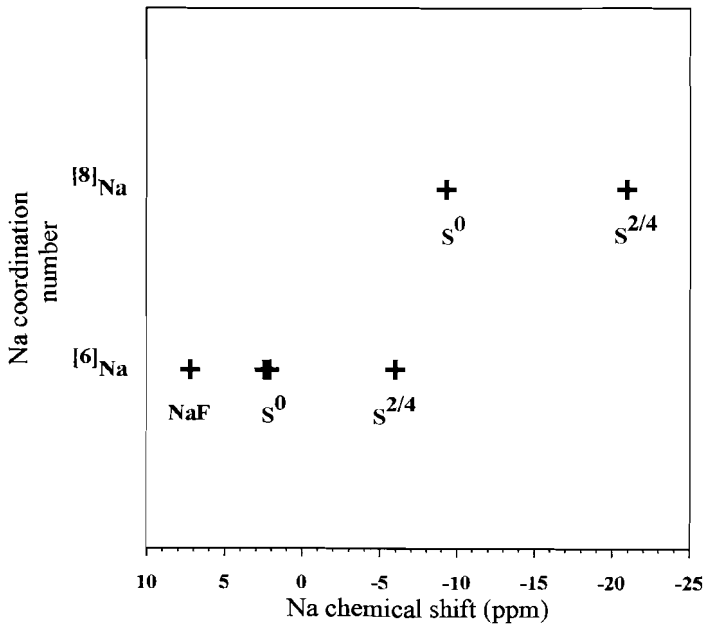


**Figure 5.** *Graphical representation of the $^{23}Na$ chemical shift of sixfold and eightfold-coordinated Na in alkalifluoroaluminates.*

## $^{23}Na$

$^{23}Na$ NMR data can add important information in elucidating polymerisation effects of $AlF_6$ octahedra in alkali fluoro-aluminates. It is possible to assign specific resonances of Na to crystallographic sites. In the case of NaF, the 7.2 ppm peak obviously results from a very regular octahedral coordination of Na by 6 fluorine atoms.

Based on crystallography, the cryolite-structure contains twice as much 8- as 6-coordinated Na. As a result, the $^{23}Na$ resonance with the lowest intensity should be assigned to 6 coordinated Na (figure 2). Therefore, the 2.4 ppm peak represents 6 coordinated Na and the -9.3 ppm peak represents 8-coordinated Na. This is in accordance with the general observation, that more shielded nuclei with more ligands resonate at higher fields (Engelhardt and Michel, 1987). Moreover, 6 coordinated Na in NaF resonates at 7.2 ppm, which is reasonably close to the 2.4 ppm in cryolite. Compared with cryolite, two 8 coordinated Na sites are occupied by K in elpasolite. The remaining octahedrally coordinated Na atom resonates at 2.1 ppm, very close to the 2.4 ppm in cryolite, which is another argument for assigning the 2.4 ppm peak to the 6-coordinated site.

In chiolite, the 6-coordinated Na has a chemical shift of -6 ppm. Again, the 8 coordinated Na atoms are more shielded and have a peak position of -21 ppm. Clearly, $^{23}Na$ NMR is sensitive to the coordination number, just as $^{29}Si$ and $^{27}Al$ NMR. Previously, Phillips et al (1988) observed a much more continuous change in chemical shift with a change in Na/(Na+K) ratio in an alkali feldspar solid solution. The continuous change in the Na/(Na+K) ratio causes the effective Na coordination number to increase, causing a continuous decrease in chemical shift. As for Al, the graphical representation of the $^{23}Na$ chemical shifts (figure 5) evidently shows, that the chemical shifts of 6- and 8 coordinated Na are determined by the number of $AlF_6$ octahedra per Na atom in the structure. In NaF, with a chemical shift of 7.2 ppm, no $AlF_6$ octahedra are present. The chemical shift of $^{23}Na$ decreases to 2.4 ppm in cryolite (0.3 $AlF_6$ octahedron on 1 Na) and -6 ppm in chiolite (0.6 $AlF_6$

octahedron on 1 Na). In the case of 8-coordinated Na, the trend is from -9.3 ppm in cryolite to -21 ppm in chiolite.

The fact, that both $^{27}Al$ and $^{23}Na$ chemical shifts correlate with the degree of polymerisation of the $AlF_6$ octahedra points to a complex interaction of Al-F polymerisation and Na-F bonds.

**Comparison $^{27}AlF_6$ - $^{27}AlO_6$**

Isotropic $^{27}Al$ chemical shift data of octahedrally coordinated Al in compounds other than silicates are available only for the $Al_2O_3$-polymorph corundum (16.0 ppm, Skibsted et al, 1991) and Yttrium Aluminum Garnet (0.8 ppm, Massiot et al, 1990). Peak positions in oxialuminates other than of sodium have been reported by Müller et al (1981) and de Jong et al. (1983) and range from 5 ppm for $BaO{\cdot}6Al_2O_3$ to 22 ppm for spinel, $MgAl_2O_4$. Comparing Al-O compounds to Al-F compounds, $^{27}Al$ isotropic chemical shifts of oxialuminates are at least 20 ppm less shielded than $^{27}Al$ chemical shifts of fluoroaluminates. The 3-dimensional network structures $Al_2O_3$ and $AlF_3$ have chemical shifts of 16 and -13 ppm, resp. It is interesing to compare the mean bond lengths of $^{[6]}Al$-O and $^{[6]}Al$-F. $^{[6]}Al$-O interatomic distances are approximately 0.07 Å longer than for $^{[6]}Al$-F (Shannon and Prewitt, 1969). This might be a reason why there is a difference in chemical shielding for the two types of ligands.

## 2.7 Conclusions

1. Isotropic $^{27}Al$ chemical shifts systematically decrease with the increase in the degree of polymerisation of $AlF_6$ octahedra in sodium fluoroaluminates. This trend can be explained by considering the number of bridging fluorines per octahedron (NBF/O).

2. Na coordinated by 8 fluorines has more negative isotropic chemical shifts than Na coordinated by 6 fluorines.

3. Isotropic $^{23}Na$ chemical shifts of 6- and 8-coordinated Na become more shielded as the $AlF_6$ polymerisation increases.

4. Al nuclei in $AlF_6$ octahedra are at least 20 ppm more shielded than Al nuclei octahedrally coordinated by O.

5. Second coordination sphere effects of alkali cationic substitution on $^{23}Na$ and $^{27}Al$ NMR are of very small influence.

*Slechts dwazen kennen*
*twijfel noch onzekerheid*

Montaigne

# Chapter 3

## Solid State $^{27}$Al MAS NMR Study of Pentameric Aluminosilicate Groups with 180° Intertetrahedral Al-O-Si Angles in Zunyite and Harkerite

### 3.1 Abstract

The minerals zunyite ($Al_{13}Si_5O_{20}(OH,F)_{18}Cl$) and harkerite ($Ca_{24}Mg_8[Al-Si_4(O,OH)_{16}]_2(CO_3)_8(BO_3)_8(H_2O,Cl)$ have been studied by solid state $^{27}$Al MAS NMR. These minerals contain $Si_5O_{16}$ (Zunyite) and $AlSi_4(O,OH)_{16}$ (Harkerite) pentamers. These pentameric groups are unique because their T-O-Si angles are (almost) 180°. Chemical analysis of the zunyite sample shows, that it has excess Al in its lattice: the Al/Si ratio is 2.9, compared to the ideal of 2.6.

High speed spinning (11-13kHz) $^{27}$Al MAS NMR spectra show two additional signals as compared to the spectra obtained by Kunwar et al. (1984). The signal with $\delta_{iso}$= 46.8 ppm represents the excess Al which enters the central Si(1) site of the $Si_5O_{16}$ pentamer. This assumption is confirmed by the fact, that $\delta_{iso}$ of Al in the $AlSi_4(O,OH)_{16}$ pentamer in harkerite is 44 ppm. Additional proof comes from comparing the electrostatic energy and the quadrupole interaction of Al in either a Si(1) or Si(2) configuration.

The Al site in the pentamers of zunyite and harkerite can be considered as a $q^4$(4Si) site. In this case Al-O-Si angles are correlated with the $^{27}$Al chemical shift (Lippmaa et al., 1986). This correlation holds well for the $^{27}$Al data of harkerite. The value for zunyite indicates, that the structure adapts to the incorporation of Al in the Si(1) site by narrowing of the Al-O-Si angle to 171°. The lower limit of the chemical shift range for Al in framework aluminosilicates is decreased by 12 ppm from 55.8 ppm for mordenite to 44 ppm for harkerite.

### 3.2 Introduction

The mineral zunyite, $Al_{13}Si_5O_{20}(OH,F)_{18}Cl$, (Pauling et al., 1933; Kamb, 1960; Louisnathan and Gibbs, 1973; Baur and Ohta, 1982) contains two rare crystallographic units. The first is a pentameric $Si_5O_{16}$ group and the second a tridecameric $Al_{13}$ group. The $Si_5O_{16}$ group is special because its Si-O-Si intertetrahedral angles are 180°. The $Si_5O_{16}$ group is very similar to the $AlSi_4(O,OH)_{16}$ group in the mineral harkerite, $Ca_{24}Mg_8[Al-Si_4(O,OH)_{16}]_2(CO_3)_8(BO_3)_8(H_2O,Cl)$(Tilley, 1951; Guiseppetti et al., 1977). The pentamer in harkerite has Al-O-Si intertetrahedral angles of 176°.

The $Al_{13}$ group occurs in nature only in zunyite. Similar to it are $Al_{13}$ groups in synthetic $Al_{13}$ salts (Johansson, 1960). The $Al_{13}$ complex as it occurs in solution can be used for the pillaring of clay minerals, making them useful catalysts (Plee et al., 1985; Kloprogge, 1992).

Magic Angle Spinning Nuclear Magnetic Resonance (MAS-NMR) spectroscopy is an important technique to determine the coordination state and local symmetry of structural units such as $(Si,Al)O_4$, $AlO_5$ or $AlO_6$ polyhedra within crystalline and amorphous solids. In general, increased shielding of a nucleus by its ligands and an increase in coordination number results in an upfield chemical shift. In the case of Al, chemical shifts for 4-, 5- and

6-coordination fall into the range 50-80, 35-40 and -10-+15, respectively (Müller et al, 1981; Kirkpatrick, 1988; Smith, 1993). The same effect has been shown for Si (Stebbins, 1989, 1991b) and Na (Phillips et al., 1988; Dirken et al., 1992; Xue and Stebbins, 1993). On top of determining the coordination state, NMR is also sensitive to polymerization effects, next nearest neighbours effects and bond lengths/angles.

It is well known, that the Al-O-Si angle is correlated with the $^{27}$Al chemical shift in framework aluminosilicate structures (Lippmaa et al., 1986). Until now, the maximum Al-O-Si angle used in this correlation was 153.7° for the mineral mordenite. This correlation is important in structural studies of glasses, because it can give an estimate of the size of rings building up aluminosilicate glasses (Oestrike et al., 1987; Dirken et al., submitted). It is also used in $^{27}$Al NMR studies of Si,Al ordering in leucite (Philips et al., 1989) and zeolites (Engelhardt and Michel, 1987) to assign signals in the NMR spectrum to sites in the lattice.

Previous $^{27}$Al NMR investigations on zunyite and $Al_{13}$ salts established the existence of a signal from fourfold and sixfold coordinated Al (Lampe et al., 1982; Kunwar et al. 1984). These NMR data, however, were collected using slow spinning conditions ($\approx$3 kHz), with overlapping resonances and spinning sidebands.

We present $^{27}$Al NMR data of the pentamer in harkerite and compare it to $^{27}$Al NMR data of a zunyite sample with excess Al. The use of fast MAS (11-13 kHz), in contrast to the slow-spinning conditions used by Kunwar et al. (1984), reveals two extra Al signals for zunyite, one of which is proven to be due to the excess Al which is incorporated into the Si pentamer. The Al chemical shift of this signal is used for assigning Al to the Si(1) or Si(2) site of zunyite.

Additionally, we try to extend the correlation mentioned above to 180° Al-O-Si angles. This is the widest possible angle in aluminosilicates, it might help refining models on atomic structure of minerals and glasses.

## 3.3 Experimental

### Samples

Chemical analyses of the samples were determined with a Jeol Jx-8600 Superprobe, using a 15 kV accelerating voltage and a 1 μm spot size. Secondary phases were examined with optical microscopy and with a Philips PW 1050/25 X-ray powder diffractometer using CuK$\alpha$ radiation.

Zunyite

The zunyite sample is from the type locality, Zuñi mine, San Juan county, Colorado, USA. Chemical analyses were consistent with previous analyses (Turco, 1962; Baur and Ohta, 1982). The Al/Si ratio is 2.9, compared to 2.6 for the ideal ratio. The sample contained several secondary phases, viz. rutile, galenite, pyrite, kaolinite and a ($PO_4$-$SO_4$) phase with varying $PO_4/SO_4$ ratios, some of which had a considerable amount of Ca, Sr, Ce and Th. This composition could correspond to a florencite, which has an alunite type structure (Burt,

1985). Important for the NMR experiments is the coordination of Al. In kaolinite and the alunite-type phases all Al is present in octahedral coordination.

Harkerite

The harkerite sample is from the type locality at Camas Malag on the isle of Skye, Scotland. Harkerite is identified by X-ray diffraction and optical microscopy. The mineralogical assemblage of this skarn locality has been described by Tilley (1951). Tilley reports monticellite ($CaMgSiO_4$), calcite ($CaCO_3$), and diopside ($CaMgSi_2O_6$) as the principal associates of harkerite. Calcite is formed as an alteration product of harkerite.

Our microprobe and X-ray diffraction analyses reveal the existence of additional kirschteinite ($CaFe^{2+}SiO_4$) , periclase (MgO) and serpentine ($Mg_3Si_2O_5(OH)_4$). Kirschteinite forms a solid solution series with monticellite.

Important with respect to the $^{27}Al$ NMR experiments is the Al content of these secondary phases. Monticellite, kirschteinite and serpentine contain 1 wt% $Al_2O_3$. Diopside contains 0.1 wt% $Al_2O_3$, considerably less than the value of 3.6 wt% given by Tilley (1951). Their wet analyses are believed to be less reliable, however, than our microprobe analyses.

Determining the exact stoichiometry of harkerite by means of microprobe analyses is difficult because boron is too light to be analysed. The relative contents of Al, Si, Ca, and Mg, however, are consistent with the analysis of Tilley (1951) and Barbieri (1977).

**NMR spectroscopy**

The solid state $^{27}Al$ NMR experiments were performed on Bruker CXP-300, AM-500 and AMX-600 spectrometers, operating at 78.2 MHz ($B_0$=7.1 T), 130.3 MHz ($B_0$=11.7 T) and 156.4 MHz ($B_0$=14.1 T), respectively. A home-built probehead with a Doty MAS assemblage was used.

As Al is a quadrupole nucleus, care has to be taken to assure relative saturation of the $^{27}Al$ resonances (Samoson and Lippmaa, 1983; Dec and Maciel, 1990; Alemany, 1993). Therefore, short pulse excitations (0.7 μs = $\pi/10$) were used, with 0.5 s relaxation delays and 100 kHz spectral widths. Per measurement 5000-20000 FID's were collected. The $^{27}Al$ chemical shifts are determined relative to an external standard of 1 M aqueous $AlCl_3$ solution. Processing of the FID was carried out without any filtering. The quadrupole interaction and the isotropic chemical shifts ($\delta_{iso}$) are determined by using the second order quadrupole induced shift of the center of gravity of the peak (Meadows et al., 1983; Engelhardt and Michel, 1987).

The $^{29}Si$ NMR spectrum of zunyite was collected on an AM-500 spectrometer using a 5 s relaxation delay, 50 kHz spectral width, a 5 μs pulse length ($\pi/2$) and a spinning speed of 3.7 kHz. 28000 FID's were collected, referenced to the -89.2 ppm resonance of a Zeolite-A standard. Integration of the intensities was carried out on a SUN microcomputer using NMRi software.

## 3.4 Crystallography

### Harkerite

Harkerite ($Ca_{24}Mg_8[AlSi_4(O,OH)_{16}]_2(CO_3)_8(BO_3)_8(H_2O,Cl)$) from a skarn deposit in Skye (Scotland) was described by Tilley (1951). It is structurally similar to Sakhaite ($2\{Ca_{24}Mg_8[(BO_3)_8(CO_3)_8(H_2O)\}$). The main difference between the two structures is the replacement of the aluminosilicate pentamer by 4 $BO_3$ in sakhaite (Davies and Machin, 1970; Machin and Davies, 1976). Harkerite crystallizes in the (pseudo-cubic) trigonal space group $R\bar{3}m$ with lattice parameters a = 18.131 Å, and $\alpha = 33.46°$ (Machin and Miehe, 1976; Guiseppetti et al., 1977). The crystal structure has an incomplete cubic close packing of O and Ca with Mg in octahedral sites, Si and Al in tetrahedral sites and B and C in triangular groups with O (figure 1a). The $[AlSi_4(O,OH)_{16}]$ pentamer is unique and only related to the $Si_5O_{16}$ pentamer in zunyite (Pauling, 1933; Baur and Ohta, 1982). In NMR terminology it can be summarized as four $Q^1$(1Al) Si atoms arranged around one $q^4$(4Si) Al atom with intertetrahedral angles of 176° (figure 1b).

Some discrepancies remain between the idealized and actual chemical composition, probably as a consequence of substitution of aluminosilicate, borate and carbonate, hydroxy or water groups (Barbieri et al. 1977).

### Zunyite

The crystal structure of zunyite ($Al_{13}Si_5O_{20}(OH,F)_{18}Cl$) was first described by Pauling (1933) and refined later by Kamb (1960), Turco (1962) and Baur and Ohta (1982). The last authors give an excellent systematic description of this complicated structure. It consists of two crystallographic units, a $Si_5O_{16}$ pentamer and a Keggin-molecule-type (Furrer et al., 1992) group with an $Al_{13}O_{16}(OH)_{24}$ stoichiomety (figure 2a). The $Si_5O_{16}$ cluster consists of a central $Q^4$(4Si) Si atom and four $Q^1$(1Si) Si atoms with Si-O-Si intertetrahedral angles of 180° (figure 2b). The $Si_5O_{16}$ pentamer is surrounded by $AlO_3(OH)_3$ octahedra from the $Al_{13}$ group. Twelve Al atoms are arranged in groups of each three $AlO_6$ octahedra around a central Al atom in fourfold coordination. The $Al_{13}$ group and the pentamer alternate in a 1:1 ratio, resulting in the $Al_{13}Si_5O_{20}(OH,F)_{18}Cl$ stoichiometry. F can substitute for the OH groups and Cl resides between 2 $Al_{13}$ groups or an $Al_{13}$ and a $Si_5O_{16}$ group.

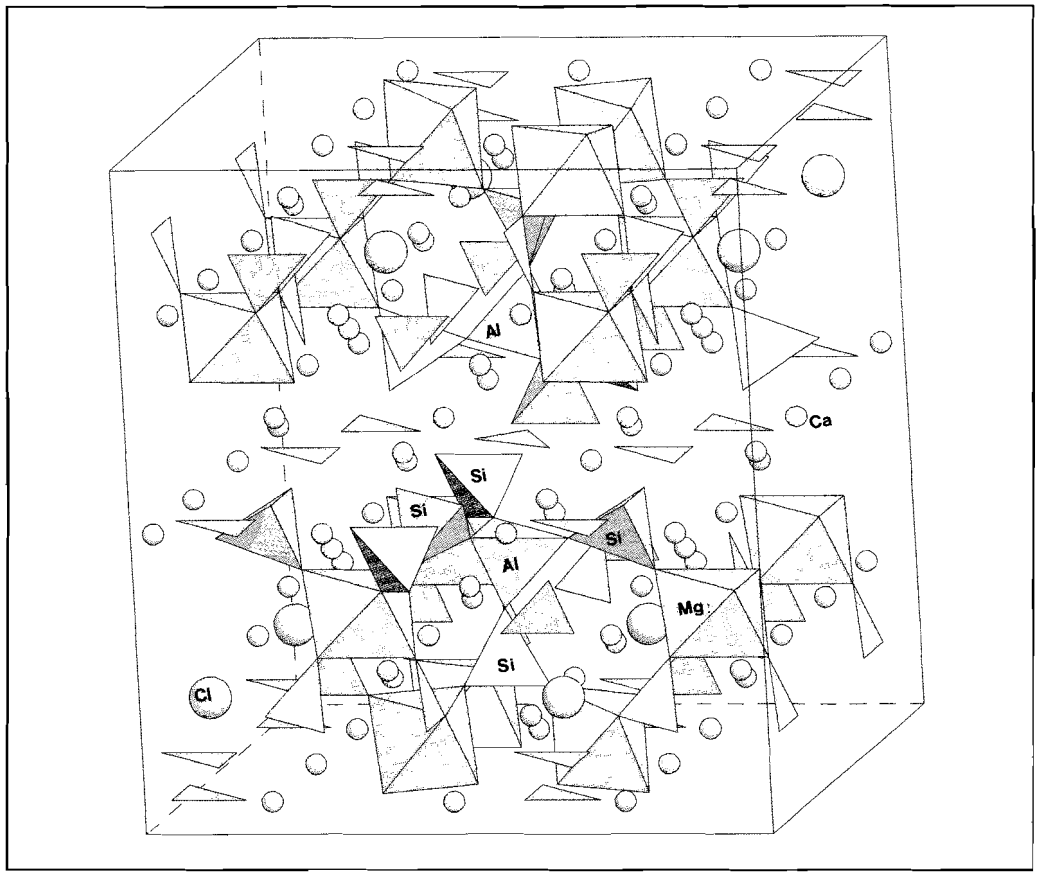


**Figure 1. a.** *The crystal structure of harkerite with the $AlSi_4O_{16}$ pentamer as indicated. The planar triangular groups are $CO_3$ or $BO_3$ groups.*

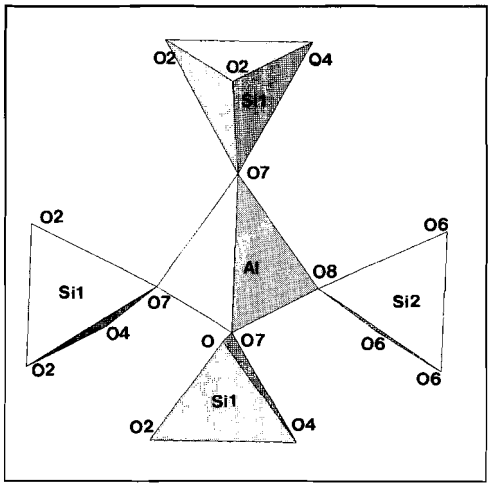


**Figure 1 b.** *The $AlSi_4O_{16}$ pentamer of harkerite.*

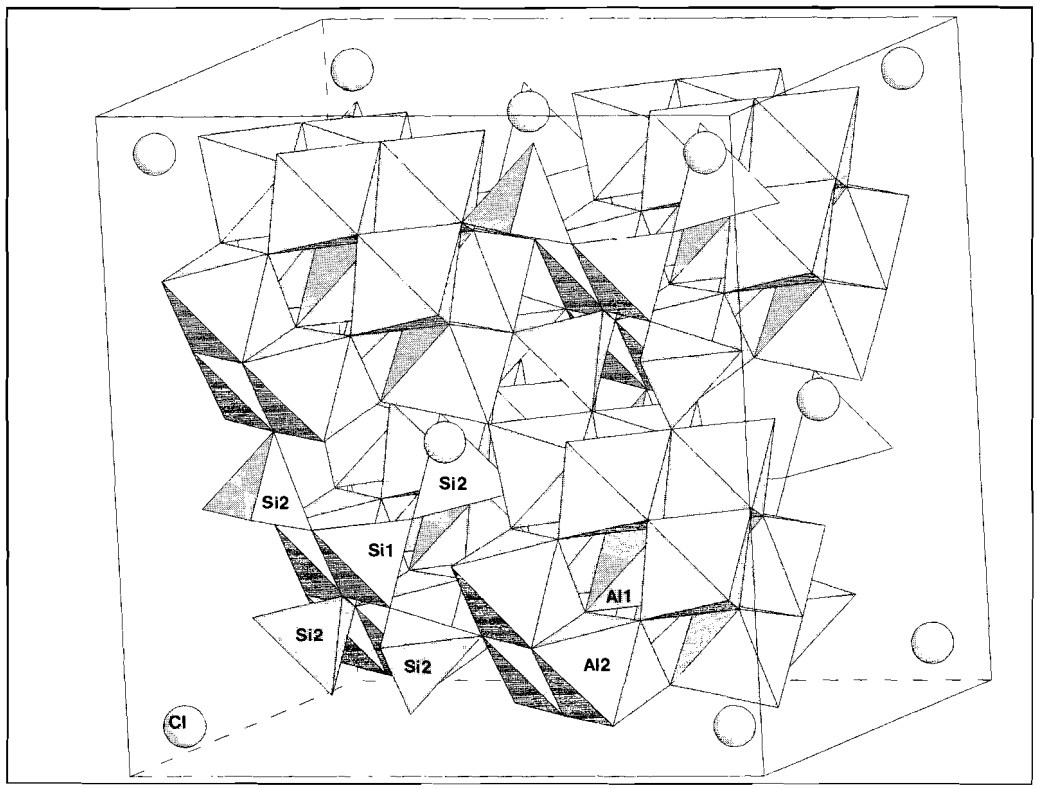


**Figure 2 a.** *The crystal structure of zunyite with the $Si_5O_{16}$ pentamer as indicated.*

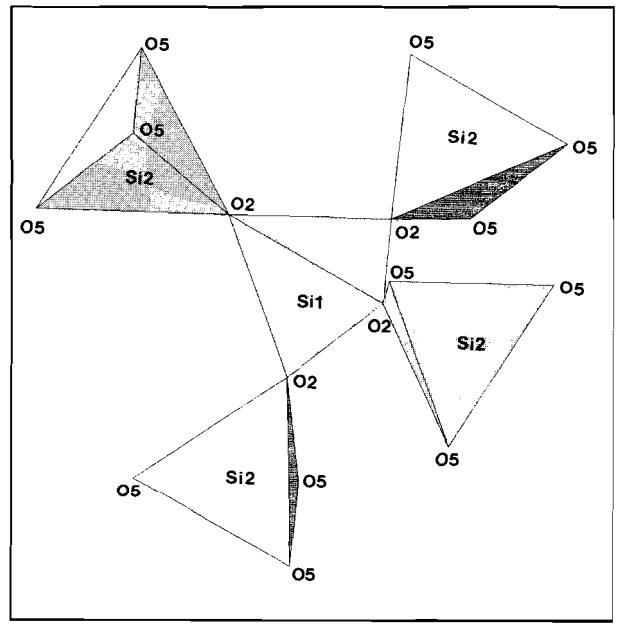


**Figure 2 b.** *The $Si_5O_{16}$ pentamer of zunyite.*

## 3.5 Results and discussion

### Harkerite

The $^{27}Al$ NMR spectrum of harkerite at a magnetic field $B_0$ of 11.7 T is shown in figure 3. It is dominated by a set of intense spinning sidebands. These sidebands belong to the peak at 44 ppm, as can be determined by varying the spinning speed. The strong intensities of the spinning sidebands is caused by the presence of $Fe^{3+}$ in the lattice. Magnetic coupling of unpaired electrons with Al causes line broadening and intensity of the center band to be lost into the sidebands (Watanabe et al., 1983; Murdoch et al., 1985). Indeed, Tilley (1951) reports a $Fe_2O_3$ content of 0.85 wt%. The peak position of the -1/2↔1/2 transition is not affected by the presence of Fe (Engelhardt and Michel, 1987).

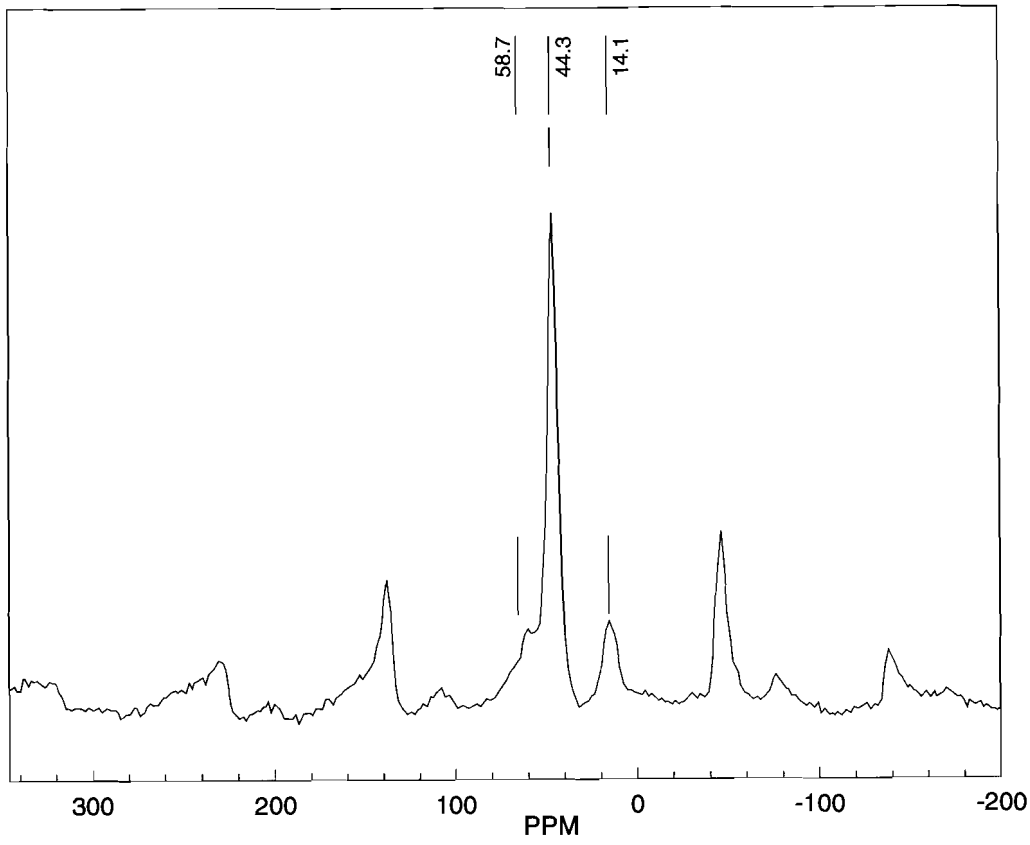


**Figure 3.** *$^{27}Al$ MAS NMR spectrum of harkerite at a magnetic field of 11.7 T.*

The peak position is 44.3 ppm at 11.7 T, 43.9 ppm at 7.1 T, and 43 ppm at 14 T. As the error in the peak position is about 1 ppm, the quadrupole interaction is very small (« 1 MHz), and the isotropic chemical shift is 44 ± 1 ppm.

The 44 ppm value falls outside the range generally accepted for $AlO_4$ (50-80 ppm) and $AlO_5$ (30-40 ppm) (Smith, 1993). It fits, however, well the correlation of the $^{27}Al$ chemical shift with the Al-O-Si angle in framework silicates (Lippmaa et al., 1986). These authors give the following equation for this correlation:

$$\delta_{iso}(Al) = (-0.50\ \theta + 132)\ ppm$$

with $\delta_{iso}(Al) = {}^{27}Al$ isotropic chemical shift;
$\theta$ = Al-O-Si intertetrahedral angle;

With $\theta = 176°$ (Guiseppetti et al., 1977) $\delta_{iso}$ becomes 44 ppm, which is exactly the experimental value (figure 4). Of course, the harkerite structure is not a framework structure in the

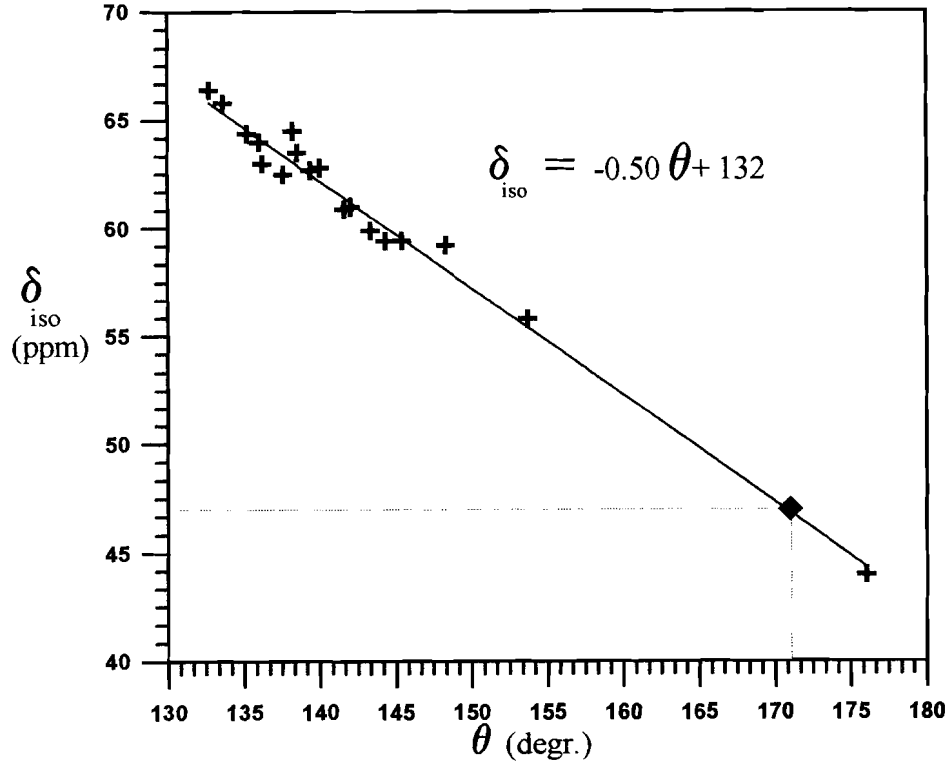


**Figure 4.** *Correlation between the isotropic chemical shift $\delta_{iso}$ and the Al-O-Si intertetrahedral angle $\theta$ for framework silicates. Crosses represent data from Lippmaa et al. (1986), and this study (harkerite at $\theta$ = 176°). The square represents zunyite.*

strict sense, since it is essentially a carbonate/borate mineral. However, from the point of view of the central Al atom it resembles a framework structure, because the $AlO_4$ group is surrounded by 4 $Si(O,OH)_4$ tetrahedra, i.e. it is a $q^4(4Si)$ Al atom (Engelhardt and Michel, 1987).

The peak at 58.7 ppm is due to Al in fourfold coordination in a secondary phase, most probably monticellite/ kirschteinite. The 14 ppm value arises from Al in sixfold coordination. This signal is ascribed to Al in serpentine. Because of the bad S/N ratio of the $^{29}Si$ spectrum and the severe linebroadening and overlap of peaks because of the Fe content of the various minerals, no attempt was made to analyse the Si spectrum.

**Zunyite**

Zunyite has been studied previously by $^{27}Al$ NMR by Kunwar et al. (1984). They report two signals in a 1:12 intensity ratio. These signals are also present in our spectra (figure 5). The 71.5 ppm signal represents Al from the central $AlO_4$ tetrahedron, the 7.8 ppm

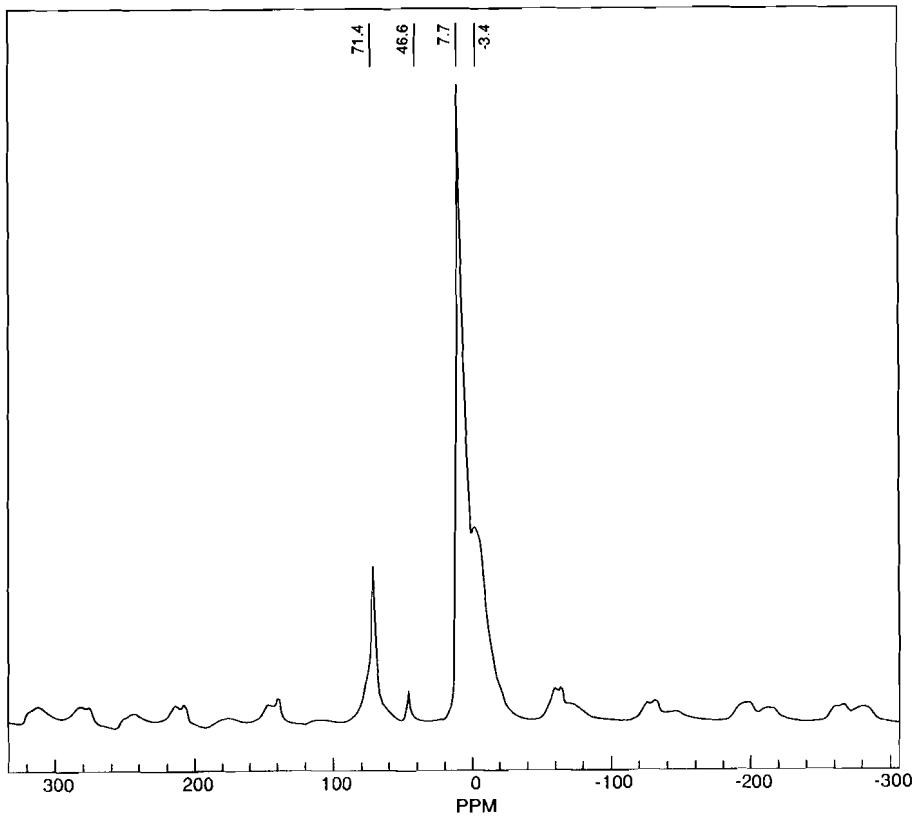


**Figure 5.** *$^{27}Al$ MAS NMR spectrum of zunyite at a magnetic field of 11.7 T*

signal with the highest intensity represents Al from the 12 $AlO_6$ octahedra around the $AlO_4$ group. The isotropic chemical shifts and quadrupole data, all determined by using the field dependent second order quadrupole induced shift are given in table 1 together with the data of Kunwar et al. (1984).

**Table 1.** *Data for $^{27}Al$ of zunyite*.*

| Site | $\delta_{iso}$ (ppm) | | QCC (MHz) | | $\eta$ | Q.B.** (Hz) | | FWHH*** (Hz) |
|---|---|---|---|---|---|---|---|---|
| | 1 | 2 | 1 | 2 | | 1 | 2 | |
| $^{[4]}Al$ ($Al_{13}$) | 72 | 71.6 | 0.6 | 0.8 | 0 | 20 | 30 | 520 |
| $^{[6]}Al$ ($Al_{13}$) | 8 | 8.9 | 2.2 | 2.2 | 0 | 280 | 280 | 900 |
| $^{[4]}Al$(penta) | -- | 46.8 | - | 0.5-1 | 0 | - | 30 | 250 |

*: 1:Data from Kunwar et al., 1984; 2:Data from this study;
**: Q.B.: Second order quadrupole broadening at $B_0$ = 11.7 T;
***: FWHH: Full width at half height at $B_0$ = 11.7 T.

In addition to these two signals, there are signals at 46.6 ppm and -2.4 ppm. Both resonances could in principle arise from the secondary phases present in the zunyite. However, the secondary phases all have Al in octahedral coordination with possible chemical shifts between -15 and +15 ppm. Only the -2.4 ppm resonance is therefore caused by these impurities. The 46.6 ppm is believed to be from the zunyite itself.

The 46.6 ppm peak ($B_0$ = 14.1 T) shifts to 46.1 and 46.3 ppm at magnetic fields of 7.1 and 11.7 T, respectively. This corresponds with an isotropic chemical shift of 46.8 ppm and a QCC of 0.5-1.0 MHz. It falls outside the range for octahedral Al, but is close to the value of 44 ppm for Al in the pentamer of harkerite. It seems plausible to assume, therefore, that the excess Al known from chemical analyses is incorporated into the $Si_5O_{16}$ pentamer.

Baur and Ohta (1982) concluded from the shortening of the O(2)-O(5) edge in the $Si(2)O_4$ tetrahedron and the increase in the O(5)-O(5) edge (figure 2b), that Al occupies the Si(1) site. Sherriff et al. (1991) do not give an unambiguous interpretation of their X-ray and $^{29}Si$ NMR study of zunyite. They state, that both the Si(1) and Si(2) site are potential recipients for the excess Al. Zagalskaya and Belov (1964) propose that the $Si_5O_{16}$ pentamer is in reality a $AlSi_4O_{16}$ pentamer and that Si partly occupies the fourfold coordinated Al site of the $Al_{13}$ group. Louisnathan and Gibbs (1972), however, consider this to be in error, since the Al-O(2) bond length (1.73-1.8 Å) is not compatible with the value derived from structure refinements (1.628 Å). This value however, is also not compatible with an occupation by Si alone.

Incorporation of more than one Al atom into the pentamer can be ruled out, since it would involve the formation of $Al^{[4]}$-O-$Al^{[4]}$ bridges. It is energetically more favourable to form two $Al^{[4]}$-O-Si bridges than one Si-O-Si and one $Al^{[4]}$-O-$Al^{[4]}$ bridge. This is called the Loewenstein rule (Loewenstein, 1954; Liebau, 1985).

In addition to the arguments proposed by Baur and Ohta (1982) there are a number of arguments that suggest, that Al is in a (central) Si(1) site.

First of all, incorporation of $Al^{3+}$ into the central $Si^{4+}$(1) site causes four O(2) bonds to be polarized, in contrast to only one O2 for incorporation into the $Si^{4+}$(2) site. If Al would enter the Si(2) site, an Al-O(5)-Al bond (last Al from an $Al_{13}$ group) is formed and polarization of the O(5 ) is lost. This polarization leads to an additional bonding energy, which favours an $Al(1)Si(2)_4O_{16}$ pentamer over an $Al(2)Si(1)Si(2)_3O_{16}$ pentamer. This effect has previously been used to explain the preference of various ions for crystallographic sites in the spinel structure (Blasse, 1964; Hill et al., 1979).

A second argument for positioning Al on the Si(1) site is the close resemblance in structure and NMR data between harkerite and zunyite. The Al in harkerite, which is in a coordination comparable to Al in a Si(1) site in zunyite, fits the correlation between the $^{27}Al$ chemical shift with the Al-O-Si angle for framework aluminosilicates (*vide supra*). The $^{27}Al$ isotropic chemical shift in the pentamer of zunyite differs only by 2.8 ppm from that of harkerite. The value of 46.8 ppm does not fit an Al-O-Si angle of 180°, however. The 46.8 ppm value for zunyite must correspond to an angle smaller than 176°, since this is the value for a known Al-O-Si angle in harkerite. In fact, 46.8 ppm corresponds to an Al-O-Si angle of 171.2° (figure 4). It must be noted, that this value is based on an extrapolation of the data of Lippmaa over 25° to one datapoint for harkerite. As a result, the error in the Al-O-Si angle for zunyite might be large (<5°).

A third argument for of Al in the Si(1) site comes from the quadrupole data. Nuclei with a spin I>1/2 are quadrupole nuclei. These nuclei have a non-spherical charge distribution. The quadrupole moment can interact with the electric field gradient at the nucleus (Cohen and Reif, 1957) and causes line-broadening and displacement of the peak from the isotropic value (Müller, 1982). The magnitude of the interaction is described by the quadrupole coupling constant (QCC) and the asymmetry parameter $\eta$. The quadrupole interaction can be determined in various ways (Smith, 1993).

The quadrupole interaction can be used to give an estimate of the distortion of the first coordination sphere of an atom in a particular site. The larger the quadrupole coupling constant (QCC), the higher the distortion of the site. Ghose and Tsang (1973) relate the $^{27}Al$ QCC of fourfold coordinated Al to the so called shear strain $\Psi$ in crystalline aluminosilicates. The shear strain is a measure of the departure of the individual bond angles from the ideal value of 109.47°. It is defined for Al in fourfold coordination as

$$\Psi = \sum_i \left|\tan(\theta_i - 109.47°)\right|$$

Here $\theta_i$ are the individual O-Al-O angles of the actual tetrahedron.

Since the crystal structure of zunyite is known, the shear strain of Al in a Si(1) site and Al in a Si(2) site and the corresponding QCC can be calculated and compared to the experimental value. The oxygen shell around Si(1) is arranged as a regular tetrahedron, with all Si-O-Si angles equal to 109.47°. This leads to a $\Psi$ value of 0. Theoretically, the QCC would therefore have to be 0. The *empirical* correlation of Ghose and Tsang, reports for a site with $\Psi$=0, a QCC of 1 MHz., very close to our experimental value of 0.5-1 MHz. This is a very small value for Al in aluminosilicates. Freude and Haase (1993) recently reviewed

quadrupole effects in solid state NMR and report the QCC values of Al in a wide variety of aluminosilicate phases. The only phases with Al QCC values comparable to our value for zunyite are a number of sodalites (QCC = 590-890 kHz). This is an indication, that indeed Al is located in a site with a very high symmetry.

If we calculate the shear strain value for Al in a Si(2) configuration, the shear strain $\Psi$ becomes 0.102. If we apply the empirical correlation of Ghose and Tsang to this $\Psi$ value, the QCC is calculated to be 2 MHz. The error in the correlation is rather large (approxemately ± 1MHz), but it is apparent, that in the case of Al in a Si(2) configuration, the QCC would be larger than the value for Al in a Si(1) configuration.

This assumption is strengthened by the use of a point charge model used to calculate the E.F.G. at the Al nucleus (Koller et al., 1994; chapter 4 of this thesis). The calculation model is a model in which each ion is considered as a point charge, with an effective charge (taken to be -1 for O, as is found in many theoretical studies of aluminosilicates (van Genechten et al., 1988), and +1 for the alkali ion). This models predicts a QCC of 0 MHz for Al in a Si(1) configuration and 0.5 MHz for a site in a Si(2) configuration. In this model an equal effective charge is presumed for all four oxygen atoms around. This holds well if Al is in the Si(1) site, but because of polarisation effects (*vide supra*), this will not hold for Al in the Si(2) site. As a result, the electric field gradient is larger than it would be if purely geometric considerations were taken into account. Therefore the calculated QCC for Al in a Si(2) environment may well be larger than 0.5 MHz.

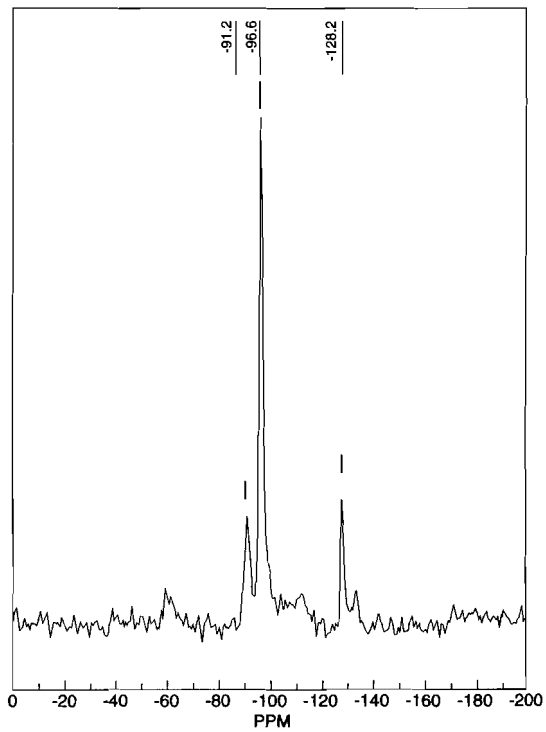


**Figure 6.** *$^{29}$Si MAS NMR spectrum of zunyite.*

Although both models cannot be used to accurately predict the electric field gradient, the general trend is, that Al in a Si(2) site has a larger QCC than that in a Si(1) site. As the experimental QCC is very small, this is an additional indication that the excess Al in the zunyite structure occupies the Si(1) site. Our Si spectrum (figure 6) is comparable to those previously reported (Grimmer et al., 1983; Sherriff et al., 1991).

The -95.6 ppm peak is from Si in a $Q^1$(1Si) configuration with Si-O-Si angles of 180°. The -128.2 ppm peak is from Si in a $Q^4$(4Si) configuration also with Si-O-Si angles of 180°. The relative intensities of the $Q^1$(1Si) and $Q^4$(4Si) have been determined by integration of the peak areas and are 1:4, as expected from the stoichiometry of the pentamer. Both chemical shifts are extremely

shifted as a result of the 180° intertetrahedral angles. This effect is well known and described for $^{29}Si$ by Smith and Blackwell (1983). It is equivalent with the dependence of the $^{27}Al$ chemical shift on the Al-O-Si angles (Lippmaa et al., 1986).

The -91.2 ppm peak is reported in all Si spectra zunyite. It is assumed by Grimmer et al. (1983) and Sherriff et al. (1991) to arise from nacrite which is present as a secondary phase. We report kaolinite as a secondary phase, which is closely related to nacrite.

It must be noted, however, that the value of -91.2 ppm is the value that is to be expected for a Si atom in a $Q_1(1Al)$ site with Si-O-Al angles of 180°. This site is formed by incorporating Al into the Si(1) site. It is well known, that per Si atom in the next nearest neighbour shell that is substituted for Al a downfield shift of 5 ppm is observed for the Si chemical shift of the central atom (Kirkpatrick, 1988). In this case, $Q_1(Al)$ should be located 5 ppm downfield from -95.6 ppm, i.e. -90.6, within analytical accuracy equal to -91.2 ppm.

Computer integration of the peak areas shows that the intensity of the -91.2 ppm is about the same as that of the $Q_4$ signal at -128.2 ppm. From these intensities we can calculte the amount of kaolinite present in the sample, assuming all of the intensity of the -91.2 ppm. If nacrite is responsible for this signal, that would mean that 11 wt% kaolinite is present in the zunyite sample. From X-ray diffraction and optical microscopy, a 5-10 wt% kaolinite content can be deduced. It is apparent, that kaolinite is responsible for most of the intensity at -91.2 ppm. However, it cannot be ruled out, that part of the intensity (up to 50%) is due to the Si in a $Q_1(1Al)$ in the zunyite sample itself. The samples that have been measured previously by NMR (*vide supra*) all come from the Zuni mine, and therefore all have excess Al in the lattice. The -91 ppm signal in these studies could, therefore well be due to Si in a $Q_1(1Al)$ site in the zunyite.

This ambiguity can only be solved by obtaining $^{27}Al$ and $^{29}Si$ NMR spectra of a (synthetic or natural) zunyite which has no excess Al. Baur and Ohta (1982) report a structure refinement of such a zunyite from Quartzsite, Arizona.

### 3.6 Conclusions

Until now, $q^4(4Si)$ sites and their $^{27}Al$ NMR chemical shifts were reported from mordenite ($\delta_{iso}$ = 55.8 ppm, Al-O-Si = 153.7°) to scolecite ($\delta_{iso}$ = 66.4 ppm; Al-O-Si = 132.7°). From this study it is apparent, that this range can be extended to 44 ± 1 ppm for Al sites in framework aluminosilicate structures with Al-O-Si angles of 176°.

Excess Al in the zunyite structure occupies the central Si(1) site of the $Si_5O_{16}$ pentamer. Prove for this comes from a comparison of the data of zunyite with harkerite, and by studying the quadrupole interaction and expected electrostatic energies of a $Al(1)Si(2)_4O_{16}$ pentamer compared to a $Al(2)Si(1)Si(2)_3O_{16}$ pentamer.

The zunyite structure adapts to the presence of excess Al by narrowing the Al-O-Si angle from 180° to 171°.

*Armoede aan aardse goederen is gemakkelijk te verhelpen; armoede van de geest is ongeneeslijk*

Montaigne

# Chapter 4

## Off-resonance Nutation NMR Study of Framework Aluminosilicate Glasses with Li, Na, K, Rb or Cs as charge balancing Cation

### 4.1 Abstract

Framework aluminosilicate glasses with varying charge-balancing cation (Li, Na, K, Rb, and Cs) have been studied with $^{27}Al$ and $^{29}Si$ MAS NMR and $^{27}Al$ on-resonance and off-resonance nutation NMR spectroscopy. The first application of off-resonance nutation NMR proves that it is a very powerful technique for the determination of quadrupole interactions in glasses. Line widths for Al and Si decrease systematically with increasing size of the cation. In case of Al this decrease is due to a decrease of the quadrupole interaction from 5.0 ± 0.1 MHz for the Li-glass to 2.8 ± 0.1 MHz for the Cs glass. A simple point charge model effectively predicts the decrease in the quadrupole interaction. This indicates, that the alkali ion is located close to aluminum. The Al and Si chemical shift dispersion do not change significantly with the type of alkali ion. The data are consistent with a change in the number of tetrahedra per ring. The larger the cation, the larger the number of tetrahedra per ring.

### 4.2 Introduction

A better knowledge of the atomic structure of aluminosilicate melts is essential to the understanding of the relationship between their microscopic and macroscopic properties. The importance of the topic is made clear by the fact, that viscosity, atomic diffusion, and thermodynamic properties are temperature and composition dependent (Perchuk and Kushiro, 1991). Diffraction and vibrational studies and recent solid state NMR studies on both melts and their supposed low temperature equivalents have shown that aluminosilicate melts consist of $(Si,Al)O_4$ tetrahedra (Taylor and Brown, 1979a, b;Eckert, 1992). These tetrahedra are connected via bridging oxygens, the relative number of which is an indication of the degree of polymerization. The larger the number of bridging oxygens per tetrahedron, the higher the degree of polymerization (Mysen, 1988; de Jong, 1983, 1987; Kirkpatrick, 1988). It is now believed, that silicate glasses consist of rings of tetrahedra and that the number of tetrahedra per ring and the inter-tetrahedral angles are subject to large variations. Especially Raman spectroscopy was very useful in determining the amount of each type of structural $(Si,AlO_4)_n$ species present in the melt (Mysen, 1990).

However, it was not until the rise of high resolution solid state NMR and especially MAS NMR, that coordination changes of Al and Si in glasses could be shown. NMR at ambient and high temperatures (Farnan and Stebbins, 1990; Stebbins, 1991a; Coté et al., 1992) is very sensitive to the number of ligands and the way in which they are arranged around the central ion (Müller et al., 1981, 1986; Phillips et al., 1988; Dirken et al., 1992).

Five- and sixfold coordinated Al has been observed in $SiO_2$-$Al_2O_3$ glasses with excess $Al_2O_3$ (Risbud et al., 1988; Sato et al., 1991), and fluorine containing jadeite glasses (Kohn

et al., 1991). Five-coordinated Si has been reported (Stebbins, 1987, 1991b). A wealth of information exists linking $^{27}Al$ and $^{29}Si$ chemical shifts with structural species in silicates (Smith et al., 1983; Lippmaa et al., 1980).

Very little attention has been paid, however, to the network modifying cations in aluminosilicates. Line width effects of $^{29}Si$ in Na, K and Ca containing silica and aluminosilicate glasses have been studied (Murdoch et al., 1985). There is an increase in the chemical shift dispersion with increasing cationic size. The $^{23}Na$ chemical shift in framework aluminosilicate glasses becomes less shielded with decreasing Na/(Na + K) ratio, a trend which is opposite to that in the crystalline phases (Oestrike et al., 1987). Due to the small chemical shift range, possible correlations between the $^{23}Na$ chemical shift and structure are difficult to trace until a good reference system is developed.

Another approach to obtain information on the influence of the alkali cation on the structure of aluminosilicate melts is to replace Na by other alkali ions. Variations in the properties of the network forming cations can be related to intrinsic properties of the alkali ions.

In this study we present a $^{27}Al$, and $^{29}Si$ study of Li, Na, K, Rb and Cs-charge balanced aluminosilicate glasses. Besides chemical shift data, line width effects and quadrupole parameters (in case of Al) are studied. The $^{27}Al$ quadrupole interaction is determined with two-dimensional off-resonance nutation NMR (Kentgens, 1993) and the field dependent 2$^{nd}$ order quadrupole shift at 7.1, and 11.7 T. The glass composition of $MAlSi_{5.3}O_{12.6}$ (M = Li, Na, K, Rb, Cs) is that of the haplogranitic eutectic at 1 kbar (Manning, 1981).

## 4.3 Experimental

### Materials

The glasses are synthesized from gels (Hamilton and Henderson, 1968) which were melted at 1550 °C for 3 hours in a Pt crucible and rapidly quenched by putting the bottom of the crucible in silicon oil. All glasses were checked for crystalline phases and phase separation by X-ray powder-diffraction (XRD) and Transmission Electron Microscopy (TEM). X-ray diffraction was carried out on a Philips PW 1050/25 diffractometer using CuK$\alpha$ radiation and the TEM analyses on a Philips CM 20 using an accelerating voltage of 200 kV. Both methods showed the glasses to be homogeneous, without phase separation and crystalline phases down to a scale of less than 10 Å.

### $^{27}Al$ NMR Spectroscopy

The solid state $^{27}Al$ NMR experiments were performed on Bruker CXP-300, and AM-500 spectrometers operating at 78.1 MHz ($B_0$=7.1 T), and 130.3 MHz ($B_0$=11.7 T), respectively. The spectra were obtained using a home-built probe equipped with a high-speed Doty MAS assembly, spinning at 12-13 kHz. As Al is a quadrupole nucleus, care has to be taken to assure relative saturation of the $^{27}Al$ resonances (Massiot et al., 1990; Samoson and Lippmaa, 1983a, b). Therefore, short pulse excitations (0.7 $\mu$s = $\pi$/10) were used, with 0.5

s relaxation delays and 100 kHz spectral widths. Per measurement 500-1000 FID's were collected. The $^{27}Al$ chemical shifts are determined relative to an external standard of 1 M aqueous $AlCl_3$ solution. Processing of the FID was carried out without any filtering.

The two-dimensional on- and off-resonance nutation experiments were carried out on the AM-500 spectrometer. The on-resonance spectra were recorded at an rf-field strength of 50 kHz, with a 1s recycle delay, 100 kHz $F_2$ spectral width, 256 $t_1$-increments of 2.0 μs, corresponding with an $F_1$ spectral width of 250 kHz. Per experiment 200 FIDs were collected. The off-resonance nutation spectra were recorded at an rf-field strength of 50 kHz, with a 1 s recycle delay, 256 $t_1$-increments of 1 μs, corresponding to an $F_1$ spectral width of 500 kHz. Per experiment, 250-350 FIDs were recorded. The on-resonance nutation spectra were recorded at a spinning speed of 2-3 kHz, slow enough not to affect the nutation spectra. The off-resonance spectra were recorded statically. FIDs were processed on a SUN microcomputer system, using NMRi software. The theoretical nutation spectra were calculated on IBM compatible PC 's (Kentgens et al., 1987; Kentgens, 1993).

### $^{29}Si$ NMR Spectroscopy

It is well known that $^{29}Si$ can have very long relaxation times $T_1$ (up to one day), especially in anhydrous glasses without any paramagnetic impurities (Kirkpatrick, 1988). A series of experiments with increasing relaxation delays was performed on the Na-containing glass to deduce the shortest possible relaxation delay which preserves all the information. Changes in the relative line intensities occurred up to recycle delay of 3 min. The $^{29}Si$ spectra were collected on an AM-500 spectrometer using a 180 s relaxation delay, a 6 μs pulse length ($\pi/2$) and a spinning speed of 4.5 kHz. 140 FID's were collected per measurement. The spectra are referenced relative to the -89.2 ppm resonance of a Zeolite-A standard and processed without filtering.

## 4.4 Results and discussion

### $^{27}Al$ MAS NMR spectroscopy

The $^{27}Al$ NMR spectra of Li, Na, K, Rb and Cs glass both at 7.1 T and 11.7 T magnetic field strengths show one broad peak at approximately 40-50 ppm (figure 1). This is consistent with the composition of the glasses, especially the molar M/Al ratio of 1 (M = Li, Na, K, Rb or Cs), which predicts, that all Al should be in 4-coordination in a 3-dimensional connected network with 4 Si nearest neighbours (Engelhardt and Michel, 1987). All the $^{27}Al$ resonances have a steep low field side and a more gradually decreasing high field side characteristic for the tetrahedral $^{27}Al$ resonance in aluminosilicates. This effect has previously been noticed (Kohn et al., 1989) and is due to a spread in the electric field gradient (E.F.G.) of the Al nuclei, due to the quadrupolar character of Al. Nuclei with a large E.F.G. have a larger quadrupole induced shift and thus contribute more to the high field side of the line than nuclei with a small E.F.G..

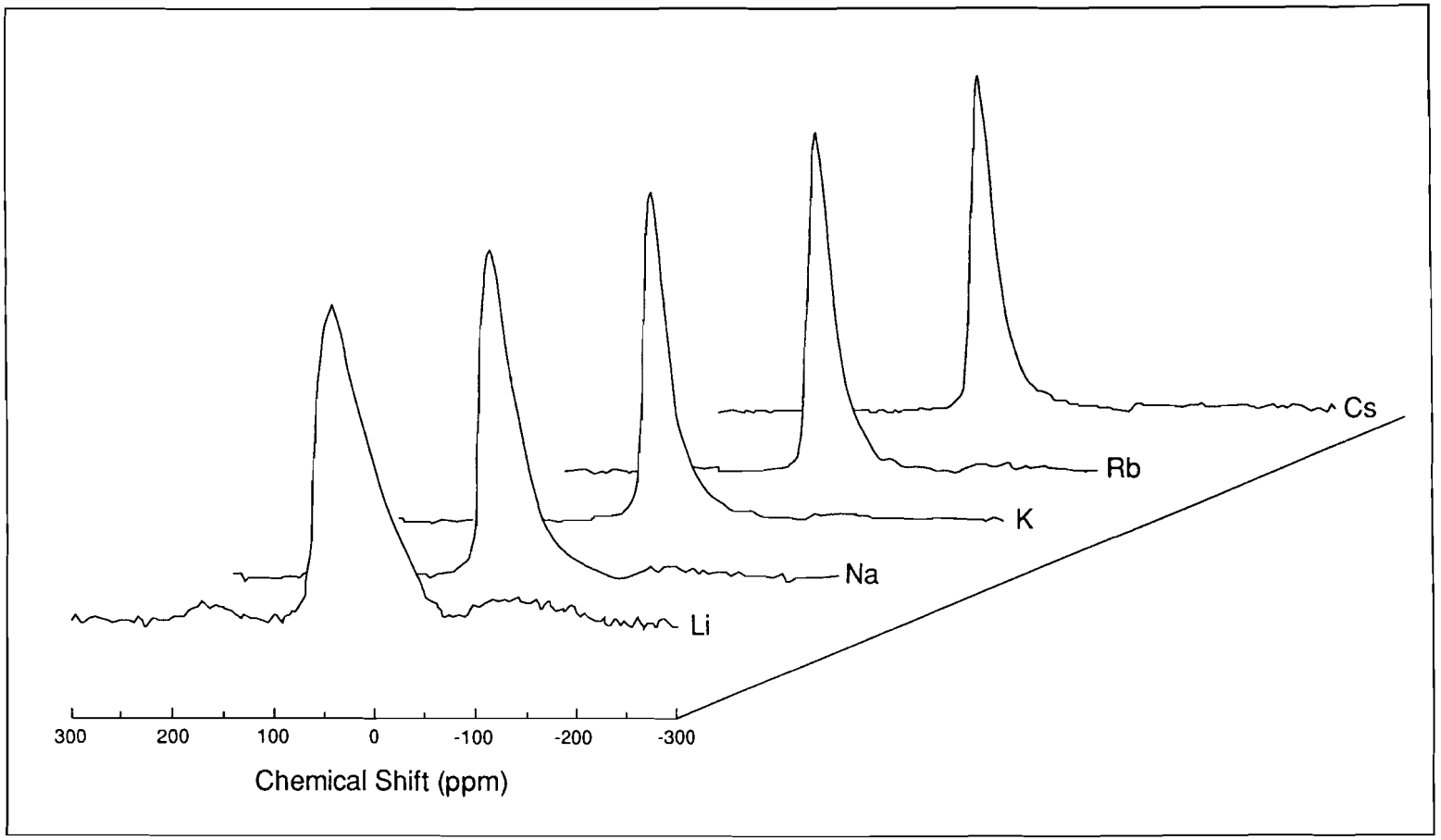


**Figure 1.** *$^{27}Al$ spectra of Li, Na, K, Rb, and Cs glass at a magnetic field of 7.1 T.*

Figure 1 clearly shows a decreasing line width going from the Li-glass to the Cs-glass, while the high-frequency side remains at about the same position. There are several effects that contribute to the line width of 1D resonances of quadrupole nuclei. The first group of line-broadening contributions is formed by the dipole-dipole interaction and chemical shift anisotropy effects, which are averaged to zero by MAS. They are thus not present in our spectra.

The second important line broadening effect is the quadrupole interaction. This is the interaction of the nuclear electric quadrupole moment with the electric field gradient at the nucleus (Cohen and Reif, 1957). This interaction is described by the Quadrupole Coupling Constant (QCC) and asymmetry parameter ($\eta$). For nuclei with spin I > 1/2 more than one transition is possible. In most cases, however, only the 1/2, -1/2 transition is observed, which is broadened by the quadrupole interaction only in second order. The second order interaction is not averaged to zero by MAS, so that in principle characteristic powder patterns are obtained. If these patterns are well-resolved, which is often not the case, theoretical calculations can be used to yield the quadrupole parameters (Abragam, 1961). All other transitions are affected by the quadrupolar interaction in first order and therefore broadened beyond detection.

The third contribution to the line width is the chemical shift dispersion (C.S.D.). It is caused by disorder of the structural environment of the atom under study.

A fourth broadening effect is caused by the transfer of magnetization of the observed nucleus to paramagnetic impurities (Engelhardt and Michel, 1987). This contribution can be neglected in this study since it is concerned with synthetic samples, free of paramagnetic impurities.

Summarizing, line width changes of MAS NMR resonances of quadrupole nuclei in the samples under study can be attributed to changes in the quadrupole interaction and to changes in the chemical shift dispersion due to disorder. The quadrupole interaction can be determined from the experimental 1D spectra either by studying the shift dependence of the center of gravity or by the linewidth of the resonance as a function of field strength. Once having obtained the quadrupole parameters one can determine the true isotropic chemical shift of the resonance and get information concerning a possible distribution of this shift. These procedures are discussed in some detail below and the results are summarized in table 1.

**Quadrupole induced shift.** It is well known that the center of gravity of the (1/2,-1/2) transition is shifted from the isotropic value in second order by the quadrupole interaction and that this shift is field dependent (Meadows et al., 1982; Lippmaa et al., 1986):

$$\Delta_{cg}=-\frac{\nu_Q^2}{30\nu_L}\left[I(I+1)-\frac{3}{4}\right]\left(1+\frac{1}{3}\eta^2\right) \qquad (1)$$

Where $\nu_Q = \frac{3e^2Q}{2I(2I-1)h}$

$\nu_L$= Larmor frequency;
$\eta$ = asymmetry parameter.

By collecting the 1D NMR spectra at more than one field, both the quadrupole interaction and the isotropic chemical shift can be calculated from the shift of the center of gravity of the peak. Until now, this is the most widely used method. Because of the very asymmetric character of the line the peak maximum does not coincide with the center of gravity. This is why it is incorrect to use the peak maxima as a tool to calculate the quadrupole interaction. The center of gravity is in fact the weight average of the chemical shift and the intensity:

$$\delta_{CG} = \sum_{i=1}^{n} \frac{(I_i \delta_i)}{I_{tot}} \qquad (2)$$

Where n = number of points covering the peak;
$I_i$ = intensity of point i with chemical shift $\delta_i$;
$I_{tot}$ = summation of $I_i$ over n points.

From the difference in $\delta_{CG}$ between the 7.1, and 11.7 T data, the quadrupole coupling constant is calculated. Using these results, the isotropic chemical shift can then be determined using equation 1. Apparently, the QCC decreases from 6.0 to 4.8 from the Li glass to the Cs glass, as is summarized in table 1. These results, however, seem to be in conflict with the obtained line widths as a function of the field strength. As the chemical shift dispersion is proportional to the field strength, whereas the contribution of the quadrupole interaction to the line width is inversely proportional to the field, the separate contributions at 7.1 T and 11.7 T can be obtained in the following way:

$$\begin{aligned} FWHH^{exp}_{7.1} &= C.S.D._{7.1} + Q.B._{7.1} \\ FWHH^{exp}_{11.7} &= 5/3 C.S.D._{7.1} + 3/5 Q.B._{7.1} \end{aligned} \qquad (3)$$

In which $FWHH^{exp}_B$ = Full width at half height at field B.
$C.S.D._B$ = Chemical shift dispersion at field B.
$Q.B._B$ = Second order quadrupole broadening at field B.

**Table 1.** *$^{27}Al$ data for the Li, Na, K, Rb and Cs glasses. FWHH is the full width at half height; Q.C.C. is the quadrupole coupling constant; C.S.D. is the chemical shift dispersion; Q.B. is the second order quadrupole broadening of the central transition; $\delta_{iso}$ is the isotropic chemical shift and ∠Al-O-Si is the Al-O-Si intertetrahedral angle.*

| | FWHH 7.1 T (Hz) | FWHH 11.7 T (Hz) | Q.C.C.[1] 2nd. shift (MHz) | Q.C.C.[2] nutation (MHz) | Q.C.C.[3] model (MHz) | C.S.D.[4] 7.1 T (Hz) | C.S.D[4]. 11.7 T (Hz) | Q.B.[4] 7.1 T (Hz) | Q.B.[4] 11.7 T (Hz) | $\delta_{iso}$ (ppm) | ∠ Al-O-Si (°) |
|---|---|---|---|---|---|---|---|---|---|---|---|
| Li | 4420 | 3480 | 6 | 5.0 | 4.5 | 780 | 1300 | 3640 | 2180 | 60.5 | 143 |
| Na | 2850 | 2390 | 5.2 | 3.9 | 2.6 | 640 | 1060 | 2210 | 1330 | 56 | 152 |
| K | 2000 | 1970 | 4.8 | 2.9 | 1.5 | 720 | 1200 | 1280 | 770 | 56 | 152 |
| Rb | 2050 | 1920 | 5.1 | 2.9 | 1.3 | 650 | 1080 | 1400 | 840 | 55 | 154 |
| Cs | 1920 | 1900 | 4.9 | 2.8 | 1.0 | 710 | 1190 | 1210 | 730 | 55 | 154 |

1: data from the induced shift as a function of field strength;
2: data from off-resonance nutation spectra;
3: data from point charge model calculations (see text);
4: data from field dependent linewidth (equation 3).

As the lines are featureless it is not possible, however, to obtain accurate quadrupole parameters from these data. In fact to our knowledge, the accuracy of the above described methods has never been studied explicitly. Therefore we turned to nutation NMR spectroscopy.

**Nutation NMR.** On-resonance nutation NMR (Samoson and Lippmaa, 1988; Kentgens et al., 1987) is a two-dimensional NMR measurement, in which the evolution of the spin system ($t_1$ period) is studied as a function of the pulse length. Projection of the resulting 2D spectrum in the $F_2$ direction yields the normal 1D spectrum, while the $F_1$ projection is the nutation spectrum. This 1D spectrum is a function of the ratio between the quadrupole interaction ($\omega_Q$) and the field strength ($\omega_{rf}$). Unfortunately, the range in $\omega_{rf}$ is limited in standard solid state NMR probes, so that the ratio $\omega_Q/\omega_{rf}$ is limited as well. Typically, field strengths of 40-70 kHz are used, corresponding with quadrupole interactions ranging from 1 MHz to 4 MHz (for nuclei with spin I=5/2). In these intermediate cases, the nutation spectrum is well resolved, and can easily be calculated to give the exact Quadrupole Coupling Constant (QCC) and asymmetry parameter ($\eta$). Quadrupole interactions larger than 4 MHz result in just one nutation frequency at (I+1/2) $\omega_{rf}$. At small quadrupole interactions, say <1 MHz, the nutation spectrum again consists of just one frequency at 1 $\omega_{rf}$. In this case it is possible to lower the field strength, so that smaller interactions can be determined, but then the resonance offset, which is negligible at high field strengths, becomes an important factor and obscures the nutation spectra.

Off-resonance nutation NMR, a recent development in nutation NMR, extends the range of quadrupole interactions to be measured, by irradiating the spins with an off-resonance rf-field (Kentgens, 1993). The choice of the appropriate resonance offset introduces additional transition frequencies into the nutation spectrum, so that it no longer consists of one line at $3\omega_{rf}$. Again, these spectra can be calculated, and experimental and calculated spectra can be compared to give the right quadrupole interaction. Furthermore, the use of more than one frequency offset allows a more accurate determination and gives an indication of a possible distribution of the quadrupole parameters.

In case of the Cs glass, there is a reasonably well resolved on-resonance nutation spectrum which points to an intermediate (1-4 MHz) quadrupole interaction. The simulated spectrum corresponds to a QCC of approximately 2.7 MHz and an asymmetry parameter of 0.5-1.0. For the other glasses, the spectrum is dominated by a peak at $3\omega_{rf}$. This is most pronounced for the Li glass (figure 2).

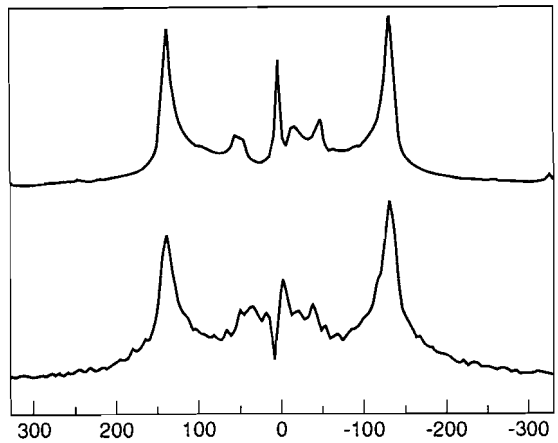


**Figure 2.** *On-resonance nutation NMR spectrum of the Li glass at an $\omega_{rf}$ of 50 kHz.*

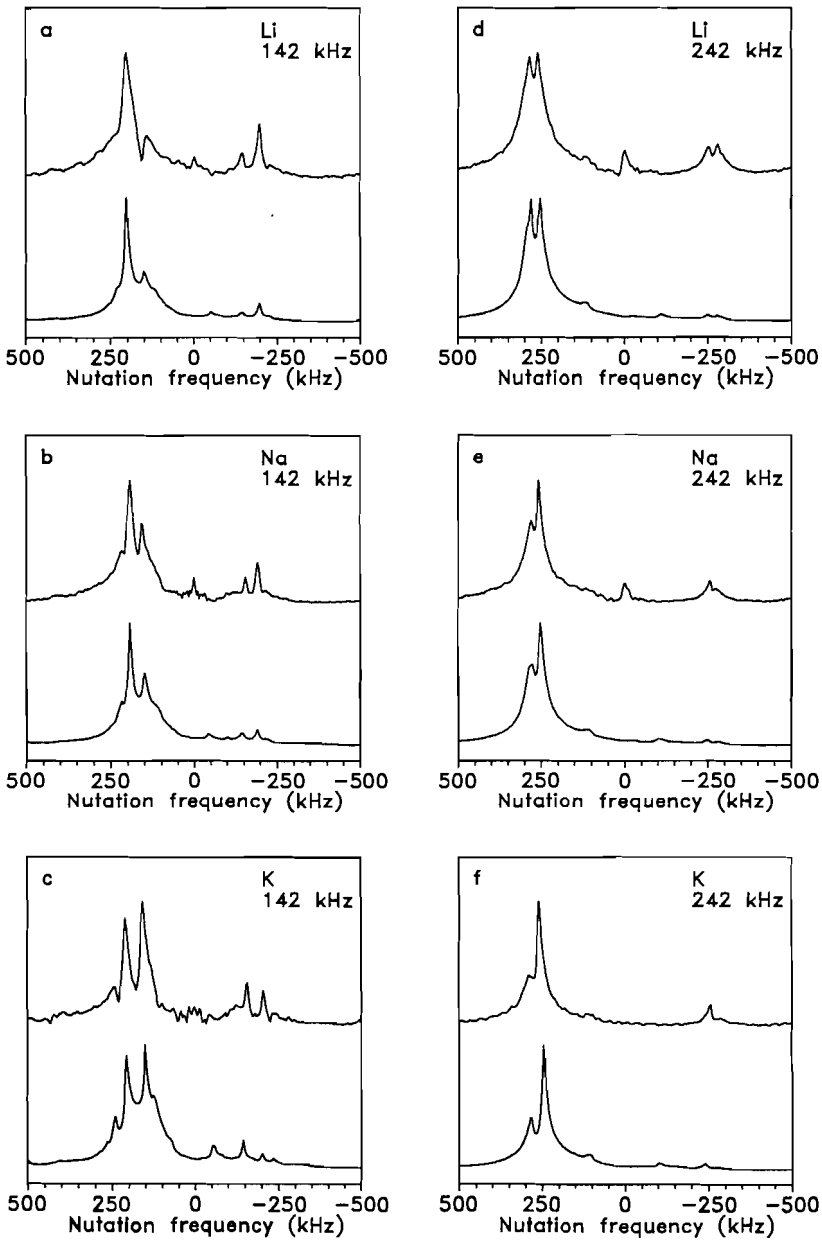


**Figure 3.** *Off-resonance nutation NMR spectra of Li, Na, K, Rb, and Cs glass at an* $\omega_{rf}$ *of 50 kHz and a resonance offset of 142 kHz, and 242 kHz.*

As there is very little structure in the on-resonance nutation spectra, the quadrupole interaction cannot be determined accurately. To be able to determine the QCC for all the samples we performed off-resonance nutation NMR experiments at an offset of 142 kHz and 242 kHz. Figure 3 displays the experimental as well as the simulated off-resonance spectra of the Li, Na and K glass. The spectra of the Rb and Cs glass are comparable to the spectrum of the K glass and are therefore omitted from figure 3. The off-resonance spectra show additional frequencies compared to the on-resonance spectra. The main features of the spectra consist of three distinct lines at an offset of 142 kHz and two at an offset of 242 kHz.

Results of simulations of the spectra (Table 1), show, that the QCC first decreases sharply from 5.0 MHz for the Li glass to 3.9 MHz for the Na glass. Then the QCC falls more gradually to 2.8 for the Cs glass. Comparison of the data from the two offsets indicates, that the QCC values are correct within 0.1 MHz. The spectra are not as sensitive to the asymmetry parameter as to the QCC, but the asymmetry parameter ranges from 0.5 to 1.0. Clearly, the QCC values obtained by nutation NMR do not correspond to values obtained by using the quadrupole induced shift. They do, however, agree well with the linewidth data. This shows, that nutation NMR is a superior method to obtain accurate quadrupole parameters. The induced shift data appear to overestimate the quadrupole coupling constants and can only be used to determine a relative trend.

From the off-resonance nutation spectra it can be seen, that the line widths of the nutation lines also decrease considerably going from the Li to Cs glass. It is not clear which interaction is the main contributor to this linewidth. Dipolar interactions (the experiments are performed statically) and a range in quadrupole interactions seem to be the most likely. A comprehensive study of the distribution of the quadrupole interaction is in progress.

In case of an $AlO_4$ tetrahedron, the charge distribution is determined by the position of the oxygen atoms and second sphere influences. In this study, the latter can be nearby location of $SiO_4$ groups or of an alkali ion. Dispositioning of the O atoms by changing the O-Al-O angle and/or changing the Al-O distances has a large impact on the QCC. It has, however, been pointed out by several theoretical studies (Navrotsky et al., 1985; Kubicki and Sykes, 1993), that in glasses, the $Si/AlO_4$ tetrahedra themselves are very stable. The changes in conditions or composition are mainly incorporated by changes in the Si/Al-O-Si intertetrahedral angle. Thus we don't expect the QCC to change as a function of the alkali ion. Therefore, second sphere influences must play an important role in the amount of distortion of the direct Al environment. The location of an alkali ion near the $AlO_4$ tetrahedron may cause charge to be drawn away from the tetrahedron, distorting it and increasing the electric field gradient at the Al nucleus. This is reflected in an increase in the QCC.

A simple measure for the strength of this type of interaction is the polarising power of the alkali ion. The polarising power is in fact the amount of charge per unit of surface, i.e. $z/r^2$ (z= valence of the alkali ion, r is the atomic radius of the alkali ion). Figure 4 shows a plot of $z/r^2$ against the QCC. There is a more or less linear correlation with the polarising power. This proves, that there is a strong interaction between the alkali ion and the $AlO_4$ tetrahedra in our glass samples. Additionally, we can assume, that the decrease in the quadrupole interaction in our glass samples is not due to dispositioning of the oxygen

atoms around Al. It is merely caused by perturbation of the electron cloud around Al by a nearby alkali ion.

This assumption is strengthened by the use of a point charge model used to calculate the E.F.G. at the Al nucleus with an adjacent alkali ion. The configuration used is that of figure 5. The tetrahedron is an ideal one, with Al-O distances of 1.73 Å (Brown and Shannon, 1973) and O-Al-O angles of 109.24°. The distance between the Al atom and the alkali is increased as the size of the alkali increases. The calculation model is a model in which each ion is considered as a point charge, with an effective charge (taken to be -1 for O, as is found in many theoretical studies of aluminosilicates (van Genechten and Mortier, 1988), and +1 for the alkali ion). The coordinating ions interact with the central atom and cause an electric field gradient (0 for the initial perfect tetrahedron).

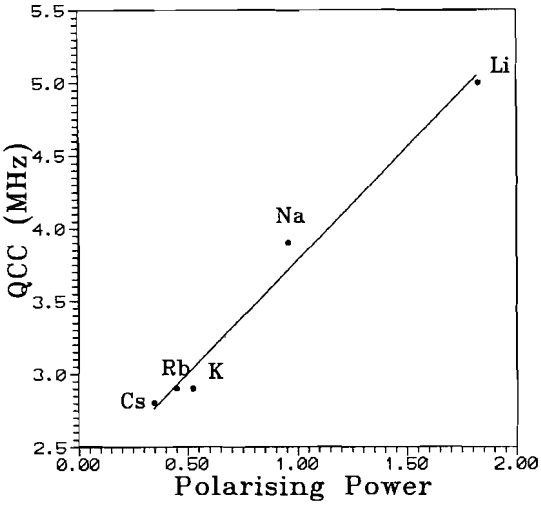


**Figure 4.** *Correlation of the quadrupole coupling constant (QCC) with the polarising power of the alkali cation.*

Table 1 shows, that the model effectively predicts the decrease in the QCC with increasing size of the alkali ion. Also, it predicts the rate of decrease: an initial sharp decrease from Li to Na and K and a slower decrease from K to Cs. This is completely consistent with our experimental data. Other influences like the Al-O-Si angle changes and small deviations from perfect tetrahedral symmetry of the $AlO_4$ unit are responsible for the difference in absolute values of the E.F.G.. Moreover, the point charge model obviously is a gross simplification. The trends in the model and our experiments are, however, very much alike.

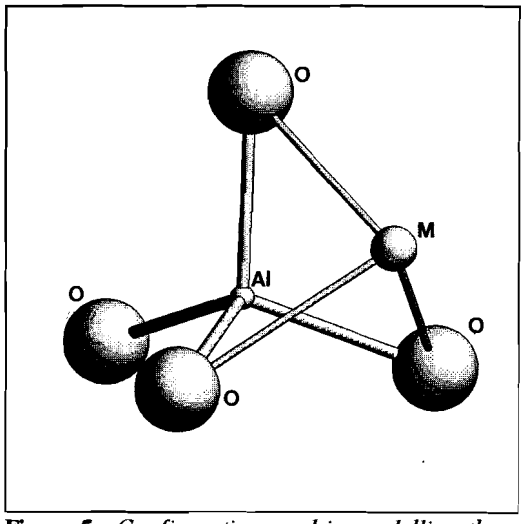


**Figure 5.** *Configuration used in modelling the interaction between an $AlO_4$ tetrahedron and an alkali cation (M).*

The values of the quadrupole parameters obtained from the off-resonance nutation spectra are used in line shape calculations of the 1D spectra (Müller, and Bentrup, 1989) in order to obtain the isotropic chemical shift. The chemical shift distribution was obtained from the field dependent line width. The isotropic shift appears to decrease when going from the Li

to the Cs glass. The chemical shift dispersion, however, varies only slightly and is not correlated with the type of alkali.

The Al-O-Si angle is known to be correlated with the $^{27}Al$ chemical shift (Lippmaa et al., 1986). It has been noted, that nepheline glass consists of six-membered rings and anorthite glass of four-membered rings (Taylor and Brown, 1979b). Also, recent molecular orbital calculations on $H_6Si_2AlO_9$, $H_6SiAl_2O_9$ and $H_6Al_3O_9$ cyclic molecules suggest, that at least in case of framework aluminosilicates with small cations like Na, three and possibly four membered Si,Al-O rings are stable (Kubicki and Sykes, 1993). Table 1 gives the $\delta_{iso}$ for the various glasses and the corresponding mean Al-O-Si angle. The Al-O-Si angle increases as the size of the alkali ion increases. The network accommodates the larger cations by expanding the rings which form the glass. An expansion of the rings can be achieved by increasing the number of tetrahedra per ring.

Summarizing, our data point to two mechanisms: 1. The alkali is closely bound to Al, perturbing its charge distribution, but leaving the $AlO_4$ tetrahedron itself geometrically unchanged. 2. The size of the alkali determines the size of the rings building up the glass network. The distribution of Al-O-Si angles in the glasses remains constant.

### $^{29}Si$ MAS NMR spectroscopy

A typical $^{29}Si$ MAS NMR spectrum for the Li, Na, K, Rb, and Cs glasses is shown in figure 6. It displays a peak at -104 ppm, consistent with Si in a $Q^4$ configuration with 4 Si next neighbours ($Q^4$) (Kirkpatrick, 1988; Engelhardt and Michel, 1987) and a small shoulder resulting from Si sites in a $Q^4$ site with one Si replaced by Al, i.e. $Q^4(1Al)$. Within analytical error, the peak position of the spectra shows no correlation with the type of alkali (table 2).

**Table 2.** *$^{29}Si$ data for the Li, Na, K, Rb, and Cs glasses.*

| | FWHH (Hz) | $\delta$ (ppm) |
|---|---|---|
| Li | 1860 | -104.5 |
| Na | 1800 | -104.0 |
| K | 1720 | -105.0 |
| Rb | 1720 | -105.0 |
| Cs | 1630 | -104.5 |

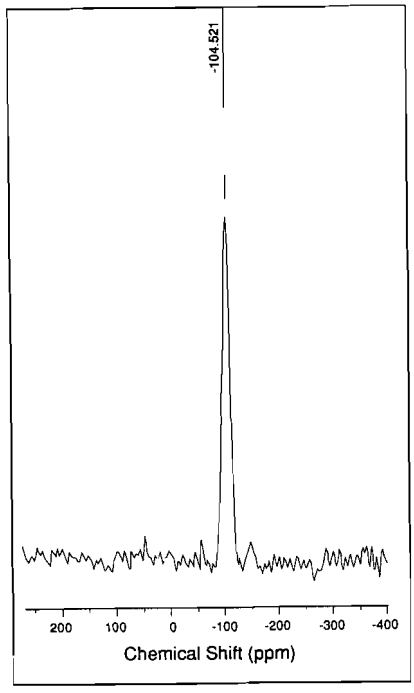


**Figure 6.** *$^{29}Si$ MAS NMR spectrum of the Li glass at an $\omega_r$ of 50 kHz and 11.7 T magnetic field.*

This is consistent with recent correlations of silicate structure and $^{29}Si$

chemical shifts, stating, that in case of alkali charge balanced (alumino)silicates the chemical shift of the separate Q-species is independent of the type of alkali ion (Prakabar et al., 1991). The line width, given in table 2, however, decreases slightly from 1860 Hz for the Li-glass to 1630 Hz for the Cs-glass. Because Si is not a quadrupolar nucleus, linewidths are entirely determined by the variation in the bond lengths and angles, i.e. by the chemical shift dispersion. $^{29}$Si NMR in $SiO_2$ polymorphs and aluminosilicates is correlated with mean Si-O-Si bond angles (Lippmaa et al., 1980; Dupree and Pettifer, 1984). Correlations of this kind in aluminosilicate glasses are not warranted (Oestrike et al., 1987), since there are not only $Q^4$(0Al) sites, but also $Q^4$(1Al). As a consequence, a variation of peak positions, peak widths and intensities have to considered. It is hard to predict how each species will react to changing charge balancing ion. Most probably, it will affect the $Q^4$(1Al) sites most, since the alkali ion is closely bound to Al. Additionally it has been noticed, that the Si chemical shift in framework aluminosilicate glasses is more strongly influenced by the Si/(Si+Al) ratio, which is held constant in this study. The small variation in the $^{29}$Si peak width is in agreement with the small spread in the chemical shift dispersion for the $^{27}$Al data.

## 4.5 Conclusions

Off-resonance nutation NMR is a powerful tool for the determination of the quadrupole interaction and as a result the mean isotropic chemical shift of Al in aluminosilicate glasses. Applying this technique to framework aluminosilicate glasses shows, that the Al quadrupole interaction decreases as the size of the charge-balancing alkali ion increases. A correlation between the QCC and the polarising power of the alkali ion and a point charge model predicting this correlation indicates, that Al is closely bound with the alkali ion.

The known correlation between the Al chemical shift and the Al-O-Si intertetrahedral angle shows, that the mean ring size in framework aluminosilicate glasses increases as the size of the alkali ion increases. This can be attributed to an increase in the number of tetrahedra per ring. The range in chemical shift for Al and Si remains constant as the size of the charge-balancing alkali ion increases.

In contrast to past studies of aluminosilicate glasses, $^{27}$Al NMR is much more informative than $^{29}$Si NMR.

# Chapter 5

# Corundum ($\alpha$-$Al_2O_3$) : a useful standard in quantitative Al NMR spectroscopy?

## 5.1 Introduction

One of the greatest advantages of NMR spectroscopy is the strict proportionality between signal intensity in the NMR spectrum and the number of nuclei giving rise to this signal. For spectral assignment it is useful in determining exact relative populations of crystallographic sites in a sample (Massiot et al., 1990; Pearson and Schramm, 1990; Alemany et al., 1991). In the case of spin I=1/2 nuclei such as $^{29}Si$, this proportionality is easily observed.

However, in the case of half-integer quadrupolar nuclei (viz. $^{11}B$ (I=3/2), $^{23}Na$ (I=3/2), $^{27}Al$ (I=5/2), or $^{71}Ga$ (I=7/2)), quantitative measurements are complicated by the presence of a quadrupole moment. The excitation of the nuclei in the sample becomes dependent on the magnitude of the quadrupole interaction. This is usually overcome by using a very short excitation pulse (Samoson and Lippmaa, 1983b). This means however, that good care has to be taken concerning experimental conditions. An important point is, that part of the intensity can be unobservable by NMR. For instance it has been shown by quantitative $^{27}$ Al NMR on zeolites, that part of Al in extra-framework alumina is "invisible" (Ernst et al., 1993). These sites have NMR signals, that are broadened beyond detection due to the large quadrupole interaction. Sato et al. (1991) used quantitative $^{27}Al$ NMR to prove, that in case of $SiO_2$-$Al_2O_3$ glasses all Al is detected. It is therefore important to have a reliable standard in order to account for all of the observed intensity in one's spectra.

For pulse spectrometers, the probe is tuned and matched upon changing the sample. Tuning on a solid or on a fluid may have considerable consequences for the magnitude of the rf field (Freude and Haase, 1993). Calibration of solid intensities on fluid standards is therefore doubtful.

Consequently, quantitative NMR spectroscopy could benefit from having a suitable solid state standard. A logical candidate seems corundum, $\alpha$-$Al_2O_3$. It is readily available, cheap, it has a high Al content from one well-defined crystallographic site with an accurately determined quadrupole interaction. Additionally, it is easy in use, i.e. it is inert, and not hygroscopic or poisonous. In fact, in some studies it has already been used as a standard (Sato et al., 1991)

In order to establish corundum as a reference for quantitative $^{27}Al$ NMR measurements, we studied the excitation behaviour of a wide variety of synthetic and natural corundum samples.

Additionally, we performed spin-echo Fourier $^{27}Al$ NMR at high rf powers ($\approx$200 kHz). The spin-echo technique may offer advantages for the investigation of sites with large QCC values (Haase and Oldfield, 1993). These sites can suffer from spectrometer dead times, resulting in signal loss and lineshape distortion (Kunwar et al., 1986). Moreover, spin-

echo NMR can be used to distinguish between different chemical species through differences in spin-echo decay ($T_{2E}$) values. This technique has been used recently to study Si-OH-Al sites in a dehydrated H-ZSM-5 zeolite structure (Ernst et al., 1993). These authors were able to observe these sites for the first time. They calculated a QCC of 16 MHz for these sites. This large quadrupole interaction had earlier prevented their observation. We use this technique to check if any signal loss in the quantitative measurements can be accounted for by Al with very large quadrupole interactions, for instance in surface sites or lattice defects.

## 5.2 Corundum crystal structure

The $M_2O_3$ structure (M=Al for corundum, but can also be Fe, Cr, V, and Ti) has been described by Newnham and de Haan (1962) and Ishizawa et al. (1980). It crystallizes in the hexagonal space group $R\bar{3}c$ with a=4.754Å and c=12.99 Å. The O atoms are arranged in an almost ideal hexagonal close packing with Al atoms occupying 2/3 of the octahedral interstices. The vacant positions are arranged in an ordered way. Common impurities in corundum are Cr, Fe, and Ti. Traces (ppm) of Cr give corundum a red colour. Traces of Fe and Ti give corundum a blue colour. Red coloured gem quality corundum is called ruby, any other colour is called sapphire. The M-M distances in the corundum type structure are one of the shortest observed for oxides (2.657 Å for Al-Al).

## 5.3 Theory

The quantitative determination of spins in powdered samples is strongly influenced by the presence of a quadrupole interaction (Abragam, 1961; Fenzke et al., 1984; Man et al., 1988). The response of a quadrupolar nucleus depends on the relative values of $\omega_{rf}$ (strength of the rf excitation pulse), $\omega_Q$ (the quadrupole splitting), the pulse length $\tau$ and the spin quantum number I. This effect is used in 2D nutation NMR spectroscopy (Samoson and Lippmaa, 1983a; Kentgens et al., 1987). In this technique, the evolution of the spin system is studied as a function of the pulse length. Fourier transformation of the spectra in two directions leads to a 2D nutation spectrum. Information on the chemical shift interaction and the second order quadrupole interaction is preserved in the projection of the 2D spectrum onto the $F_2$ direction. This is in fact the "normal" 1D single pulse NMR spectrum. Projection of the 2D spectrum onto the $F_1$ direction gives the nutation spectrum which contains information about $\omega_Q$. For quantitative excitation, however, this effect can be a nuisance.

Two extreme cases have to be distinguished. The first is where $\omega_{rf} \gg \omega_Q$. In this case, all the energy levels are perturbed, and the excitation is called non-selective. In the nutation spectrum, one single nutation frequency is observed at $\omega_{rf}$. The intensity of the m↔m+1 transition is given by (Freude and Haase, 1993):

$$G^{ns}_{m,m+1}(0) = \sin(\omega_{rf}\tau)\,\frac{3\{I(I+1) - m(m+1)\}}{2I(I+1)(2I+1)} \qquad [1]$$

If m=-1/2, the intensity of the central transition -1/2↔1/2 is equal to the intensity obtained from continuous wave experiments and becomes:

$$G^{ns}_{-1/2,1/2}(0) = \frac{3(2I+1)}{8I(I+1)} \sin(\omega_{rf}\tau) \qquad [2]$$

The second case is where $\omega_{rf} \ll \omega_Q$. In this case, only two neighbouring energy levels are perturbed, and the excitation is called selective. In the nutation spectrum, again, one single nutation frequency is observed at $(I+1/2)\omega_{rf}$. The intensity of the m↔m+1 transition are in this case given by:

$$G^{s}_{m,m+1}(0) = \frac{3W_m}{I(I+1)2I+1)} \sin(2W_m\omega_{rf}\tau) \qquad [3]$$

Where $$W_m = 1/2\sqrt{I(I+1)-m(m+1)}$$

If m=-1/2, the intensity of the central transition -1/2↔1/2 becomes (Freude and Haase, 1993):

$$G^{s}_{-1/2,1/2}(0) = \frac{3}{4I(I+1)} \sin\{(I+1/2)\,\omega_{rf}\tau\} \qquad [4]$$

Finally, if $\omega_Q \approx \omega_{rf}$, every spin packet has its own nutation frequency and the nutation spectrum has a complex lineshape. This lineshape can be calculated numerically to give the quadrupole coupling constant ($e^2qQ/h$) and the asymmetry parameter ($\eta$) (Kentgens, 1987).

For very short pulses $\tau$, $\sin[\omega_{rf}\tau] = \omega_{rf}\tau$ and $\sin[(I+1/2)\omega_{rf}\tau] = (I+1/2)\omega_{rf}\tau$. Equations [2] and [4] then become identical. For this to be true, Freude and Haase (1993) give as a critical pulse length (intensity error <10%):

$$\omega_{rf}\tau < \sqrt{\frac{0.6}{I(I+1)-3/4}} \approx \frac{\pi}{4(I+1/2)} \qquad [5]$$

As long as equation [5] is obeyed, the intensity of the central transition is independent of $\omega_Q$, and the intensities can be compared directly.

Man et al. (1988) and Fenzke et al. (1984) calculated the intensities of the central transition as a function of $\omega_Q$ and $\tau$ and found, that in case of non-selective excitation, the maximum intensity for the -1/2 ↔1/2 transition is 9/35 times the total. This is at a pulse length one third of that of the maximum for selective excitation. Kentgens (1991) proposed a quantitative excitation experiment, in which the carrier frequency is swept using a frequency-stepped adiabatic half-passage (FSAHP). In principle the full magnetization of the central transition can be recorded by a FSAHP.

In order to be sure that condition [5] is obeyed, an accurate determination of $\omega_{rf}$ is essential. Only then, pulse lengths and angles can be related. For this purpose, excitation curves/nutation spectra are obtained. In order to obtain uniform excitation of the central transition the experiments are performed on-resonance and without magic angle spinning (MAS).

Additional to excitation phenomena, there are a number of experimental conditions, that have to be met with in order to obtain quantitative results. First, the reference sample and the experimental sample should both have the same size and position with respect to the coil, since the rf field is inhomogeneous. Secondly, repetition times between the pulses must be larger than 5 times the spin-lattice relaxation time $T_1$. Thirdly, intensities and linewidths of the absorption lines of the experimental and reference sample should be similar.

## 5.4 Experimental

### Samples

Five different corundum samples have been studied, three synthetic and two natural samples. The first synthetic sample (Sample Corundum A) was prepared by heating 1 gram of $Al(OH)_3$ powder at 1100 °C for 4 days. The second synthetic sample (Sample Verneuil corundum) is a single crystal of about 1 $cm^3$ prepared by the Verneuil method. The third synthetic sample was obtained by annealling 250 mg of the Verneuil type corundum hydrothermally for 5 days at 610 °C and 2.6 kbar in a cold-seal pressure vessel. The natural samples are a number of red and blue coloured corundum crystals from Bamble (Norway) and the Isle of Naxos, respectively.

The natural and Verneuil type corundum crystals were crushed into fine grained powder in a Tungsten Carbide (WC) ball-mill.

The corundum structure of all the samples was confirmed by X-ray powder diffraction with a Philips PW 1050/25 diffractometer using CuK$\alpha$ radiation.

The Al content of all the samples was checked independently by using X-ray fluorescence spectroscopy (Philips PW1400/00) and electron microprobe (Jeol Jx-8600 Superprobe) analyses. Within analytical accuracy, the chemical analyses of all the samples from both techniques agrees with the $Al_2O_3$ stoichiometry. The Bamble sample contains 0.2 wt % $Fe_2O_3$, and 0.3 wt% $Cr_2O_3$, which gives it its red colour. The Naxos sample contains 0.5 wt% $Fe_2O_3$ , and 0.1 wt% $TiO_2$ , giving it its blue colour.

**NMR spectroscopy**

The 1D $^{27}$Al MAS NMR spectra were collected on Bruker AM-500 and AM-600 spectrometers, operating at 130.3 MHz ($B_0$ = 11.7 T) and 156.3 MHz ($B_0$ = 14.1 T). A home-built probe was used, equipped with a Doty MAS assembly. A 0.7 μsec. pulse was used with an rf field strength $\omega_{rf}$ of approximately 50 kHz and a 100 kHz spectral width. The delay between subsequent pulses was 1 s. Per experiment 200 FIDs were acquired.

The quantitative Al NMR measurements were performed on a Bruker AM-500 spectrometer operating at 130.3 MHz for $^{27}$Al ($B_0$ =11.7 T). All experiments were performed in a home-built high power (maximum $\omega_{rf} \approx 200$ kHz) probe under static conditions. The volume of the sample and the position of the sample within the coil were kept constant. Therefore, samples of 10-50 mg with approximately the same volume were carefully weighed and put into the sample holder at a constant position. Between the measurements the probe was tuned and matched, but adjustments were minimal. The excitation curves were collected as standard nutation NMR experiments: 64 experiments of 32 scans exactly on-resonance were performed with a pulse increment of 1 μs, 100 kHz spectral width and 5 s delay. In stead of a 2D Fourier transformation -as is done to obtain the 2D nutation spectrum- the spectra were Fourier transformed and phase corrected only in the $F_2$ direction on a SUN microcomputer using NMRi software. Projection of the sum of the $F_2$ spectra onto the $F_1$ direction resulted in the required excitation curves.

The spin-echo experiments were also collected on a Bruker AM-500 spectrometer, prior to the collection of the nutation spectra. A phase cycled selective echo sequence ($\pi/2_{0.5\mu s}$ , $delay_{20\mu s}$, $\pi_{1\mu s}$) was used with a 0.5 s delay and 250 kHz spectral width, similar to the methods used by Ernst et al. (1993). The rf field strength $\omega_{rf}$ was $\approx$200 kHz. The experiments were performed under static conditions.

## 5.5 Results.

A typical 1D $^{27}Al$ NMR spectrum of corundum is given in figure 1. Despite the moderate quadrupole interaction (quadrupole coupling constant (QCC) = 2.38 MHz, asymmetry parameter ($\eta$) = 0.0) (Lee and Bray, 1991; Skibsted et al., 1991), no powder pattern is observed.

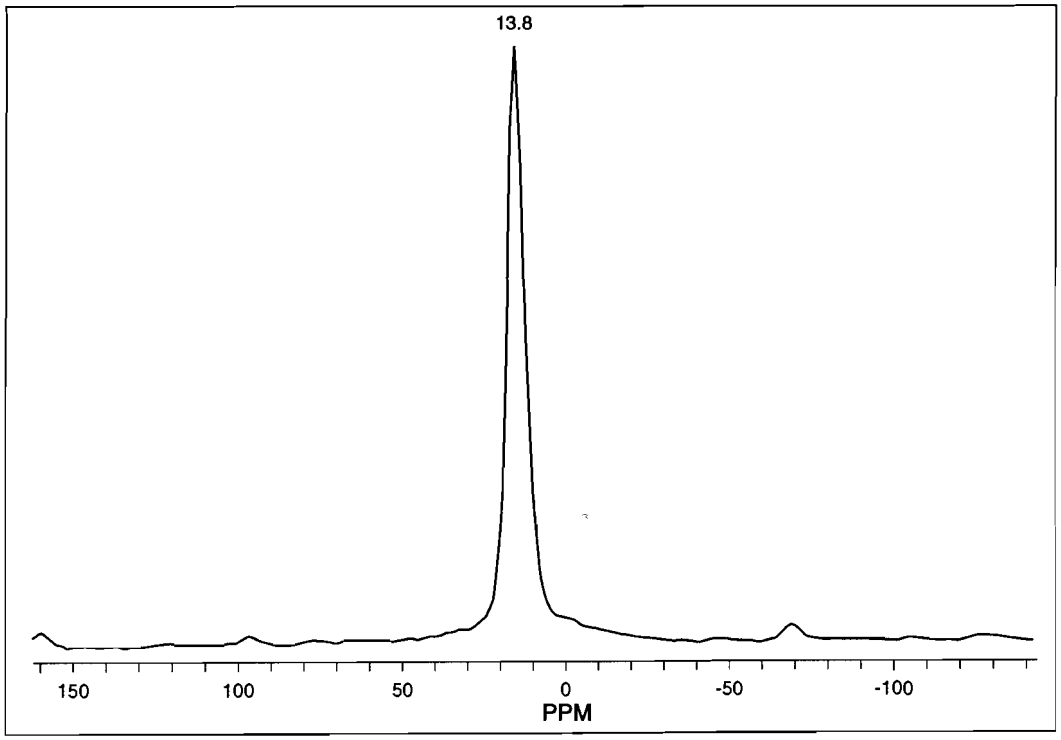


**Figure 1.** *1D $^{27}Al$ MAS NMR spectrum of corundum A at a magnetic field of 11.7 T and 11 kHz spinning speed.*

This might be an indication of strong broadening due to homonuclear (Al-Al) dipolar interactions. As has been pointed out in the section on the corundum crystal structure, the Al-Al distance is rather short (2.657 Å). In fact, the broadening due to homonuclear dipolar interactions ($\Delta\omega$) between like spins is inversely proportional to the internuclear distance $r_{ik}$ (Abragam, 1961):

$$\langle \Delta\omega \rangle^2 = \frac{9}{5} \left( \frac{\mu_0}{4\pi} \gamma_{Al}^2 \hbar \right)^2 F_I \frac{1}{r_{ik}^6} \qquad [6]$$

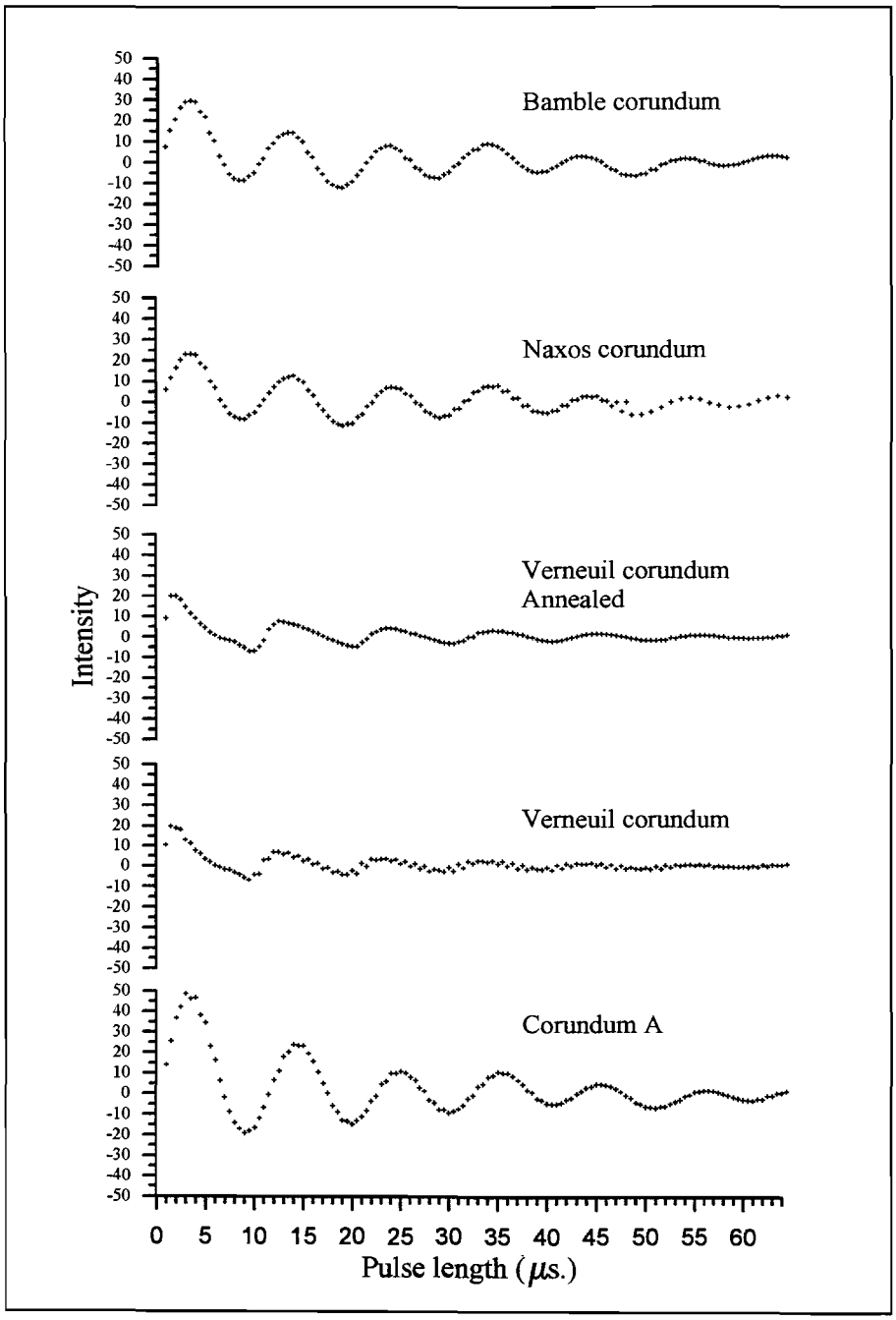


**Figure 2.** *$^{27}Al$ excitation curves for the various corundum samples.*

where

$$F_I = \frac{4I(I+1)}{27} + \frac{[2I^2(I+1)^2+3I(I+1)+13/8]}{18(2I+1)}$$

and

| | |
|---|---|
| $\mu_0$ | permeability of free space; $4\pi \cdot 10^{-7}$ Wb/Am; |
| $\gamma_{Al}$ | gyromagnetic ratio of aluminium; $6.9763 \cdot 10^7$ $(s \cdot A/m)^{-1}$; |
| $h$ | $(=2\pi\hbar)$ Planck's constant; $6.6262 \cdot 10^{-34}$ J s; |
| I | spin quantum number |

For $r_{ik}$ = 2.657 Å and I = 5/2, $\Delta\omega$ becomes 4880 Hz. The experimental linewidths are 5800-6000 Hz (under static conditions and at a magnetic field strength of 11.7 T) for the synthetic samples and 7000, and 8100 Hz for the Bamble and Naxos samples, respectively. The results of the synthetic samples are in good agreement with the data of Huggins and Ellis (1992). If magic angle spinning (MAS) is applied, linewidths are 700 for the synthetic and 1000-1050 for the natural corundum samples. Of this linewidth, 350 Hz can be attributed to the second order quadrupole broadening. The extra linebroadening of the natural samples, as compared to the synthetic samples, is due to the presence of paramagnetic impurities. It can be seen, that dipolar interactions are responsible for 60-80 % of the linewidth. This is probably the reason, why no powder pattern is observed under static conditions. In principle, MAS should average dipolar interactions to zero. In the case of strong interactions, however, residual linebroadening is still observed. For corundum, these residual dipolar interactions obscure a quadrupole structure in the MAS spectrum as well.

Collecting the 1D spectra at more than one magnetic field strength makes it possible to calculate the quadrupole coupling constant using the field dependent second order quadrupole shift (Samoson et al., 1986). At a magnetic field of 11.7 T, the peak position for all the corundum samples is 13.8 ± 0.1 ppm, and increases to 15.0 ± 0. ppm at 14.1 T. This corresponds with a QCC of 2.44 ± 0.3 MHz, assuming $\eta$ = 0. The 2.44 MHz value is in reasonable agreement with previous studies: Lee and Bray (1991) and Skibsted et al. (1991) report a QCC of 2.38 and asymmetry parameter of 0.0.

The excitation curves for all the corundum types are given in figure 2. The curves are normalised to the intensity of 100 mg of $Al_2O_3$. The shape of all the curves is approximately sinusoidal, as one would expect from selective excitation of the central transition. Only in case of the Verneuil type there is a large departure of the ideal shape. This is reflected in the nutation spectrum, which is in fact a Fourier transform of the excitation curve. The nutation spectrum for the Verneuil type corundum is shown in figure 3. Additional to the intensity at 1 and 3 $\omega_{rf}$, there is also considerable intensity at nutation frequencies of 6 and $9\omega_{rf}$. This is probably a result of too short a relaxation delay (Kentgens, 1987).

For the Naxos and Bamble type corundum, there is also a slight departure from the ideal sinusoidal shape. This can be explained as follows. In the case of selective excitation only one frequency is observed, giving rise to an ideal sinusoidal shape of the excitation curve. If the condition of selective excitation is not entirely met with, additional frequencies in the excitation curve will cause the shape of the curve to become more complex. This

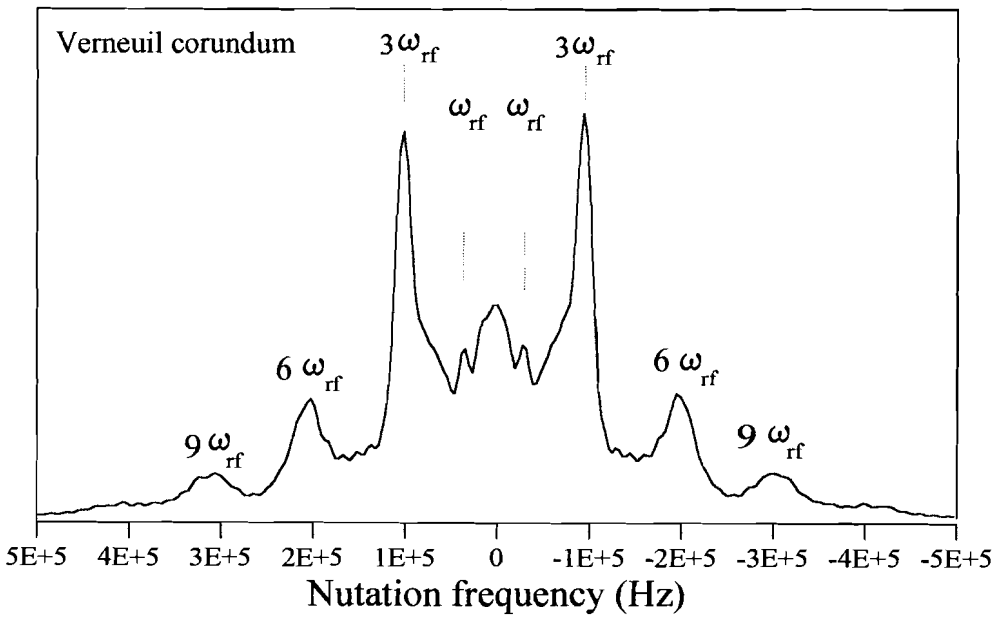


**Figure 3.** *Nutation NMR spectrum of the Verneuil type corundum.*

effect is of course exploited in nutation NMR. For corundum at the conditions described in this study, the excitation is not perfectly selective. There is also a contribution to the signal from sites with nutation frequencies of 1 $\omega_{rf}$ and as a result, there is a departure from the sinusoidal form. Figure 4a and 4b show calculated excitation curves together with experimental curves for the corundum A sample and the Bamble type sample. Calculation has been carried out using the programme Antiope by Stickney de Bouregas and Waugh (1992) and the parameters are QCC = 2.38 MHz, and $\eta$ = 0. Values for $\omega_{rf}$ were derived from nutation spectra (*vide infra*). Comparison of the two samples reveals, that the Bamble type corundum follows the theory correctly. For a perfect sinusoidal shape, the second minimum and the fourth maximum in the curve are too low and too high, respectively . The corundum A sample, however, does not agree well with the parameters given above. The curve is more sinusoidal in shape. This is an indication, that the 1 $\omega_{rf}$ signal has less intensity, as compared to the Bamble type sample.

The corresponding nutation spectra (figure 5a and 5b) clearly reveal that indeed the relative intensities of the $1\omega_{rf}$ and $3\omega_{rf}$ signals differ for the two samples. The $1\omega_{rf}$ (at 35 kHz) signal of the corundum A sample is less intense than the $1\omega_{rf}$ signal (at 35.5 kHz) of the Bamble type corundum.This is rather surprising, because it points to the presence of sites in the corundum A sample with a larger quadrupole interaction than 2.38 MHz. In fact, the spectrum of corundum A can only be simulated by an (avarage) QCC of 2.6 MHz.

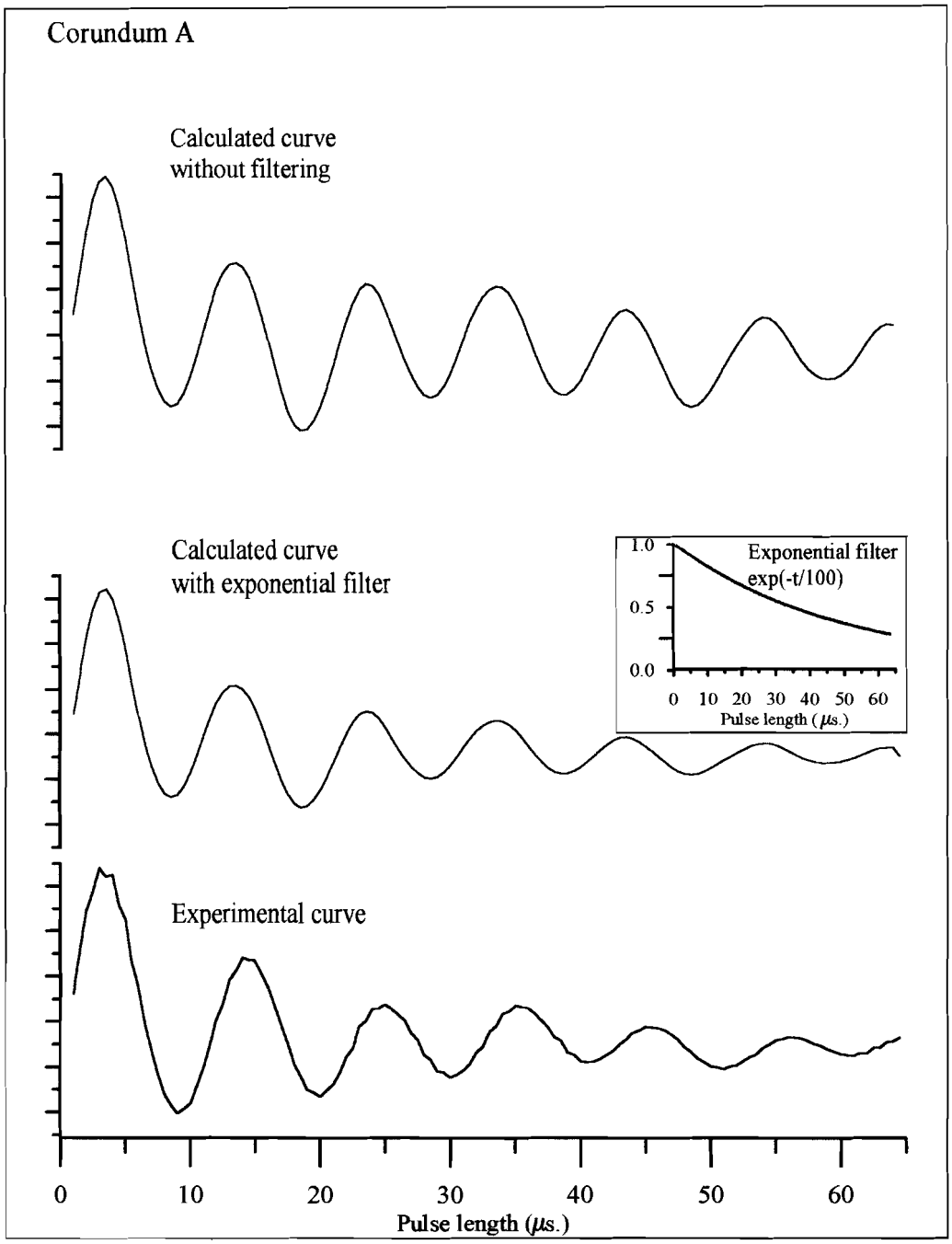


**Figure 4a.** *Experimental and calculated excitation curves for the corundum A sample. The vertical scale represents the intensiy.*

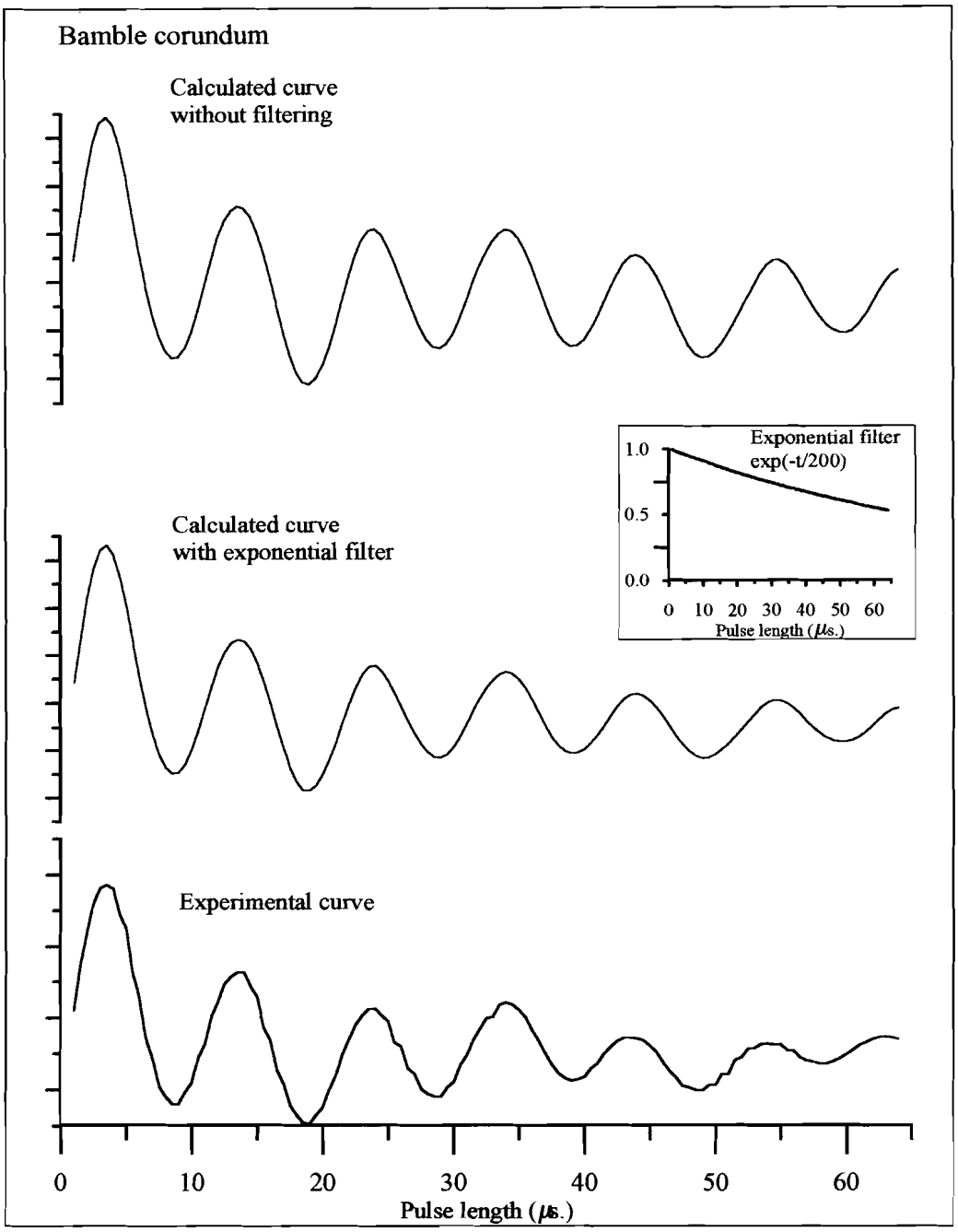


**Figure 4b.** *Experimental and calculated excitation curves for the Bamble type corundum sample. The vertical scale represents the intensiy.*

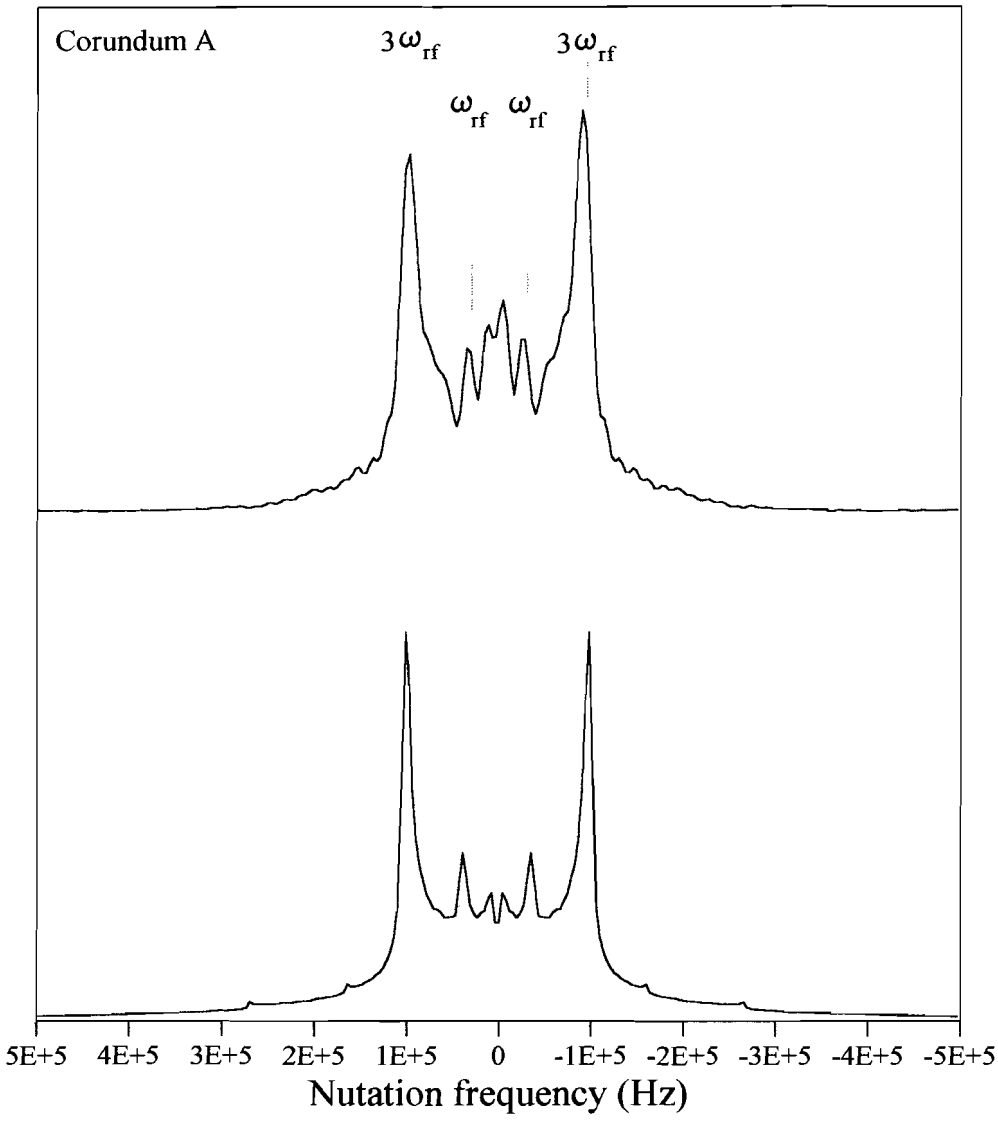


**Figure 5a.** *Experimental and simulated nutation spectra for the corundum A sample.*

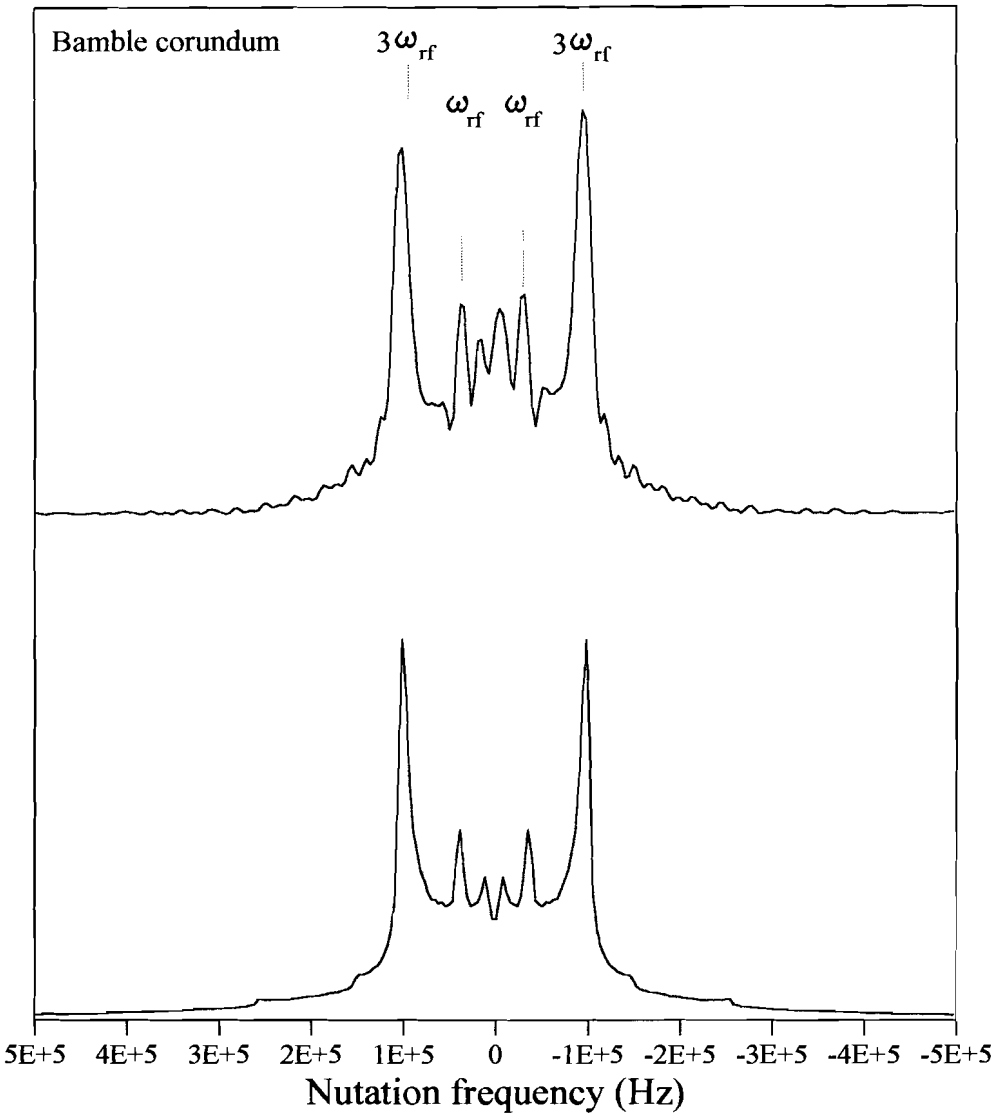


**Figure 5b.** *Experimental and simulated nutation spectra for the Bamble type corundum sample.*

The first part of the excitation curves in figure 2 is in all cases linear, making it indeed possible to perform quantitative measurements. However, despite the fact that all experimental conditions are identical (the experiments were performed during one session), there are large differences in intensity between the various corundum samples. Table 1 gives a numerical representation of figure 2 with a pulse length of 1 up to 6 μs. Corundum A has the highest intensity (48.8) at a pulse of 3 μs. The maxima of the Bamble and Naxos type corundum samples are about at the same pulse length (3 and 3.5 μs) and have intensities of 29.6 and 23.0, respectively. The Verneuil type corundum and its annealed derivative have their highest intensity (20.0 and 20.3) at a pulse length of 1.5 μs.

**Table 1.** *Intensities of corundum samples as a function of pulse length.All intensities have been normalised to 100 mg. of* $Al_2O_3$.

| | Corundum type | | | | |
|---|---|---|---|---|---|
| Pulse length | Corundum A | Verneuil | Verneuil annealed | Naxos | Bamble |
| | | | Intensity | | |
| (μs) | | | (arbitrary unit) | | |
| 1 | 14.0 | 10.7 | 9.4 | 6.2 | 7.6 |
| 1.5 | 25.5 | 20.0 | 20.3 | 11.9 | 15.5 |
| 2 | 36.7 | 19.0 | 19.8 | 16.6 | 20.6 |
| 2.5 | 42.2 | 18.0 | 18.4 | 20.4 | 26.1 |
| 3 | 48.8 | 13.1 | 14.9 | 23.0 | 28.9 |
| 3.5 | 46.3 | 11.3 | 11.6 | 23.0 | 29.6 |
| 4 | 46.8 | 7.6 | 9.2 | 22.6 | 28.9 |
| 4.5 | 38.3 | 6.3 | 6.5 | 18.6 | 24.3 |
| 5 | 34.4 | 3.4 | 4.5 | 16.5 | 21.7 |
| 5.5 | 22.9 | 2.2 | 2.3 | 10.0 | 14.0 |
| 6 | 16.4 | 0.2 | 0.9 | 7.0 | 10.2 |

At a 1μs pulse length and $\omega_{rf}$=30 kHz (obeying equation [5] for a linear pulse response of the intensity) there are also considerable differences between the various types of corundum. Relative to corundum A, the intensities of the single crystal, Naxos and Bamble type corundum are 24.7 %, 56.0 %, and 46.9 % lower.

Additional spin-echo experiments were used to check if any signal loss could be attributed to "invisible" sites, i.e. sites with a very large quadrupole interaction due to a large distortion of the nearest neighbour oxygen shell around aluminium. If there are any such sites in the corundum samples, linewidths and lineshapes of single pulse and spin-echo experiments will be different. This has been shown by Ernst et al. (1993) for Si-OH-Al sites in H-ZSM-5 zeolites. A typical spin-echo spectrum is shown in figure 6 for the Naxos type corundum. There is no significant difference between the single pulse (static) spectra and the spin-echo spectra. The linewidths of the echo NMR signal for all the samples are 1-1.5 kHz larger than for the single pulse experiments. Unfortunately, relaxation delays of the echo experiments were much shorter (0.5 s) than the delays for the single pulse experiments. Therefore, it is difficult to compare the results more systematically. In any case, there is no

indication of any sites with very large quadrupole interactions (>10 MHz) present in our samples.

Finally, in an additional session, the Al intensity of corundum A has been compared to the Al intensity of a sample and an aluminium nitrate solution (A. Bos, 1993). In order to obey equation [5] a 10° pulse length was used for the solution, corresponding to a 30° pulse length for the solid state. $NH_4Al(SO_4)_2 \cdot 12H_2O$ has a very low quadrupole interaction (QCC = 0.456 MHz; $\eta$ = 0 (Freude and Haase, 1993)) and as a result, all Al is detected. Comparison of the signal intensities of the three samples shows, that within 10 %, all Al in the corundum A sample is observed.

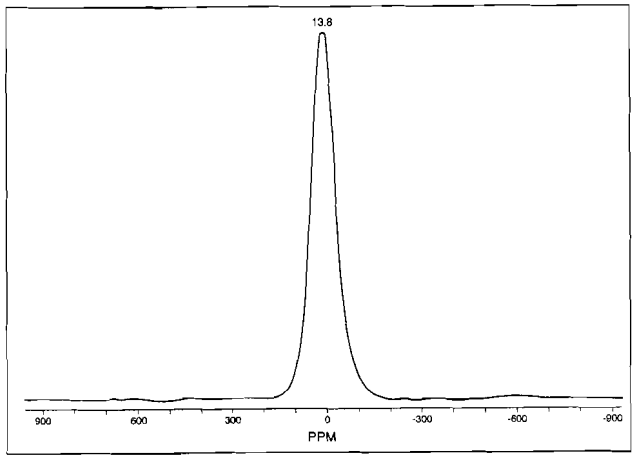


**Figure 6.** *$^{27}Al$ spin-echo spectrum of the Naxos type corundum sample at a 11.7 T magnetic field and an rf field of 200 kHz.*

## 5.6 Discussion

$^{27}Al$ intensity measurements of the various corundum samples vary considerably. The natural and Verneuil type corundum lose up to 56 % of their intensity.

Nuclei in certain chemical environments may not give rise to any NMR signal. Examples are nuclei close to paramagnetic electron spins (Eckert, 1992). These impurities cause a very rapid relaxation of closely bound nuclei (in this case Al) and as a result these nuclei are not observed. In case of the Naxos and Bamble type corundum, paramagnetic impurities may be responsible for the intensity loss. The fact that the samples are coloured already points to presence of impurities and they have also been observed in microprobe analyses (*vide supra*).

It is interesting to compare the two synthetic samples in this study. The Verneuil type sample loses part of its intensity, probably because of a too short delay between the rf pulses. The corundum A sample, however, recovers 100 % of its intensity. Both do not contain paramagnetic impurities. The only difference between the samples is the way in which they were prepared. The Verneuil type sample is a good quality single crystal, while the corundum A sample is a very fine grained powder made by dehydrating $Al(OH)_3$. As a result, the surface area and the nature of the surface of the two samples will differ considerably. It is well-known that the nature and the area of the surface of $\alpha$-, $\gamma$- and transition aluminas is subject to large variations. This makes them of great use in catalytic processes. O'Reilly (1960) performed $^{27}Al$ solid-state NMR of transition aluminas (including

$\alpha$-$Al_2O_3$). He concluded, that at the surface of these compounds there were sites with very large electric field gradients, making them unobservable by NMR techniques. Huggins and Ellis (1992), however, show that this effect is due to dynamic effects at the surface. It is known, that $^{27}Al$ relaxation is achieved almost entirely by quadrupolar relaxation (Pound, 1950) and more importantly, by fluctuating electric field gradients (Freude and Haase, 1993). This can be achieved through motion of lattice defects (Becker, 1982) or paramagnetic centers (Pound, 1950). Our excitation curves and nutation spectra indicate that in corundum A sites are present which have large quadrupole interactions. This points to the presence of defects at the surface. Motion of these defects along dislocations could cause efficient relaxation of Al both at the surface and in the bulk of the sample. This reduces the average spin-lattice relaxation time as compared to the Verneuil sample, in which defects are present at a much lower level. As a result, much more intensity is observed for the corundum A sample than for the single crystal Verneuil sample.

In addition to paramagnetic impurities, the absence of many defects in the natural corundum samples may also contribute to loss of intensity. The quality of the natural corundum samples is comparable to that of the synthetic single crystal. They are of good quality and have a low specific surface.

There is no significant difference between the standard single crystal sample and the annealed sample. This is an indication, that surface defects with very large E.F.G.'s (>10 MHz) are not the cause of the observed low intensity. Annealing the sample reduces the number of these defect sites and results in a higher observed intensity. This is not observed in our experiments. This is in agreement with the quantitative Al measurements on Yttrium Aluminium Garnet (YAG) by Massiot et al. (1990). In this study, identical quantitative results were obtained for a polycrystalline sample obtained from sol-gel synthesis and a single crystal. This is also supported by the spin-echo experiments.

## 5.7 Conclusions

There is a large difference in the intensity response of $^{27}Al$ as a function of the pulse length in a variety of synthetic and natural corundum samples. The natural samples and the single crystal sample all have much lower intensities than the corundum A sample for which all Al intensity is observed. We show, that the relaxation behaviour of various samples governs the outcome of the quantitative measurements. The presence or absence of defects influences the number of nuclei that are observed on the NMR time scale. In case of the natural samples, the presence of paramagnetic impurities causes very rapid relaxation of Al nuclei causing signal loss. In case of the synthetic single crystal made by the Verneuil method, the low level of defects (impurities or others) causes very long relaxation times and loss of signal. Comparison of the Al intensity of the corundum A sample with an aluminium nitrate solution and $NH_4Al(SO_4)_2 \cdot 12H_2O$, a sample with a very small quadrupole interaction, shows, that all Al is observed in corundum A. This is probably the result of defect sites, which cause a relaxation rate that is just right for the observation of most of the nuclei in the sample.

## References cited


Abragam, A. The Principles of Nuclear Magne tism, Oxford University Press, London, 1961.

Akitt, J.W. (1989) Multinuclear studies of aluminium compounds. In J.W. Emsley, J. Feeney and L.H. Sutcliffe, Eds., Progress in Magnetic Resonance Spectroscopy, 21, 1-149, Pergamon Press plc, Oxford.

Alemany, L.B. (1993) Critical factors in obtai ning meaningful fast MAS NMR spectra of non-integral spin quadrupolar nuclei. A review with particular emphasis on $^{27}Al$ MAS NMR of catalysts and minerals. Applied Magnetic Resonance, 4, 179-201.

Alemany, L.B., Massiot, D., Sherriff, B.L., Smith, M.E., and Taulelle, F. (1991) Observationand accurate quantification of $^{27}Al$ MAS NMR spectra of some $Al_2SiO_5$ polymorphs containing sites with large quadrupole interactions Chemical Physics letters, 177, 301-306.

Barbieri, M., Cozzupoli, D., Federico, M., Fornaseri, M., Merlino, S., Orlandi, P., and Tolomeo, L. (1977) Harkerite from the Alban Hills, Italy. Lithos, 10, 133-141.

Barth, T., and Lunde, G. (1927) Über das Mi neral Villiaumit. Zentrallblatt für Mineralogie,Geologie und Petrologie, A, 57-66.

Baur, W.H., and Ohta, T. (1982) The $Si_5O_{16}$ pen ta-mer in zunyite refined and emperical relationsfor individual Silicon oxygen bonds. Acta Crystallografica, B38, 390-401.

Becker, K.D. (1982) Nuclear magnetic relaxation induced by the dynamics of lattice defects in solids (I=3/2, I=2, and I=5/2). Zeitschrift für Naturforschung, 37a, 697-705.

Blasse, G. (1964) Crystal chemistry and some magnetic properties of mixed metal oxides with spinel structures. Philips Research Reports Supplement, nr. 3.

Bøggild, O.B. (1953) The mineralogy of Greenland. Meddelelser om Grønland, 149(3), 1-442.

Bos, A. (1993) Kwantitatieve interpretatie van $^{27}Al$-spectra m.b.v. puls- en sweepmethoden. Quaterly report, volume 1.

Brown., I.D., and Shannon, R.D. (1973) Emperical bond-strength-bond-length curves for oxides. Acta Crystallografica., A29, 266-282.

Burnham, C.W. (1981) The nature of multi-component aluminosilicate melts. In: D.T. Rickard, and F.E. Wickman, Eds. Physics and Chemistry of the earth, vols. 13-14, 197-229.

Burt, D.M. (1989) Compositional and phase relations among rare earth element minerals. In Mineralogical Society of America Reviews in Mineralogy, 21, 259-308.

Cas, R.A.F., and Wright, J.V. (1987) Volcanic successions. Modern and Ancient. A geological approach to processes, products, and successions. London: Allen & Unwin.

Chmelka, B.F., Müller, K.T., Pines, A., Stebbins, J., Wu, Y., and Zwanziger, J.W. (1989) Oxygen-17 NMR in solids by dynamic-angle spinning and double rotation. Nature, 339, 42-43.

Christoph, F.J., jr., Elkton, M.D., Teufer, G., and Ford, C.H. (1965) U.S. Patent 3,178,483.

Cohen, M.H., and Reif, F. (1957) Quadrupole effects in nuclear magnetic resonance studies of solids. Solid State Physics, 5, 321-438.

Coté, B., Massiot, D., Taulelle, F., and Coutures, J.-P. (1992)$^{27}Al$ NMR spectroscopy of aluminosilicate melts and glasses. Chemical Geology, 96, 367-370.

Cowley, J.W., and Scott, T.R. (1948) The nature of precipitated fluoaluminates. Journal of the American Chemical Society, 69, 2596-2598.

Davies, W.O., and Machin, M.P. (1970) Isomorphous replacements in harkerite and the relation of sakhaite to harkerite. Canadian Mineralogist, 10, 689-695.

Dec, S.F., and Maciel, G.E. (1990) High-speed MAS NMR spectra of quadrupolar nuclides at high magnetic fields. Journal of Magnetic Resonance, 87, 153-159.

Dirken, P.J., J.B.H. Jansen, and R.D. Schuiling (1992) Influence of octahedral polymerization on $^{23}Na$ and $^{27}Al$ MAS NMR in alkali fluoroaluminates. American Mineralogist, 77, 718-724.

Dirken, P.J., Kentgens, A.P.M., G.H. Nachte gaal, and J.B.H. Jansen. Off-resonance nutation NMR study of framework aluminosilicate glasses with Li, Na, K, Rb or Cs as charge balancing cation. Submitted Journal of Physical Chemistry.

Dupree, E., and Pettifer, R.F. (1984) Determination of the Si-O-Si bond angle distribution in vitreous silica by magic angle

spinning NMR. Nature, 308, 523-525.

Eckert, H. (1992) Structural characterization of noncrystalline solids and glasses using solid state NMR. Progress in NMR spectroscopy, 24, 159-293.

Engelhardt, G., and Michel, D. (1987) High resolution solid state NMR of silicates and zeolites,. Wiley, Chichester, England.

Ernst ,H., Freude, D., and Wolf, I. (1993) Multinuclear solid-state NMR studies of Brønsted sites in zeolites. Chemical Physics Letters, 212, 588-596.

Farnan, I., and Stebbins, J.F. (1990) High temperature $^{29}Si$ NMR investigation of solid and molten silicates. Journal of the American Chemical Society, 112, 32-39.

Fenzke, D., Freude, D., Fröhlich, T., and Haase, J. (1984) NMR intensity measurements of half-integer quadrupole nuclei. Chemical Physics Letters, 111, 171-175.

Freude, D., and Haase, J. (1993) Quadrupole effects in solid state nuclear magnetic resonance. In Diehl, P., Fluck, E., Günther, H., Kosfeld, R., and Seelig, J. Progress in nuclear magnetic resonance, 29, 1-90.

Furrer, G., Ludwig, C., and Schindler, P.W. (1992) On the chemistry of the Keggin $Al_{13}$ polymer. I. Acid-base properties. Journal of Colloid and Interface Science, 149(1), 56-67.

van Genechten, K.A. and Mortier, W.J. (1988) Influence of the structure type on the intrinsic framework electronegativity and the charge distribution in zeolites with $SiO_2$ composition. Zeolites, 8, 273.

Ghose, S., and Tsang, T. (1973) Structural dependence of quadrupole coupling constant $e^2qQ/h$ for $^{27}Al$ and crystal field parameter D for $Fe^{3+}$ in aluminosilicates. American Mineralogist, 58, 748-755.

Grimmer, A.-R., Müller, D., Bentrup, U., and Kolditz, L. (1982) $^{19}F$ und $^{27}Al$-NMR-spek troskopischer Nachweis von Bewegungsvorgängen in alkalihexafluoroaluminaten. Zeitschrift für Chemie, 22, 43.

Grimmer, A.-R., Von Lampe, F., Tarmak, M., and Lippmaa, E. (1983) Solid-state high resolution $^{29}Si$ NMR in zunyite. Chemical Physics Letters, 97, 185-187.

Guiseppetti, G. Mazzi, F., and Tadini, C. (1977) The crystal structure of harkerite. American Mineralogist, 62, 263-272.

Haase, J., and Oldfield, E. (1993) Quantitative determination of nonintegral spin quadrupolar nuclei in solids using nuclear magnetic resonance spin-echo techniques. Journal of Magnetic Resonance, Series A 104, 1-9.

Hamilton, D.L., and Henderson, C.M.B. (1968) The preparation of silicate compositions by a gelling method. Mineralogical Magazine, 36, 832-838.

Hawthorne, F.C., and Ferguson, R.B. (1975) Refinement of the crystal structure of cryolite. Canadian Mineralogist, 13, 377-382.

Hepworth, M.A., Jack, K.H., Peacock, R.D., and Westland, G.J. (1957) The crystal structures of the trifluorides of iron, cobalt, ruthenium, rhodium, palladium and irdidium. Acta Crystallografica, 10, 63-69.

Hill, R.J., Craig, J.R., and Gibbs, G.V. (1979) Systematics of the spinel structure type. Physics and Chemistry of Minerals, 4, 317-339.

Hoppe, R., and Kissel, D. (1984) Zur Kenntnis von $AlF_3$ und $InF_3$. Journal of Fluorine Chemistry, 24, 327-340.

Huggins, B.A., and Ellis, P.D. (1992) $^{27}Al$ nu clear magnetic resonance study of aluminas and their surfaces. Journal of the Amercian Chemical Society, 114, 2098-2108.

Ishizawa, N., Miyata, T., Minato, I., Marumo, F., and Iwai, S. (1980) A structural investigation of $\alpha$-$Al_2O_3$ at 2170 K. Acta Crystallografica, B36, 228-230.

Jacoboni, C., Leble, A., and Rousseau, J.J.(1981) Détermination précise de la structure de la chiolite $Na_5Al_3F_{14}$ et étude par R.P.E. de $Na_5Al_3F_{14}$:$Cr^{3+}$. Journal of Solid State Chemistry, 36, 297-304.

Jäger, C., Rocha, J., and Klinowski, J. (1992) High-speed satellite transition $^{27}Al$ MAS NMR spectroscopy. Chemical Physics Letters, 188, 208 212.

Johansson, G. (1960) On the crystal structures of some basic aluminium salts. Acta Chemica Scandinavica, 14, 771-773.

de Jong, B.W.H.S., Schramm, C.M., and Parzia le, V.E. (1983) Polymerization of silicate and aluminate tetrahedra in glasses, melts, and aqueous solutions-IV. Aluminium coordination in glasses and aqueous solutions and comments on the aluminum avoidance principle. Geochimica et Cosmochimica Acta, 47, 1223-1236.

de Jong, B.H.W.S. (1987) Uneconomic bonding in glasses. Nature, 330, 422.

Kamb, W.B. (1960) The crystal structure of zunyite. Acta Crystallografica, 13, 15-24.

Kentgens, A.P.M. (1987) Two-dimensional solid state NMR. Ph.D. Thesis K.U. Nijmegen.

Kentgens, A.P.M.(1991) Quantitative excitation of half-integer quadrupolar nuclei by a frequency stepped adiabatic half-passage. Journal of Magnetic Resonance, 95, 619-625.

Kentgens, A.P.M. (1993) Off-resonance nutation NMR spectroscopy of half-integer quadrupolar nuclei. Journal of Magnetic Resonance, Series A 104, 302-309.

Kentgens, A.P.M., Scholle, K.F.M.G.J., and Veeman, W.S. (1983) Effect of hydration on the local symmetry around aluminum in ZSM-5 zeolites studied by aluminum-27 Nuclear Magnetic Resonance. The Journal of Physical Chemistry, 87, 4357.

Kentgens, A.P.M., Lemmens, J.J.M., Geurts, F.M.M., and Veeman, W.S. (1987) Two dimensional solid-state nutation NMR of half integer quadrupolar nuclei. Journal of Magnetic Resonance, 71, 62-74.

Kimura, K., and Satoh, N. (1989) High resolu tion solid state NMR of $^{27}AlF_3$ particles observed by a conventional Fourier-transform spectrometer. Chemistry Letters, 271-274.

Kirkpatrick, R.J. (1988) MAS NMR spectrosco py of minerals and glasses. In J.F. Hawthorne, Ed., Reviews in Mineralogy, Vol. 18. Spectroscopic methods in mineralogy and geology, p. 341-403. Mineralogical Society of America, Washington D.C.

Kirkpatrick, R.J. and Phillips, B.L. (1993) $^{27}Al$ NMR spectroscopy of minerals and related materials. Applied Magnetic Resonance, 4, 213-236.

Kloprogge, J.T. (1992) Pillared clays. Preparati on and characterization of clay minerals and aluminum-based pillaring agents. Geologica Ultraiectina. Mededelingen van de Faculteit Aardwetenschappen der Universiteit Utrecht, no. 91.

Kohn, S.C., Dupree, R., and Smith, M.E. (1989) A multinuclear magnetic resonance study of the structure of hydrous albite glasses. Geochimica et Cosmochimica Acta, 53, 2925-2935.

Kohn, S.C., Dupree, R., Mortuza, M.G., and Henderson, C.M.B. (1991) NMR evidence for five- and six-coordinated aluminum fluoride complexes in F-bearing aluminosilicate glasses. American Mineralogist, 76, 309-312.

Kohn, S.C., Dupree, R.D., and Mortuza, M.G. (1992) The interaction between water and aluminosilicate magmas. Chemical Geology, 96, 399-411.

Koller, H., Engelhardt, G., Kentgens, A., and Sauer, J. (1994) $^{23}Na$ NMR spectroscopy of solids: interpretation of quadrupole interaction parameters and chemical shifts. In press Journal of Chemical Physics.

Kubicki, J.D., and Sykes, D. (1993) Molecular orbital calculations of vibrations of three membered aluminosilicate rings. Physics and Che mistry of Minerals, 19, 381-391.

Kunwar, A.C., Thompson, A.R., Gutowsky, H.S., and Oldfield, E. (1984) Solid state aluminum-27 NMR studies of tridecameric Al-oxo-hydroxy clusters in basic aluminum selenate, sulfate, and the mineral zunyite. Journal of Magnetic Resonance Communications, 60, 467-472.

Kunwar, A.C., Turner, G.L., and Oldfield, E. (1986) Solid-state spin-echo Fourier transform NMR of $^{39}K$ and $^{67}Zn$ salts at high field. Journal of Magnetic Resonance, 69, 124-127.

Lampe, F. v., Müller, D., Gessner, A.-R., and Scheler, G. (1982) Vergleichende $^{27}Al$ Al-NMR-Untersuchungen am Mineral zunyite und basischen Aluminium-Salzen mit tridekameren Al-oxo-hydroxo-aquo-Kationen. Zeitschrift für Anorganische und Allgemeine Chemie, 489, 16-22.

Le Bail, A., Jacoboni, C., Leblanc, M., De Pape R., Duroy, H., and Fourquet, J.L. (1988) Crystal structure of the metastable form of aluminum trifluoride $\beta$-$AlF_3$ and the gallium and indium homologs. Journal of Solid State Chemistry, 77, 96-101.

Lee, D., and Bray., P.J. (1991) $^{27}Al$ nuclear quadrupole resonance study of crystalline aluminosilicates. Journal of Magnetic Resonance, 94, 51-58.

Liebau, F. (1985) Strucural chemistry of silica tes: structure, bonding and classification. Springer Verlag, Berlin, Germany.

Lippmaa, E., Mägi, M., Samoson, A., Engel hardt, G. ,and Grimmer, A.-R.(1980) Structural studies of silicates by solid state high-re-

solution $^{29}Si$ NMR. Journal of the American Chemical Society, 102, 4889-4893.

Lippmaa, E., Mägi, M., Samoson, A., Tarmak, M., and Engelhardt, G.(1981) Investigation of the structure of zeolites by solid-state high-resolution $^{29}Si$ NMR spectroscopy. Journal of the American Ceramic Society, 103, 4992-4996.

Lippmaa, E., Samoson, A., and Mägi, M. (1986) High-resolution $^{27}Al$ NMR of aluminosilicates. Journal of the American Chemical Society, 108, 1730-1735.

Liu, S.B., Pines, A., Brandriss, M., and Stebbins, J.F. (1987) Relaxation mechanisms and effects of motion in Albite ($NaAlSi_3O_8$) liquid and glass: a high temperatureNMR study. Physics and Chemicstry of Minerals, 15, 155-162.

Llor, A. ,and Virlet, J. (1988) Towards high resolution NMR of more nuclei in solids: sample spinning with time-dependent spinner axis angle. Chemical Physics Letters, 152, 248-253.

Loewenstein, W. (1954) The distribution of aluminum in the tetrahedra of silicates and aluminates. American Mineralogist, 39, 92-96.

Louisnathan, S.J., and Gibbs, G.V. (1972) Aluminum-silicon distribution in zunyite. Ame rican Mineralogist, 57, 1089-1108.

Louisnathan, S.J., and Gibbs, G.V. (1973) Zunyite: a comparison of neutron- and X-ray-diffraction studies. American Mineralogist, 58, 138.

Machin, M.P., and Miehe, G. (1976) $[Al(SiO_4)_4]^{13-}$ tetrahedral pentamers in harkerite. Neues Jahrbuch für Mineralogie, Monatshefte, 228-232.

Magi, M., Lippmaa, E., Samoson, A., Engel hardt, G., and Grimmer, A.R. (1984) Solid-state high resolution silicon-29 chemical shifts in silicates. Journal of Physical Chemistry, 88, 1518-1522.

Magnelli, A. (1953) Studies on the hexagonal tungsten bronzes of potassium, rubidium and cesium. Acta Chemica Scandinavica, 7, 315-324.

Majumdar, A.J., and Roy, R. (1965) Test of the applicability of the Clapeyron relationship to a few cases of solid-solid transitions. Journal of Inorganic and Nuclear Chemistry, 27, 1961-1973.

Man, P.P., Klinowski, J., Trokiner, A., Zanni, H., and Papon, P. (1988) Selective and non-selective NMR excitation of quadrupolar nuclei in the solid state. Chemical Physics Letters, 151, 143-150.

Manning, D.A.C. (1981) The effect of fluorine on liquidus phase relationships in the system Qz-Ab-Or with excess water at 1kb. Contributions to Mineralogy and Petrology, 76, 206-215.

Massiot, D., Bessada, C., Contures, J.P., and Taulelle, F. (1990) A quantitative study of the $^{27}Al$ MAS NMR in crystalline YAG. Journal of Magnetic Resonance, 90, 231-242.

McMillan, P.F., Wolf, G.H., and Poe, B.T. (1992) Vibrational spectrscopy of silicate liquids and glasses. Chemical Geology, 96, 351-366.

Meadows, M.D., Smith, K.A., Kinsey, R.A., Rothgeb, T.M., Skarjune, R.P., and Oldfield, E. (1982) High resolution solid-state NMR of quadrupolar nuclei. Proceedings of the National Academy of Sciences, 79, 1351-1355.

Mesrobian, G., Rolin, M., and Pham, H. (1972) Étude sous pression des mélanges fluorure de sodium-fluorure d'aluminium riches en fluorure d'aluminium. Revues Internationales des Hautes Température et des Refractaires, 9, 139-146.

Mozzi, R.L., and Warren, B.E. (1969) The structure of vitreous silica. Journal of Applied Crystallography, 2, 149-152.

Müller, D., Gessner, W., Behrens, H.-J., and Scheler, G. (1981) Determination of the aluminium coordination in aluminium-oxygen compounds by solid-state high-resolution $^{27}Al$ NMR. Chemical Physics Letters, 79[1], 59-62.

Müller, D. (1982) Zur Bestimmung chemischer Verschiebungen der NMR-Frequenzen bei Quadrupolkernen aus den MAS-NMR-Spektren. Annalen der Physik, 39, 451-460.

Müller, D., Gessner, W., Samoson, A., Lippmaa, E., and Scheler, G. (1986) Solid-state aluminium-27 nuclear magnetic resonance chemical shift and quadrupole coupling data for condensed $AlO_4$ tetrahedra. Journal of the Chemical Society, Dalton Transactions, 1277-1281.

Müller, D., and Bentrup, U. (1989) $^{27}Al$-NMR-

Untersuchungen an alkalifluoroaluminaten. Zeitschrift für Anorganische und Allgemeine Chemie, 575, 17-25.

Murdoch, J.B., Stebbins, J.F., and Carmichael, I.S.E.(1985) High-resolution $^{29}Si$ NMR study of silicate and aluminosilicate glasses. The effect of the network-modifying cations. American Mineralogist, 70, 332-343.

Mysen, B.O., and Virgo, D. (1985) Structure and properties of fluorine-bearing aluminosilicate melts: the system $Na_2O$-$Al_2O_3$-$SiO_2$-F at 1 atm. Contributions to Mineralogy and Petrology, 91, 205-220.

Mysen, B. (1988) Fyfe, C.A. Ed., Structure and Properties of Silicate melts. Developments in Geochemistry, Elsevier.

Mysen, B. (1990) The role of aluminum in depolymerized, peralkaline aluminosilicate melts in the systems $Li_2O$-$Al_2O_3$-$SiO_2$, $Na_2O$-$Al_2O_3$-$SiO_2$, and $K_2O$-$Al_2O_3$-$SiO_2$American Mineralogist, 75, 120-134.

Navrotsky, A., Geisinger, K.L., McMillan, P., and Gibbs, G.V. (1985) The tetrahedral framework in glasses and melts-Inferences from molecular orbital calculations and implications for structure, thermodynamics and physical properties. Physics and Chemistry of Minerals, 11, 284-298.

Newnham, R.E., and de Haan., Y.H. (1962) Refinement of the $\alpha$-$Al_2O_3$, $Ti_2O_3$, $V_2O_3$ and $Cr_2O_3$ structures. Zeitschrift für Kristallografie, 117, 235-237.

Oestrike, R., Yang, W.-H., Kirkpatrick, R.J., Hervig, R.L., Navrotsky, A., and Montez, B. (1987) High-resolution $^{23}Na$, $^{27}Al$, and $^{29}Si$ NMR spectroscopy of framework aluminosilicate glasses. Geochimica et Cosmochimica Acta, 51, 2199-2209.

O'Reilly, D.E. (1960) Magnetic resonance techniques in catalytic research. Advances in Catalysis, 12, 31-116.

Pauling, L. (1933) The crystal structure of zu nyite $Al_{13}Si_5O_{20}(OH,F)_{18}Cl$.Zeitschrift für Kristallo-gra-fie, 84, 442-452.

Pearson, R.M., and Schramm, C.M. (1990) Quantitation of aluminum-27 NMR spectra of high-surface-area-oxides. Colloids and surfaces, 45, 323-334.

Perchuk, L.L, and Kushiro, I., Eds. Advances in Physical Geochemistry, vol. 9, Springer-Verlag, 1991.

Phillips, B.L., Kirkpatrick, R.J., and Hovis, G.L. (1988) $^{27}Al$, $^{29}Si$ and $^{23}Na$ MAS NMR study of an Al,Si ordered alkali feldspar solid solution series. Physics and Chemistry of Minerals, 16, 262,275.

Phillips, B.L., Kirkpatrick, R.J., and Putnis, A. (1989) Si,Al ordering in leucite by high-resolution $^{27}Al$ MAS NMR spectroscopy. Physics and Chemistry of Minerals, 16, 591-598.

Plee, D., Borg, F., Gatineau, L., and Fripiat, J.J. (1985) High-resolution $^{27}Al$ and $^{29}Si$ nuclear magnetic resonance study of pillared clays. Journal of the American Chemical Society, 107, 2362-2369.

Pound, R.V. (1950) Nuclear electric quadrupole interactions in crystals. Physical Review, 79, 685 702.

Prakabar, S., Rao, K.J., Rao, C.N.R. (1991) $^{29}Si$ NMR chemical shifts in silicates. Chemical Physics Letters, 183, 176-182.

Risbud, S.H., Kirkpatrick, R.J., Taglialavore, A.P., and Montez, B. Solid-state NMR evidence of 4-, 5-, and 6-fold aluminum sites in roller-quenched $SiO_2$-$Al_2O_3$ glasses. Journal of the American Ceramic Society, 70, C10-12.

Robie, R.A., Hemingway, B.S., and Fisher, J.R. (1978) Thermodynamic properties of minerals and related substances at 298.15 K and 1 Bar ($10^5$ Pascals) pressure and at higher temperatures. United States Geological Survey Bulletin, 1452, United States Government Printing Office, Washington, D.C.

Sabelli, C. (1987) Structure refinement of elpasolite from Cetine mine, Tuscany, Italy. Neues Jahrbuch der Mineralogie, Monatsheft 11, 481-487.

Samoson, A. (1985) Satellite transition high-resolution NMR of quadrupolar nuclei in powders. Chemical Physics Letters, 119, 29-32.

Samoson, A., and Lippmaa, E. (1983a) Central transition NMR excitation spectra of hal-integer quadrupole nuclei. Chemical Physics Letters, 100, 205-208..

Samoson, A., and Lippmaa, E. (1983b) Excita tion phenomena and line-intensities in high-resolution NMR powder spectra of half-integer quadrupolar nuclei. Physical Reviews B., 28, 6567-6570.

Samoson, A., and Lippmaa, E. (1988) 2D NMR nutation spectroscopy in solids. Journal of

Magnetic Resonance, 79, 255-268.

Samoson, A., Lippmaa, E., and Pines, A. (1988) High resolution solid-state N.M.R. Averaging of second-order effects by means of a double-rotor. Molecular Physics, 65, 1013-1018.

Sato, R.K., McMillan, P.F., Dennison, P., and Dupree, R. (1991) High-resolution $^{27}Al$ and $^{29}Si$ MAS NMR investigation of $SiO_2$-$Al_2O_3$ glasses. Journal of Physical Chemistry, 95, 4483-4489.

Satoh, N., and Kimura, K. (1990) High-resolu tion solid-state NMR in liquids. 2.[1] $^{27}Al$ NMR study of $AlF_3$ ultrafine particles. Journal of the American Chemical Society, 112, 4688-4692.

Shannon, R.D., and Prewitt, C.T. (1969) Effec tive ionic radii in oxides and fluorides. Acta Crystallografica, B25, 925-946.

Sherriff, B.L., Grundy, H.D., and Hartman, J.S. (1991) The relationship between $^{29}Si$ MAS NMR chemical shift and silicate mineral structure. European Journal of Mineralogy, 3, 751-768.

Shinn, D.B., Crocket, D.S., and Haendler, H.M. (1966) The thermal decomposition of ammonium hexafluoroferrate(lll) and ammonium hexafluoroaluminate. A new crystalline form of aluminum fluoride. Inorganic Chemistry, 5(11), 1927-1933.

Skibsted, J., Nielsen, N.C., Bildsoe, H., and Jakobsen, H.J. (1991) Satellite transitions in MAS NMR spectra of quadrupolar nuclei. Journal of Magnetic Resonance, 95, 88-117.

Slichter, C.P. (1992) Principles of Magnetic Re sonance. 3rd ed., Springer Verlag, New York.

Smith, M.E. (1993) Application of $^{27}Al$ NMR techniques to structure determinations in solids. Applied Magnetic Resonance, 4, 1-64.

Smith, K.A., Kirkpatrick, R.J., Oldfield, E., and Henderson, D.M. (1983) High-resolution silicon-29 nuclear magnetic resonance spectroscopy of rock-forming silicates. American Mineralogist, 68, 1206-1215.

Smith, J.V., and Blackwell, C.S. (1983) Nuclear magnetic resonance of silica polymorphs. Nature, 303, 223-225.

Stebbins, J.F. (1987) Identification of multiple structural species in silicate glasses by $^{29}Si$ NMR. Nature, 330, 465-467.

Stebbins, J.F. (1988) NMR spectroscopy and dynamic processes in mineralogy and geochemistry. In J.F. Hawthorne, Ed., Reviews in Mineralogy, Vol. 18. Spectroscopic methods in mineralogy and geology, p. 405-429. Mineralogical Society of America, Washington D.C.

Stebbins, J.F., and McMillan, P.F. (1989) Five- and six-coordinated Si in $K_2Si_4O_9$ glass quenched from 1.9 GPa and 1200 °C. American Mineralogist Letters, 74, 965-968.

Stebbins, J.F. (1991a) Nuclear magnetic resonan ce at high temperature. Chemical Reviews, 91, 1353-1373.

Stebbins, J.F. (1991b) NMR evidence for five-coordinated silicon in a silicate glass at atmospheric pressure. Nature, 351, 638-639.

Stickney de Bouregas, F., and Waugh., J.S. (1992) ANTIOPE, A program for computer experiments on spin dynamics. Journal of Magnetic Resonance, 96, 280-289.

Sykes, D. and Kubicki, J.D. (1993) A model for $H_2O$ solubility mechanisms in albite melts from infrared spectroscopy and molecular orbital calculations. Geochimica et Cosmochmica Acta, 57, 1039-1052.

Taylor, M., and Brown, G.E. (1979a) Structure of mineral glasses-I. The feldspar glasses $NaAlSi_3O_8$, $KAlSi_3O_8$, $CaAl_2Si_2O_8$. Geochimica et Cosmochimica Acta, 43, 61-75.

Taylor, M., and Brown, G.E. (1979b) Structure of mineral glasses-II. The $SiO_2$-$NaAlSiO_4$. - Geochimica et Cosmochimica Acta, 43, 1467-1473.

Tilley, C.E. (1951) The zoned contact-skarns of the Broadford area, Skye: a study of boron-fluorine metasomatism in dolomites. The Mineralogical Magazine, 214, 621-666.

Tossell, J.A., and Gibbs, G.V. (1978) The use of molecular-orbital calculations on model systems for the prediction of bridging bond-angle variations in siloxanes, silicates, silicon,, nitrides and silicon sulfides. Acta Crystallografica, A34, 463-472.

Tossell, J.A., and Vaughan, D.J. (1992) Theoretical geochemistry: applications of quantum mechanics in theearth and mineral sciences. Oxford UniversityPress, New York.

Turco, G. (1962) La zunyite; recherches expérimentales physico-chimiques en liaison avec l'étude du nouveau gisement de Beni-Embarek. Bulletin de la Societé française de mineralogie et de cristallographie, LXXXV,

407-458.

Watanabe, T., Shimizu, H., Masuda, A., and Saito, H. (1983) Studies of $^{29}Si$ spin-lattice relaxation times and paramagnetic impurities in clay minerals by magic-angle spinning $^{29}Si$-NMR and EPR. Chemistry Letters, 1293-1296.

Webster, J.D. (1990) Partitioning of F between $H_2O$ and $CO_2$ fluids and topaz rhyolite melt. Implications for mineralizing magmatic-hydrothermal fluids in F-rich granitic systems. Contributions to Mineralogy and Petrology, 104, 424-438.

Xue, X., and Stebbins, J.F. (1993) $^{23}Na$ NMR chemical shifts and local Na coordination environments in silicate crystals, melts and glasses. Physics and Chemistry of Minerals, 20, 297-307.

Zachariasen, W. (1932) The atomic arrangement in glass. Journal of the American Ceramic Society, 54, 3841-3851.

Zagal'skaya, Yu.G. and Belov, N.V. (1964) Concerning the crystal structure of zunyite $Al_{13}(OH)_{18}Si_5O_{20}Cl$ = $[Al_{12}(OH)_{18}\cdot SiO_4]\cdot[Al(SiO_4)_4]Cl$. Soviet Physics-Crystallography, 8, 429-432.

## Curriculum vitae

De auteur van dit proefschrift werd op 1 augustus 1967 geboren te Geleen. In die plaats werd in 1985 het diploma Gymnasium $\beta$ behaald aan de scholengemeenschap St. Michiel. In datzelfde jaar begon hij met de studie Geologie aan de Rijksuniversiteit Utrecht. In 1986 werd het propaedeutisch examen behaald. Van 1986 tot januari 1990 heeft hij de hoofdrichting geochemie met als specialisatie kristallografie gevolgd. Als bijvakken koos hij informatica aan de Rijksuniversiteit Utrecht en keramische technologie aan de Technische Universiteit Eindhoven. Op 30 januari 1990 behaalde hij het doctoraal examen geologie. Van 1 maart 1990 tot 1 maart 1994 is hij als assistent in opleiding verbonden geweest aan de Faculteit Aardwetenschappen. Het resultaat van het onderzoek dat in die vier jaar werd uitgevoerd heeft u in de vorm van dit proefschrift voor u liggen.